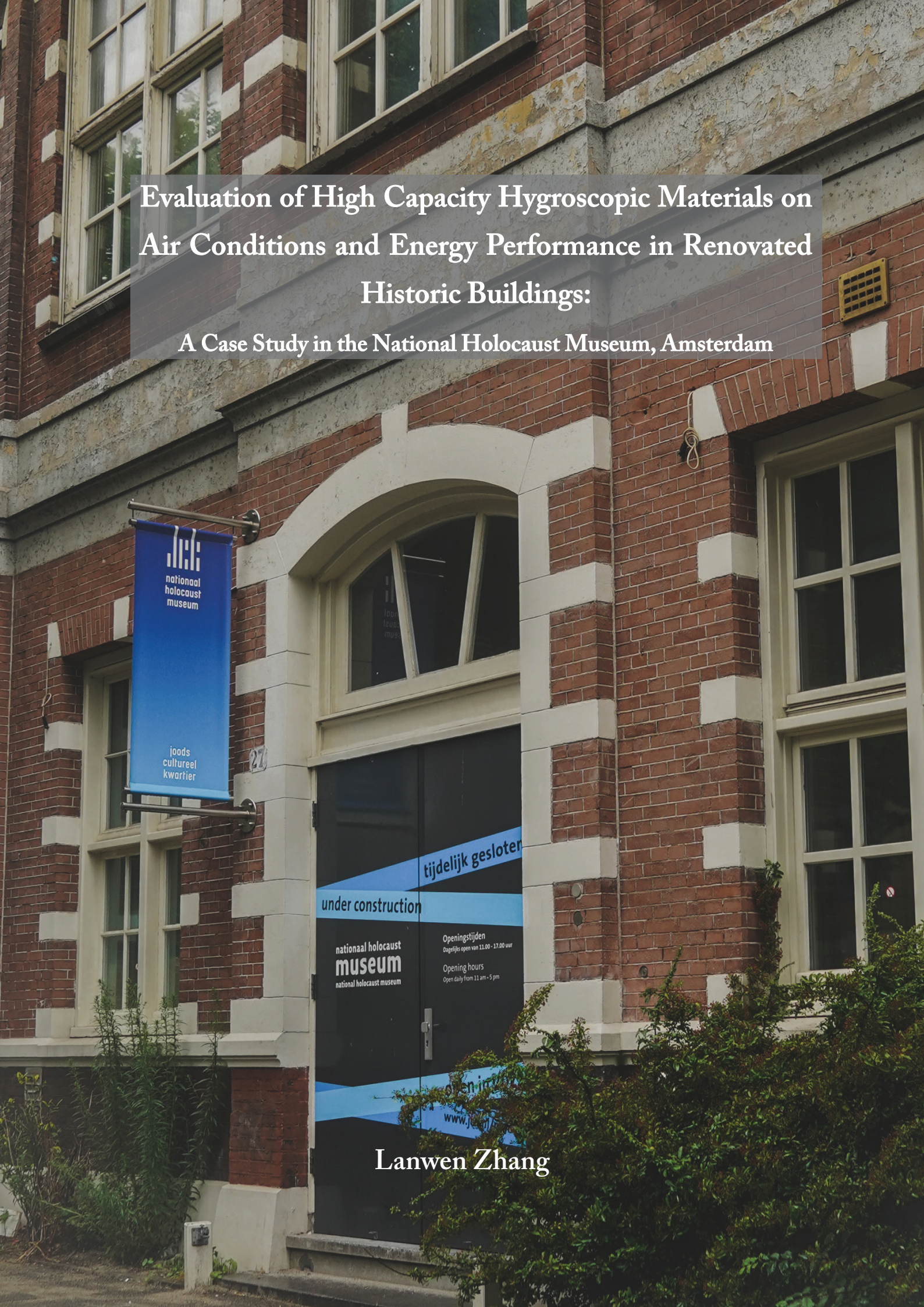


Evaluation of High Capacity Hygroscopic Materials on Air Conditions and Energy Performance in Renovated Historic Buildings:

A Case Study in the National Holocaust Museum, Amsterdam



Lanwen Zhang

Evaluation of High Capacity Hygroscopic Materials on Air Conditions and Energy Performance in Renovated Historic Buildings:

A Case Study in the National Holocaust Museum, Amsterdam

To obtain the degree of
Master of Science
in Civil Engineering
Track | Building Engineering
Specialization | Building Technology & Physics

To be defended publicly on Monday September 21, 2020 at 3:00pm

Lanwen Zhang

Student number | 4829956

E-mail | lanwenzhang52@gmail.com

Telephone number | +31 6 17291993

Graduation committee:

Prof. dr. L.C.M. Itard | Chair | TU Delft

Dr. Ir. W.H. van der Spoel | Daily supervisor | TU Delft

Dr.ir. H.R. Schipper | TU Delft

Ir. Kitty Huijbers | ABT bv



Acknowledgment

I would like to express my gratitude to everyone who gives me support in the past two years of my life in the Netherlands.

First of all, a special thank is given to my graduation committee. I am particularly grateful to my daily supervisor, Willem van der Spoel who offered me a graduation internship at ABT. He is a very responsible supervisor with a great sense of humor and always gave me clear guidance and helped me develop the simulation model in time, even at his non-working time. I would like to thank the chair of my committee, Laure Itard, who is a knowledgeable professor with great kindness. She hosted each meeting and gave me detailed comments on my report. I would like to thank my mentor and graduation coordinator from the Building Engineering track, Roel Schipper, who gave me guidance when I am confused about finding a topic of graduation project at the beginning and made each step of the graduation procedure very organized. I would like to thank my supervisor at ABT, Kitty Huijbers, who is an experienced project leader. She helped me get familiar with the museum project quickly and inspired me on how to combine my research with practice. Besides, I appreciate that ABT provided me this renovation project. Although I only worked at the office for only two months due to coronavirus situations, I enjoyed the relaxing atmosphere and flexible working time and I would like to thank every friendly colleague for sharing their working experience with me.

I would like to thank my friends from the Building Engineering track. Their accompany helped me passing exams successfully, and they always encouraged me when I was dispirited. I would like to thank my lovely friends at Camelot 015, and I feel like not being lonely during the quarantine time and having great happiness with them.

Last but not least, I am very grateful to my parents who support my study abroad with their selfless dedication.

Lanwen Zhang
Delft, September 2020

Abstract

Managing climate in museums is always a challenging task since it should meet the needs of multiple stakeholders, namely the conservation of collections, the comfort of visitors, and the protection of historic buildings. The relative humidity is one of the most crucial parameters in this management process, and it is controlled by passive design and active design approaches. In the renovation of museums, it is preferable to optimize the passive design and minimize the use of the active design that results in substantial energy consumption and high cost.

The application of hygroscopic materials is one of the most effective passive design strategies, and some of them are already used on construction, such as wood and plaster. Nevertheless, silica gel, as a kind of hygroscopic materials with higher moisture capacity, is only used in the display case currently. So, the goal of this thesis is to study its application in the exhibition room and evaluate its effect on the stabilization of relative humidity, reduction in ventilation flow rate, and decrease in energy demand. The research is also combined with a case study, which is the renovation of the National Holocaust Museum in Amsterdam, and the aim of clients is to achieve climate class A1 in the exhibition room.

Model 1.0, 2.0, and 3.0 with different complexity are created in Matlab/Simulink, which forms a schematic study of modeling. With the validation implemented in Design Builder, the accuracy of model 3.0 is proved, and it is determined as the main simulation tool. Model 3.0 consists of the thermal part, the hygric part, and the air handling unit part. In terms of simulation, it is based on the renovation plan of the National Holocaust Museum. A series of scenarios are defined at first, and the variables are the presence or absence of silica gel, the number of visitors, the ventilation flow rate, and the setpoint of humidity control. The simulation is done on two scales: one exhibition room and the whole building.

With the amount of silica gel equal to 0.1% of the volume of the simulated object, the fluctuation of relative humidity reduces by a factor of 2 on the level of both room and building. Furthermore, 18.9% of energy for humidification and dehumidification can be saved. There is a possibility of decreasing the ventilation flow rate from 12 L/s per person to 6 L/s per person with the almost 90% data meeting the A1 requirements at the same time.

The study shows the silica gel is capable of stabilizing the relative humidity fluctuation significantly with the additional benefits of energy savings and reduction in ventilation flow rate. It is recommended to apply this concept in practice as a trial, and further research about its hygrothermal performance can be done in the future.

Table of Contents

1	Introduction	3
1.1	Problem Contexts	3
1.1.1	General Academic Problem	3
1.1.2	Case Study in the National Holocaust Museum	4
1.2	Research Questions	4
1.3	Focus and Restriction	5
1.4	Outline	5
1.5	Methodology	6
1.5.1	Part 1	6
1.5.2	Part 2	6
1.5.3	Part 3	7
2	Literature Study	11
2.1	Indoor Climate in Museums	11
2.1.1	Climate Needs and Risks	11
2.1.2	Climate Class	13
2.1.3	Climate Mitigating Strategies	15
2.2	High Capacity Hygroscopic Materials: Silica Gel	17
2.2.1	Types	17
2.2.2	Properties	17
2.2.3	Moisture Transfer in the Packed Bed	19
2.2.4	Application in Display Case	22
2.3	Combined Heat and Moisture Transfer in the Porous Materials	22
2.4	National Holocaust Museum in Amsterdam	24
2.5	Conclusions	25
3	Feasibility Study	29
3.1	Description of Model 1.0	29
3.2	Definition of Variables	30
3.2.1	Dependent Variables	30
3.2.2	Dependent Variables	32
3.3	Division of Groups	33
3.4	Simulation Results	33
3.4.1	Group 1: 0 kg/m ² Silica Gel	34
3.4.2	Group 2: 2.5 kg/m ² Silica Gel	35
3.4.3	Group 3: 5 kg/m ² Silica Gel	36
3.4.4	Group 4: 10 kg/m ² Silica Gel	37
3.5	Analysis of Parameters	38

3.5.1	Amount of Silica Gel	38
3.5.2	Ventilation Flow Rate	38
3.5.3	Internal Humidity Load	39
3.5.4	Period	39
3.6	Conclusions	39
4	Model Development	43
4.1	Description of Model 2.0	43
4.1.1	Thermal Part	43
4.1.2	Hygic Part	45
4.1.3	AHU Part - Humidity Control	48
4.2	Description of Model 3.0	51
4.2.1	Thermal Part	51
4.2.2	Hygic Part	52
4.3	Summary of Two Models	54
5	Model Verification and Validation	57
5.1	Introduction	57
5.2	Design Builder Model	58
5.3	Model Comparison	59
5.3.1	Simulation Conditions	59
5.3.2	Comparison of Results	60
5.4	Testing of Model 3.0	63
5.4.1	Estimation of Magnitude of Moisture Transfer between Construction and Air	63
5.4.2	Hygrothermal Performance of Packed Bed	64
5.5	Conclusions	68
6	Simulation Conditions	71
6.1	Renovation Design of the National Holocaust Museum	71
6.2	Definition of Scenarios in One Room	72
6.2.1	Outside Climate Conditions and Schedule	72
6.2.2	Occupancy	72
6.2.3	Internal Humidity Load	73
6.2.4	Ventilation and Infiltration	74
6.2.5	Amount of Silica Gel	76
6.2.6	Summary of Conditions	76
6.3	Definition of Scenarios in the Whole Building	78
6.3.1	Outside Climate Conditions and Schedule	78
6.3.2	Occupancy	78
6.3.3	Ventilation	78
6.3.4	Amount of Silica Gel	78

6.3.5	Summary of Conditions	79
6.4	Simulation Setting in Matlab/Simulink	81
6.5	Summary of Scenarios	81
7	Simulation Results	85
7.1	Simulation of One Room	85
7.1.1	Results	85
7.1.2	Evaluation	86
7.2	Simulation of the Whole Building	87
7.2.1	Results	87
7.2.2	Evaluation	89
7.3	Design Concept of Humidity Control Device	93
7.4	Conclusions	95
8	Discussion	99
8.1	Chapter 2 Literature Study	99
8.2	Chapter 3 Feasibility Study	99
8.3	Chapter 4 Model Development	99
8.4	Chapter 5 Model Verification and Validation	100
8.5	Chapter 6 Simulation Conditions	100
8.6	Chapter 7 Simulation Results	100
9	Conclusions	103
9.1	Conclusions to Sub-questions	103
9.2	Conclusions to General Questions	105
10	Recommendations	109
10.1	Recommendations to Museums	109
10.2	Recommendations to Future Research	109
11	Appendix	111
11.1	Appendix A: Implementation of Model 1.0	111
11.1.1	Matlab Script	111
11.1.2	Simulink Code	112
11.2	Appendix B: Feasibility Study Data	113
11.2.1	Group 1: 0 kg/m ² Silica Gel	113
11.2.2	Group 2: 2.5 kg/m ² Silica Gel	114
11.2.3	Group 3: 5 kg/m ² Silica Gel	115
11.2.4	Group 4: 10 kg/m ² Silica Gel	116
11.3	Appendix C: Implementation of Model 2.0	117
11.3.1	Matlab Script	117
11.3.2	Simulink Code	128
11.4	Appendix D: Implementation of Model 3.0	131
11.4.1	Matlab Script	131

11.4.2	Simulink Code	132
11.5	Appendix E: Design Builder Model Settings	135
11.5.1	Activity	135
11.5.2	Construction	136
11.5.3	Opening	137
11.5.4	HVAC	138
11.6	Appendix F: Renovation Design from Winhov and ABT	139
11.6.1	Front Elevation	139
11.6.2	Back Elevation	140
11.6.3	Floor Plan of the Ground Floor	141
11.6.4	Floor Plan of the First Floor	142
11.6.5	Details of the Glazing and Ground	143
11.6.6	Details of the Facade and Glazing	144
12	Nomenclature	145
13	List of Figures	149
14	List of Tables	153
15	Reference	155

1

Introduction

1.1 Problem Contexts

1.2 Research Questions

1.3 Focus and Restriction

1.4 Outline

1.5 Methodology

1 Introduction

In this chapter, the contexts of managing climate in museums and relevant problems about weighting passive design against active design are presented in section 1.1. Then the research questions about the evaluation of high capacity hygroscopic materials on indoor climate and energy performance come up in section 1.2. Accordingly, the research framework and methodology are proposed in section 1.4 and 1.5, respectively. The focus and restriction of this thesis are explained in section 1.3.

1.1 Problem Contexts

1.1.1 General Academic Problem

Collections in museums should be preserved in the appropriate indoor climate with the passive protection of building envelop and the active control of HVAC systems. In practice, the passive and active design measurements are usually combined to obtain stable temperature and relative humidity.

To quantify the design and reduce the climate risks in museums, the climate class and corresponding benchmarks are defined in ASHRAE. The copy of the classification is presented on page 14. It is shown that the higher climate class requires the more stringent climate targets, and the complexity of climate control systems increases accordingly. To achieve climate class B, A1, A2, and AA, the precise full climate control systems in the entire space are required (Ankersmit & Stappers, 2017), which results in substantial energy consumption. Nevertheless, some research showed that the application of passive approaches improves the thermal inertia and hygroscopic capacity of buildings, which is capable of assisting or even eliminating some aspects of active systems more efficiently (Ankersmit & Stappers, 2017).

The application of hygroscopic materials as one of the most effective passive design strategies becomes attractive to scholars since it has great impacts on the stabilization of relative humidity. Based on the review of completed research, it was found that a well-controlled HVAC system integrated with hygroscopic materials reduces heating and cooling energy consumption by up to 5% and 30% (Osanyintola & Simonson, 2006). In 2019, the research on Portugal museums indicated that hygroscopic inertia can stabilize the relative humidity, even if the ventilation rate is reduced (Ferreira et al., 2020). However, completed research only focuses on the materials that can be used on construction. Silica gel, as a kind of hygroscopic material, cannot be used as building materials but has a higher moisture capacity. Carlos (2015) studied its effect inside the display case. However, there is little research about its effect on hygrothermal performance of the museum exhibition space.

1.1.2 Case Study in the National Holocaust Museum

The research involves the case study of the National Holocaust Museum in Amsterdam, which will be renovated in the near future. Currently, the aim of clients is to achieve climate class A1 or B in the exhibition room and class A1 inside the display case. As Figure 1.1 shows, the design focuses on integrated systems, and there is a 50mm moisture buffering layer that is made of lime plaster or loam between wooden beams.

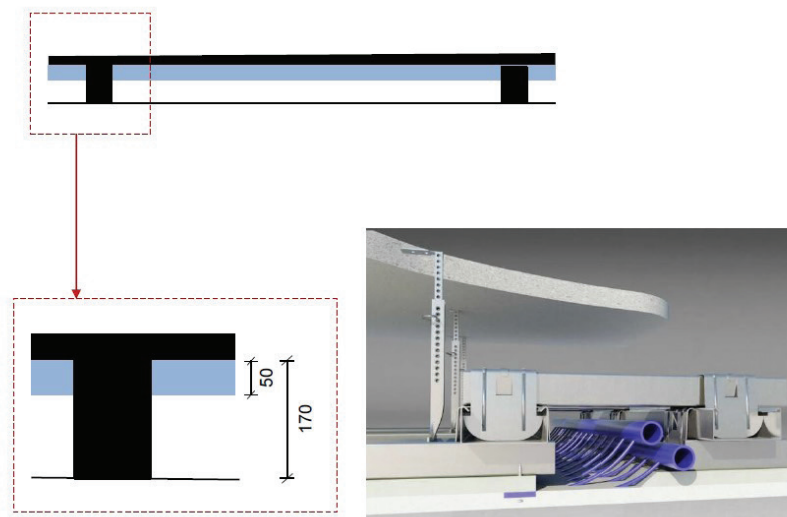


Figure 1.1: *A climate design concept in the National Holocaust Museum (ABT & Winhov, 2019)*

Since it is the design concept, it is uncertain how well moisture buffering materials perform and what kind of materials are the best option in this customized case. Furthermore, how to choose the HVAC systems with proper complexity and estimate the optimal output values in the operation phase later concerning economic values are also confronting questions.

1.2 Research Questions

Based on the problems presented in section 1.1, the main research question is raised:

What effects on air conditions and energy demand are when the high capacity hygroscopic material is applied in museums?

In relation to the main research question, sub-questions are formulated as follows:

1. What simulation tools are available and what is their expected accuracy in estimating the hygric conditions in the exhibition space?
2. To what extent can the fluctuation of relative humidity be reduced by using the high capacity hygroscopic material?

3. What is the influence on energy demand by using the high capacity hygroscopic material?
4. To what extent can the ventilation rate of the air handling unit be reduced by using high capacity hygroscopic material?
5. How can the high capacity hygroscopic material be integrated into construction or climate systems?

1.3 Focus and Restriction

In general, space in museums is divided into three zones: collection zone, people zone, and mixed zone (Ministerie van Onderwijs, 2018). The exhibition room is one of the examples of a mixed zone where the needs of both exposed collection and humans are considered, and it is the studied context in this thesis. In terms of indoor climate, the hygric conditions are studied more than the thermal conditions because the temperature does not weigh as much as the relative humidity in this project. Although there are some collections preserved in the display case, the inside microclimate is not studied.

There is a variety of high capacity hygroscopic materials globally, but only silica gel is the object of study. The properties of silica gel vary from type to type, and ProSorb is a kind of silica gel for the conservation of cultural heritage. It has the best performance among all kinds of silica gel when the relative humidity is between 40% and 60%. So, only its physical parameters are chosen for analysis.

For simplification, energy demand in this thesis only includes that for humidification, dehumidification, and ventilation. Neither heating nor cooling energy is not discussed.

1.4 Outline

The outline of the thesis is summarized in Figure 1.2. Chapter 2 is the preliminary work that includes the basic knowledge of managing indoor climate in museums, the properties and moisture transfer mechanism of silica gel, and the current situations of the National Holocaust Museum. In chapter 3 and 4, three simulation models are created in Matlab/Simulink. The feasibility study is done in model 1.0 that is the most simple one. Then, more advanced model 2.0 and 3.0 are developed in order to simulate more realistic scenarios. In chapter 5, model 2.0 and 3.0 is compared with Design Builder model to solve the first sub-question. With the definition of simulation conditions in chapter 6, the rest four sub-questions are all solved in chapter 7 where the results of relative humidity, energy demand, and ventilation flow rate are presented, and a design concept of the humidity control device is proposed as well. Chapter 8, 9, and 10 is a summary of the whole thesis. Discussion is a review of imperfections of work, and conclusions are drawn to answer the research

questions. In the end, the recommendation is written to give suggestions on museums and future research.

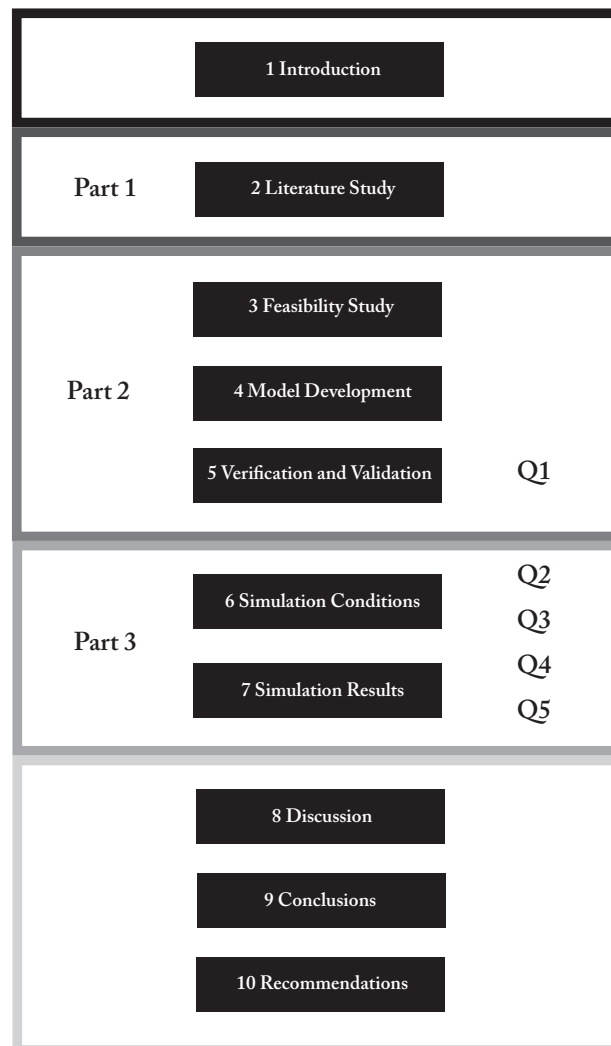


Figure 1.2: *Outline of the thesis*

1.5 Methodology

1.5.1 Part 1

The background of this project is acquired by reading literature and visiting museums. The basic knowledge about managing indoor climate in museums is summarized at first. Then, the moisture transfer mechanism both inside silica gel and on the surface of silica gel is researched theoretically and presented mathematically in a comparable way. Finally, the information about the National Holocaust Museums is collected from the museum brochure and on-site photos.

1.5.2 Part 2

All three models are created by following the same procedure. The basic assumptions are made at first. Then equations are written based on theory and implemented in Matlab/

Simulink. In order to prove validity, Design Builder as well-validated software is used as a comparison.

1.5.3 Part 3

Simulation is the main approach in this part. Reasonable scenarios are defined based on the renovation plan of the National Holocaust Museum. The simulation includes both room and building levels. The effect on relative humidity and how to integrate silica gel with climate systems are studied in the room model. Meanwhile, the impact on energy demand and the ventilation flow rate are analyzed in the building model. All the simulation data is collected to present directly or make diagrams, such as bar charts and box plots.

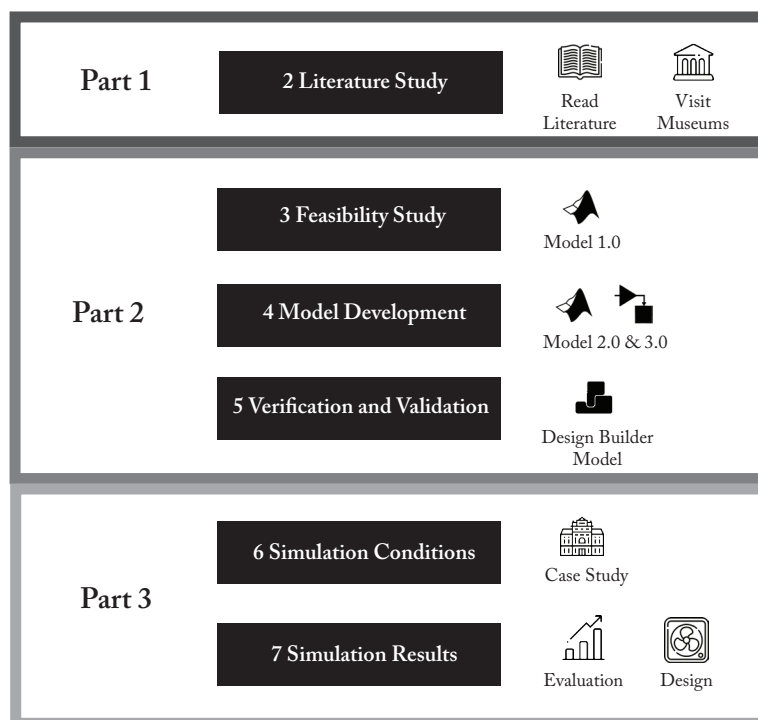


Figure 1.3: *Methodology of the thesis*

2

Literature Study

2.1 Indoor Climate in Museums

2.2 High Capacity Hygroscopic Materials: Silica Gel

2.3 Combined Heat and Moisture Transfer in the Porous Materials

2.4 National Holocaust Museum in Amsterdam

2.5 Conclusions

2 Literature Study

This chapter mainly states the theoretical background for further research. Firstly, the general information of indoor climate in museums is studied: the guideline of managing climate, the climate risks and requirements that visitors and collection have, and the control strategies. Secondly, the properties and moisture transfer mechanism of silica gel is researched. Finally, basic information about the National Holocaust Museum is collected by visiting the site.

2.1 Indoor Climate in Museums

Managing indoor climate in museums is a challenging task since multiple stakeholders are involved. It is important to take the requirement of everyone and the ambition of the project in the beginning (Ministerie van Onderwijs, 2018). Figure 2.1 gives a nine-step guideline to reach the optimal goals. Firstly, a balanced decision is made. Secondly, all the cultural values are assessed and ranked. Then, the needs and climate needs of collections, people, and the building are analyzed. Specific climate requirements are given to meet climate needs and avoid climate risks. Finally, control strategies are proposed based on climate specifications.

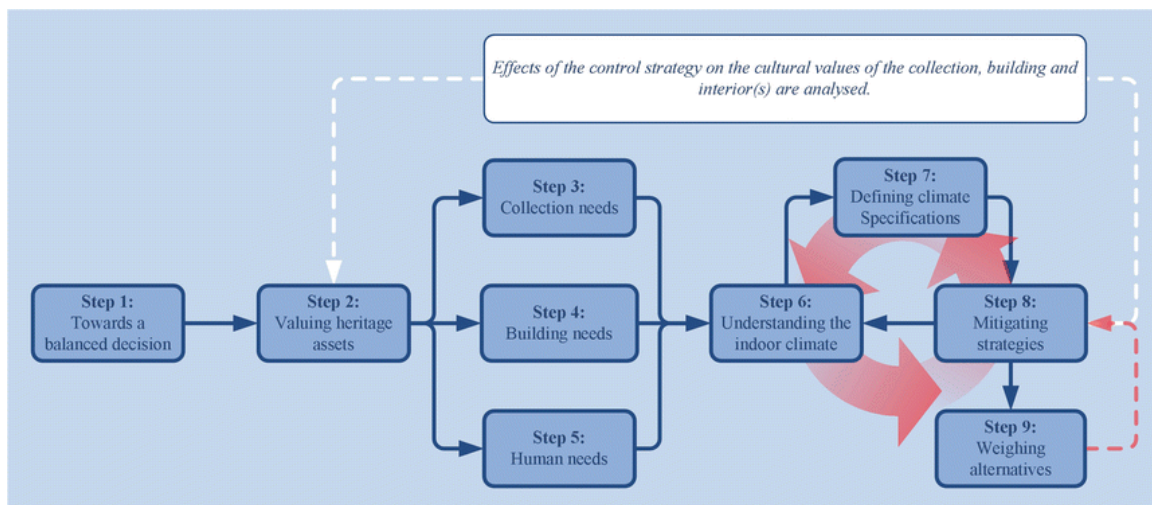


Figure 2.1: *Nine steps to manage the indoor climate in museums (Ankersmit & Stappers, 2017)*

2.1.1 Climate Needs and Risks

Temperature and relative humidity are two main parameters related to climate risks of collection and building. In terms of human needs, air quality is an additional criterion for health and comfort.

2.1.1.1 Human comfort needs

Collections are usually preserved at a lower temperature, while people prefer the relatively high temperature in the range of 19°C to 26°C (Ankersmit & Stappers, 2017). An adaptive temperature guideline is an approach that is used to assess thermal comfort. Kramer did a case study in the Museum Hermitage Amsterdam based on this approach, and it is found that 90% acceptance class is valid for temperate climates (Kramer, 2017).

Sufficient fresh air is also needed to maintain a healthy indoor environment, and its volume should be adjusted based on the CO₂ level or the number of visitors (Ankersmit & Stappers, 2017).

2.1.1.2 Climate Risks to Collection and Building

Moveable collections are sensitive to inappropriate relative humidity and temperature that include fluctuation and extreme values (Ankersmit & Stappers, 2017). Both of them are likely to damage the collection, and three types of deterioration mechanisms are defined in ASHRAE.

Biological Damage

Mold grows on the damp surface, and relative humidity, temperature, and nutrients play a crucial role in its growth. Sedlbauer (2001) combines these three parameters to the isopleth system, which displays the growth rate at specific relative humidity and temperature on different substrates. The left of Figure 2.2 shows a more comprehensive graph which is presented in ASHRAE 2019, and it consists of a study on mold growth on book materials by Groom and Panisset (1933), a general trend of culture studies by Ayerst (1968), and data from Sedlbauer (2001). In addition, the required time for mold growth is plotted on the right of Figure 2.2, and it includes the report about mold growth on the wall in the European building industry by Hens (1993) and the study on how a mixture of mold species affect mold growth. These two studies indicate the same trend.

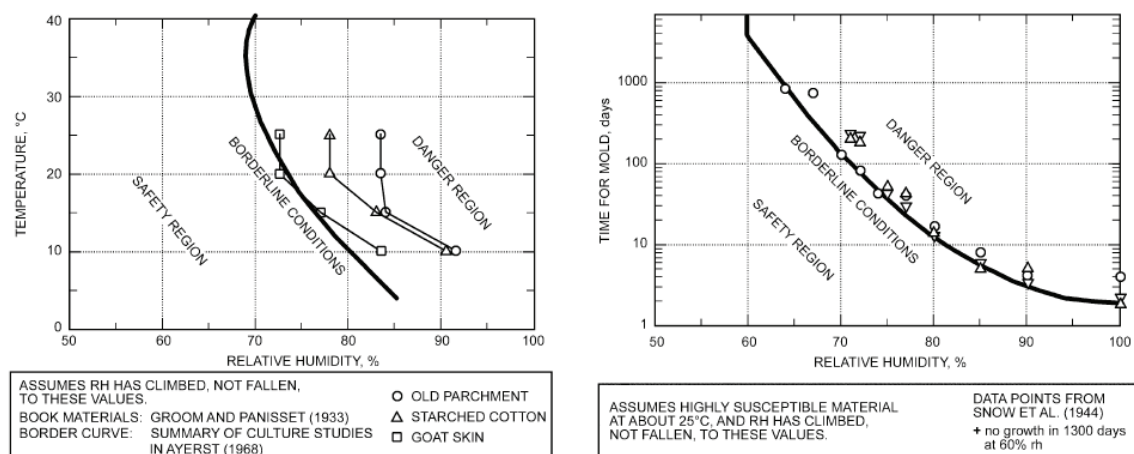


Figure 2.2: *Temperature and humidity for visible mold (left). The time required for visible mold (right)*

Some research also defined the critical value of mold growth. Ohtsuiki (1987) concluded that fungal DNA helix collapse near at RH of 55%. According to Michalski (1993), all mold growth can be prevented when the RH in the room is lower than 60%.

Mechanical Damage

Mechanical damage occurs in the form of internal or external restraint when the relative humidity or temperature reaches a very low value or fluctuates. For hygroscopic materials, the dimensional change occurs with absorption or desorption of moisture (ASHRAE, 2019).

The characteristics of mechanical deterioration of four typical objects in museums were summarized by Martens (2012). For instance, mechanical damage of panel paintings is caused by the relative humidity gradient. Panel paintings shrink, and cracks appear on the surface when RH drops. When they expand, cracks do not show immediately because the surface is under compression. There is no damage on the pictorial layer of panel paintings if the change is smaller than 15% RH.

The research community concluded that 50% RH is the safe reference value, but the permissible fluctuation and magnitudes vary from aspects to aspects (Kramer, 2017).

Chemical Damage

Chemical damage includes all the processes where chemical reactions are caused primarily by decay (Ankersmit & Stappers, 2017), and its process is accelerated by water (Erhardt et al., 1994). Water is absorbed by hygroscopic materials when RH increases, which results in the molecular layer of water becomes loose and tends to react. Conversely, the reaction speed decreases with lower RH values (Martens, 2012).

2.1.2 Climate Class

Different climate classes with a specific range of temperature and relative humidity are defined in the ASHRAE guideline. The benefits and risks are also summarized to give some suggestions on the feasibility and the budget of building envelope and HVAC design.

Table 2.1: Temperature and relative humidity specifications for collection (ASHRAE, 2019)

Type of Collection and Building	Type of Control	Long-Term Outer Limits	Annual Averages	Seasonals Adjustments from Annual Average	Short-Term Fluctuations plus Space Gradients	Collection Benefits and Risks
Museums, Galleries, Archives and Libraries in modern purpose-built buildings or purpose-built rooms	AA Precision control, no seasonal changes to relative humidity	$\geq 35\%$ rh $\leq 65\%$ rh $\geq 10^\circ\text{C}$ $\leq 25^\circ\text{C}$		No change to relative humidity Increase by 5 K; Decrease by 5 K	$\pm 5\%$ rh, ± 2 K	Mold germination and growth, and rapid corrosion avoided. No risk of mechanical damage to most artifacts and paintings. Some metals, glasses, and minerals may degrade if rh exceeds a critical value. Chemically unstable objects deteriorate significantly within decades at 20°C , twice as fast each 5 K higher.
	A1 Precision control, seasonal changes in temperature and relative humidity	$\geq 35\%$ rh $\leq 65\%$ rh $\geq 10^\circ\text{C}$ $\leq 25^\circ\text{C}$	For permanent collections: historic annual average of relative humidity and temperature. In public display areas, human comfort temperatures can apply.	Increase by 10% rh. Decrease by 10% rh. Increase by 5 K; Decrease by 10 K	$\pm 5\%$ rh, ± 2 K	Mold germination and growth, and rapid corrosion avoided. No mechanical risk to most artifacts, paintings, photographs, and books; small risk of mechanical damage to high-vulnerability artifact. (Current knowledge considers the specifications A1 and A2 as causing the same low risk of mechanical damage to vulnerable collections. Slow seasonal adjustment of 10% rh is estimated to cause the same mechanical risk as rapid fluctuations of 5% rh, because of significant stress relaxation occurring within three months of a slow transition.)
	A2 Precision control, seasonal changes in temperature only	$\geq 35\%$ rh $\leq 65\%$ rh $\geq 10^\circ\text{C}$ $\leq 25^\circ\text{C}$		No change to relative humidity. Increase by 5 K; Decrease by 10 K	$\pm 10\%$ rh, ± 2 K	Chemically unstable objects deteriorate significantly within decades at 20°C , twice as fast each 5 K higher
Museums, galleries, archives, and libraries needing to reduce stress on their building (e.g., historic house museums), depending on climate zone	B Limited control, seasonal changes in relative humidity and large seasonal changes in temperature.	$\geq 30\%$ rh $\leq 70\%$ rh $\leq 30^\circ\text{C}$	For permanent collection: historic annual average of relative humidity and temperature.	Increase by 10% rh Decrease by 10% rh Increase by 10 K Decrease by up to 20 K	$\pm 10\%$ rh, ± 5 K	Mold germination and growth, and rapid corrosion avoided. Chemical deterioration halts during cool winter periods. No risk of mechanical damage to many artifacts and most books. Tiny risk to most paintings, most photographs, some artifacts, some books. Moderate risk to high-vulnerability artifacts.
	C Prevent relative humidity extremes (damp or desiccation) and prevent high temperature extremes.	$\geq 25\%$ rh $\leq 75\%$ rh $\leq 40^\circ\text{C}$ g	Within 25% to 75% rh year-round. Temperature usually below 25°C		Not continually above 65% rh for longer than X days.h Temperature rarely over 30°C	Objects made with flexible paints and plastics that become brittle when cold, such as paintings on canvas, need special care when handling in cold temperatures. Chemically unstable objects deteriorate significantly within decades at 20°C , twice as fast each 5 K higher. Chemical deterioration halts during cool winter periods. Mold germination and growth, and rapid corrosion avoided. Tiny risk of mechanical damage to many artifacts and most books; moderate risk to most paintings, most photographs, some artifacts, some books; high risk to high-vulnerability artifacts Even greater care is needed than provided in B when handling objects made with flexible paints and plastics that become brittle when cold, such as paintings on canvas.
	D Prevent very high relative humidity (dampness)	$\leq 75\%$ rh	Relative humidity reliably below 75% rh		Not continually above 65% rh for longer than X days.h	Chemically unstable objects deteriorate significantly within decades at 20°C , and twice as fast each 5 K higher. Conversely, cool winter season can extend their life. Mold germination and growth, and rapid corrosion avoided. High risk of sudden or cumulative mechanical damage to most artifacts and paintings because of low-humidity fracture; but avoids high-humidity delamination and deformations, especially in veneers, paintings, paper, and photographs.
Collections in open structured buildings, historic houses						

In Table 2.1, different types of collection and buildings are displayed in the first column, together with benefits and potential risks with regard to three kinds of deterioration in the last column. The second column states the six climate classes in descending order of control complexity, and the specifications for temperature and relative humidity are summarized in columns 3 to 6.

The Long-term outer limit is applicable to many mixed collections. The upper and lower values of relative humidity are based on biological and mechanical damage, respectively. And the upper limit of temperature is based on chemical deterioration. It is assumed that design is aimed at permanent collections in column 4, local historic annual averages can be used to save energy and cost and avoid building stress. The human comfort temperature limit is allowed to apply in public display areas in climate class AA, A1, A2. However, it cannot exceed the range in column 3 (ASHRAE, 2019). Setpoints are variable at different periods: seasonal adjustments are given in column 5, and short-term fluctuations are stated in column 6.

2.1.3 Climate Mitigating Strategies

As section 2.1.2 is mentioned, the higher the climate class is required, the more complex the type of control is. Museum climate can be mitigated by improving the building envelope or changing the hygrothermal properties of air via HVAC systems (Ankersmit & Stappers, 2017). Martens (2012) investigated 21 Dutch museums with different quality of envelopes and levels of control to study the effect of the combination of passive design and active design. He concluded that a simple climate system is enough to achieve class B in old buildings, while a more elaborate system is needed to reach a higher class (Martens, 2012). Active design is mainly related to climate systems with functions of ventilation, filtering, heating, cooling, humidification, dehumidification. Passive design on the building level can be done by adding buffering materials, improving performance glazing ratio, insulating the construction (Ankersmit & Stappers, 2017), and only the buffering materials are discussed in section 2.1.3.2.

2.1.3.1 Active Design

The availability of space, reliability and robustness of components, and low energy consumption are the main criteria when climate control concepts are chosen. Museum climate can be directly controlled by a limited climate system, such as a mobile humidifier, mobile dehumidifier, electric heater, etc.

To achieve climate B, A, and AA, full climate control is required. And it is done by the HVAC system that is shown schematically in Figure 2.3

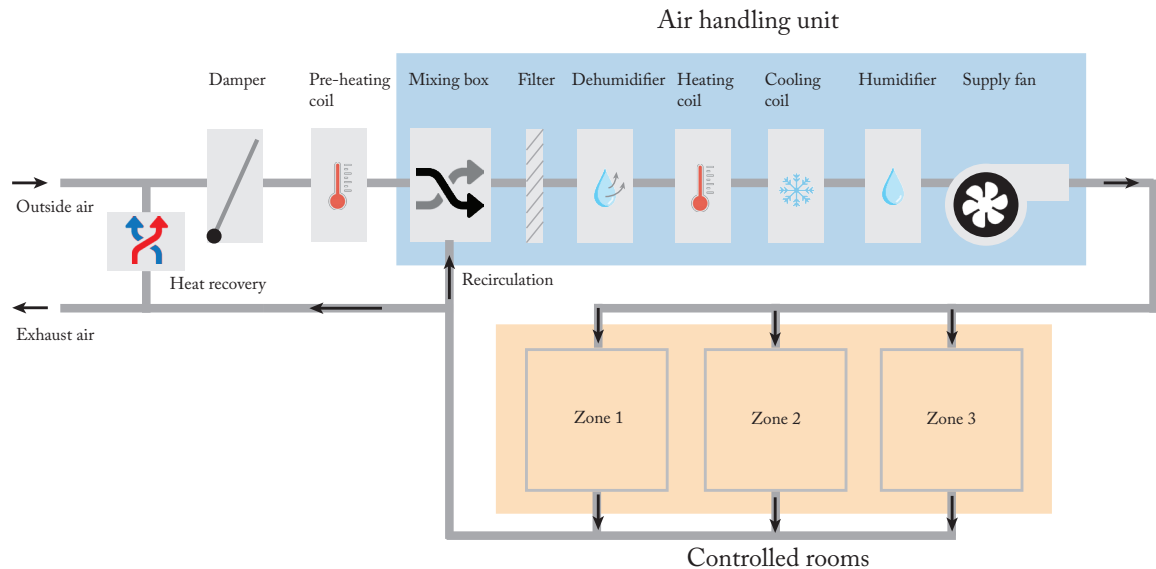


Figure 2.3: *Schematic HVAC system*

Air conditions can be controlled in the HVAC system by changing temperature and humidity ratio. With regards to thermal condition, the air taken from outside is pre-heated at first. Then it goes through the air handling unit where the temperature is regulated by mixing box, heating coil, and cooling coil. A portion of outlet air with higher temperature has heat exchange with inlet air in the heat recovery device where waste heat is reused. As for hygric conditions, the humidity ratio of supply air is changed in the mixing box, dehumidifier, and humidifier. Moreover, the ventilation rate and the percentage of fresh air are controlled by supply fan and damper, respectively. There are sensors that monitor temperature, relative humidity, and CO_2 in the room in order to give feedback to the specific component in the HVAC system. So, the corresponding change in the hygrothermal performance of air occurs, and dynamic climate control is achieved.

2.1.3.2 Passive Design: Buffering Materials

Humidity buffering materials, also known as hygroscopic materials, can reduce relative humidity fluctuation by absorbing or releasing moisture when surrounding hygrothermal conditions varies. Moreover, relative humidity can be maintained at an almost constant level when sufficient hygroscopic materials with small controlled airflow are applied (Ankersmit & Stappers, 2017).

The common hygroscopic materials include wood, paper, clay, limestone, etc. Some of them are already used on construction to stabilize the relative humidity fluctuation. Padfield studied the performance of museums walls made of absorbent materials, and he concluded that wood, cut across the grain, and unfired clay brick are the best buffering material that can be used on construction (Padfield, 1999).

Olalekan and Carey's research showed the effect of hygroscopic construction materials on energy savings. Heating and cooling energy in the optimized HVAC system can be saved by 2 - 3% and 5 - 30%, respectively. While only cooling energy drops by 0 - 20% if there is no control in the HVAC system. Also, there is a 5% reduction in both heating and cooling energy when the ventilation rate is decreased (Osanyintola & Simonson, 2006). According to C. Ferreira, the ventilation rate in maritime temperate climate zones can be minimized to 0.98 h^{-1} if lime mortar, gypsum board, and old oak are made into the finishing of walls, ceiling, and floor were respectively (Ferreira et al., 2020).

2.2 High Capacity Hygroscopic Materials: Silica Gel

Silica gel is an amorphous and porous form of silicon dioxide, and it is produced during the acidification of the solution of sodium silicates (Chang Lara, 2015). And it is one of the high-capacity hygroscopic materials that have been widely used in the display case and desiccant wheel of the HVAC system since it has a larger surface area, larger pores, and excellent dehumidification capacity (Yang et al., 2017).

2.2.1 Types

Silica gel can be classified according to different pore structures. Type A is fine pore silica gel that has a $100 - 1000 \text{ m}^2/\text{g}$ surface area, and the average pore diameter is 2 - 3 nm (White, 2013). Type B is medium pore silica gel that has a $450 - 650 \text{ m}^2/\text{g}$ surface area with an average pore diameter of 4.5 - 7 nm (Chang Lara, 2015). Type C is macro pore silica gel that has a $300 - 400 \text{ m}^2/\text{g}$ surface area, and the average pore diameter is 80 - 125nm (Chang Lara, 2015). Both type A and type C can be used as an absorbent in the cooling system (White, 2013).

Besides, there are four types of silica gel that are specially used in the display case in museums. Type E is mainly used for drying since it works best when RH is between 15% and 35%. While type M is applied to prevent condensation because it always has a large absorption capacity unless RH exceeds 90% (Chang Lara, 2015). The other two types of silica gel are ArtSorb and Prosob whose optimal performance ranges are 60 - 80% and 30 - 60%, respectively.

2.2.2 Properties

The buffering performance of silica gel can be indicated in color and quantified in sorption isotherms and specific moisture reservoir.

2.2.2.1 Color Indication

Blue and orange silica gel are two common types of indicating silica gel that show changes in color when the moisture content is different. In Figure 2.4, blue-pink silica gel turns

from blue to light blue gradually and becomes pink finally when moisture is absorbed, and it is mainly used for the dehumidification of sealed vessels.

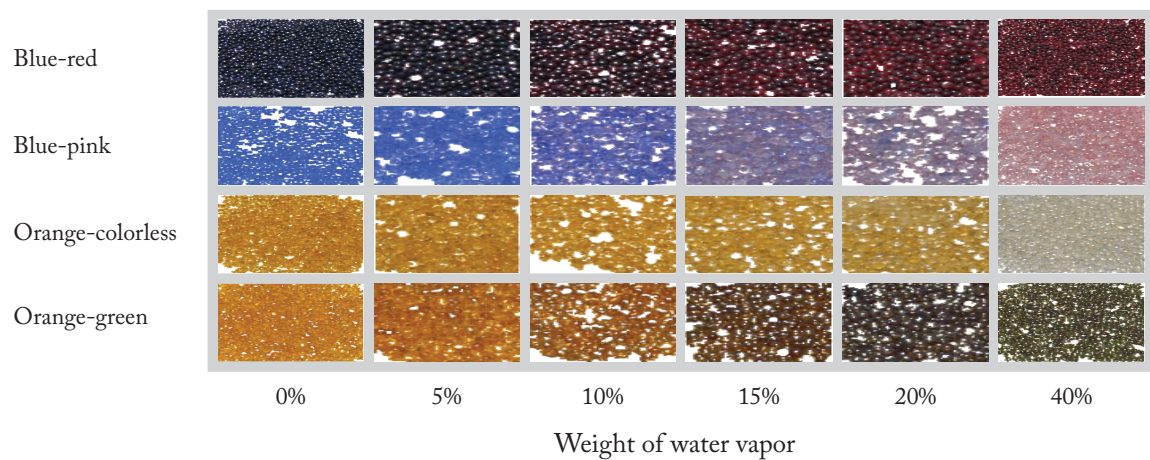


Figure 2.4: *Indicating silica gel (Giebel Adsorbents)*

2.2.2.2 Sorption Isotherms

Equilibrium moisture content (EMC) is the weight of water in the material in equilibrium at certain RH, which is expressed as a percentage of its dry weight (Weintraub, 2002). And the sorption isotherms of three typical silica gel are shown in Figure 2.5, which describes the relationship between EMC and RH. As it is mentioned in section 2.2.1, silica gel E has optimal performance in the low relative humidity range, while ProSorb works better when relative humidity is at medium level, and ArtSorb is more applicable to high humidity conditions.

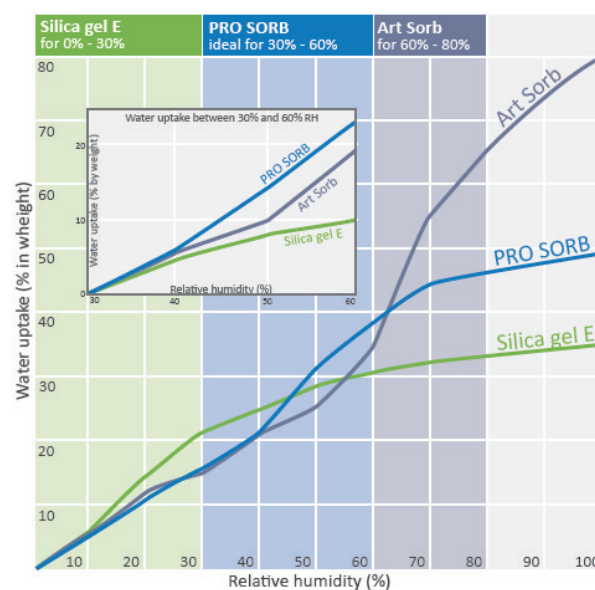


Figure 2.5: *Sorption isotherms of three types of silica gel (Long Life for Art, 2017)*

2.2.2.3 Specific Moisture Reservoir

The moisture buffering capacity of a material is defined by the specific moisture reservoir, which is expressed by M . It means that the amount of water (in grams) that is gained or lost by 1 kilogram of silica gel with each 1% change in RH (Thomson, 1977). So, it is also can be regarded as the slope of sorption isotherms. However, there is some difference in the amount of water between sorption and desorption conditions at the same RH level, and silica gel has better buffering effect when RH increases, compared with a decrease in RH (Weintraub, 2002). That is called hysteresis, and M_H is corrected value with consideration of hysteresis.

M of four types of silica gel are shown in Table 2.2

Table 2.2: *Specific moisture reservoir at 20 °C (Tétreault & Bégin, 2018)*

Type of silica gel	M: 50 ± 10% RH around 50%	M: 20% → 30% Keep RH low	M: 60% → 50% Keep RH high
Type A	1.93 ± 0.44	5.48 ± 0.40	1.47 ± 0.16
Orange silica gel	1.16 ± 0.26	4.92 ± 0.59	0.94 ± 0.14
ProSorb	5.42 ± 1.32	4.37 ± 0.10	4.25 ± 0.38
ArtSorb	4.04 ± 0.80	2.84 ± 0.47	4.18 ± 0.49

2.2.3 Moisture Transfer in the Packed Bed

The packed bed of silica gel can be assumed as the hygroscopic material since the airflow can go through the space between beads. As Figure 2.6 illustrates, moisture diffuses inside the beads. There are both diffusion and advection in the pore space. Also, moisture transfer occurs between the surface of beads and air in the pore space.

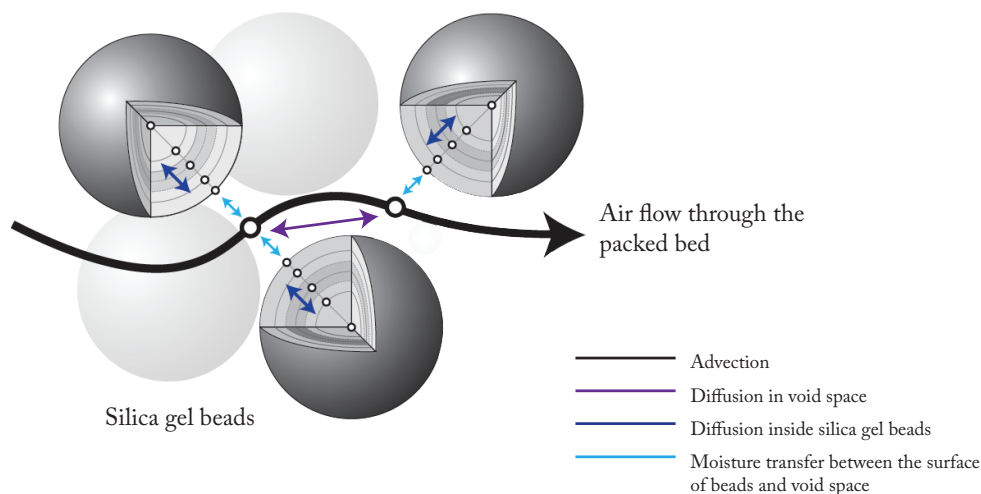


Figure 2.6: *Moisture transfer in the packed bed (Chang Lara, 2015)*

2.2.3.1 Moisture Transfer Inside Beads

According to Hagentoft (2001), it follows the basic mass transfer mechanism, and the equation is:

$$\nabla \cdot \vec{g} = \frac{\partial w}{\partial t} \quad (2.1)$$

Where \vec{g} is the mass flux density [kg/m²s]. w is the moisture content [kg/m³].

The mass transfer can be in the form of water vapor and liquid:

$$\vec{g} = \vec{g}_l + \vec{g}_v \quad (2.2)$$

Where \vec{g}_l is the mass flux density of liquid transport. \vec{g}_v is the mass flow density of water vapor transport.

If only the vapor transfer is taken into account, the equation is defined by Andersson (1985):

$$\vec{g}_v = \delta_p p_{sat} \frac{1}{\xi} \nabla w - \delta_p p_{sat} \left(\frac{\partial \phi}{\partial t} \Big|_{w,fix} + \frac{M_w L_{lv}}{RT^2} \right) \nabla T \quad (2.3)$$

Where δ_p is the moisture permeability [kg/m·Pa·s]. p_{sat} is the water vapor pressure at saturation (Pa). ξ is the specific hygroscopic moisture capacity [kg/m³], which is defined as the slope of sorption isotherm at certain relative humidity. ϕ is the relative humidity. M_w is the molar weight of water [g/mol]. L_{lv} is the specific latent heat of vaporization [J/kg].

In Carlos's thesis, ∇T was neglected since the effect of moisture content gradient is much larger than that of a temperature gradient. Besides, the mass flow by liquid transport is neglected as it is mentioned above. The equation of mass transfer inside beads is:

$$\nabla \cdot (\delta_p p_{sat} \frac{1}{\xi} \nabla w) = \frac{\partial w}{\partial t} \quad (2.4)$$

2.2.3.2 Moisture Transfer between Void Space and Surface of Beads

Carlos (2015) defined this gel-air interaction by assuming that the mass transfer is independent of diffusion in each medium, and moisture content is used as the dependent variable:

$$\beta_{c-g} A_r (w_a - w_{a-g}) \quad (2.5)$$

β_{c-g} is the moisture transfer coefficient between void space and surface of beads, and it was

defined that the value is 0.024 m/s based on the Lewis relationship (Chang Lara, 2015). A_r is the surface area where air and beads interact [m²]. w_{a-g} is the moisture content of the air right at the silica gel surface [kg/m³], and it was defined:

$$w_{a-g} = aw_a + b \quad (2.6)$$

Where w_a is the moisture content of pore space [kg/m³]. a is the slope of the left graph of Figure 2.7. b is the y-intercept of the left graph of Figure 2.7

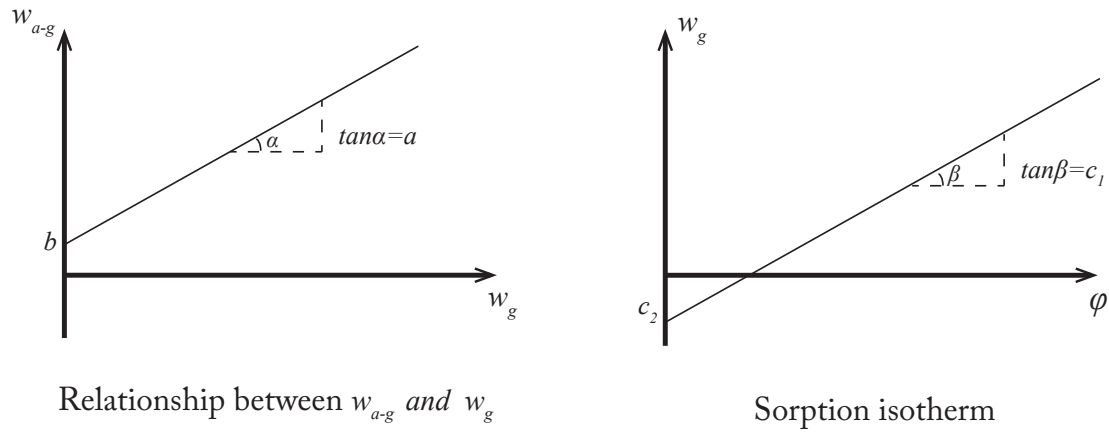


Figure 2.7: Relationship between the moisture content of silica gel beads and that of air right at the surface(left). Sorption isotherm of silica gel(right).

According to the sorption isotherm of Figure 2.7, the moisture content of silica gel beads can be calculated:

$$w_g = c_1 \phi + c_2 \quad (2.7)$$

Where c_1 is the slope of sorption isotherm. c_2 is the y-intercept of sorption isotherm.

The relative humidity is calculated based on ideal gas law:

$$\phi = \frac{R_v T}{p_{sat}} w_{a-g} \quad (2.8)$$

By combining equation 2.6, 2.7, and 2.8, the mass transfer equation between void space and the surface of beads is:

$$w_{a-g} = aw_a + b = \frac{p_{sat}}{R_v T c_1} w_g + \frac{p_{sat}}{R_v T c_1} c_2 \quad (2.9)$$

2.2.3.3 Moisture Transfer in Void Space

Moisture transfer includes both diffusion and advection in void space. The diffusion also follows the same mechanism as that inside silica gel beads:

$$\nabla \cdot (\delta_p p_{sat} \frac{1}{\xi} \nabla w) = \frac{\partial w}{\partial t} \quad (2.10)$$

2.2.4 Application in Display Case

T treault (2003) defined the equation that calculated the amount of silica gel needed in the case:

$$Q_{gel} = \frac{C_{eq} D V_{case} N t_{min}}{M_H F} \quad (2.11)$$

Where Q_{gel} is the quantity of the required silica gel. C_{eq} is the concentration of water vapor at equilibrium. D is the difference between the RH in the display case and outside RH. V_{case} is the volume of the display case. N is the air exchange rate per day. t_{min} is the minimum days that the exhibition should be preserved under the acceptable range of RH. F is the maximum acceptable range of RH fluctuation in the display case.

It was calculated that 4kg/m² ArtSorb silica gel is needed when the difference RH between inside and outside is 10%, and the acceptable range is 45 - 55% in the display case (Weintraub, 2002).

Carlos (2015) studied the application of ProSorb silica gel in the display case. The performance of the display case does not depend on one parameter. On the contrary, it is dominated by the change of outside relative humidity and temperature, the air exchange rate, the time domain, and the moisture transfer coefficient. In terms of the effect of the outside climate on the display case, it is related to the air exchange rate, and the effect becomes significant when the value is 1.33 per day. However, the temperature can affect the display case without air exchange. However, the air exchange rate has a larger influence (Chang Lara, 2015).

2.3 Combined Heat and Moisture Transfer in the Porous Materials

Water is stored in porous materials in the form of liquid and vapor. Its moisture transfer mechanism is discussed in section 2.2. When it is assumed that there is only diffusion as the main transport approach, the heat is only transfer by the conduction accordingly. Based on the Fourier's law, the conduction equation in the porous materials is:

$$\vec{q} = -\lambda \nabla T \quad (2.12)$$

Where \vec{q} is the heat flux [W/m²]. λ is the thermal conductivity of porous materials [W/m·K].

Consistent with mass flux in section 2.2.3.1, the heat is transferred in the form of sensible heat and latent heat. The former occurs in the vapor and the latter occurs in the liquid. Their equations are:

$$\vec{q}_l = \vec{g}_l h_l \quad (2.13)$$

$$\vec{q}_v = \vec{g}_v h_v \quad (2.14)$$

Where \vec{q}_l is the heat flux transferred by liquid [W/m²]. \vec{q}_v is the heat flux transferred by vapor [W/m²]. h_l is the enthalpy of liquid water [J/kg]. h_v is the enthalpy of water vapor [J/kg].

Van Belleghem (2013) assumed that the h_l and h_v can be proportional to temperature when the heat capacity is close to constant. The equation 2.13 and 2.14 can be rewritten as:

$$\vec{q}_l \approx \vec{g}_l C_l T \quad (2.15)$$

$$\vec{q}_v \approx \vec{g}_v (C_v T + L_{lv}) \quad (2.16)$$

Where C_l is the heat capacity of liquid water [J/K]. C_v is the heat capacity of water vapor [J/K]. T is the temperature [K]. L_{lv} is the specific latent heat of vaporization of water [J/kg].

The total energy stored in the porous materials includes the energy stored in the liquid water, the energy stored in the water vapor, and the energy stored in the solid materials. The equation is:

$$(\rho_s C_s + \rho_l C_l + \rho_v C_v) \frac{\partial T}{\partial t} + C_l T \frac{\partial \rho_l}{\partial t} + C_v T \frac{\partial \rho_v}{\partial t} = \nabla \cdot (\lambda \nabla T - C_l T \vec{g}_l - (C_v T + L_{lv}) \vec{g}_v) \quad (2.17)$$

Where ρ_s is the density of solid materials [kg/m³]. ρ_l is the density of liquid water [kg/m³]. ρ_v is the density of water vapor [kg/m³].

2.4 National Holocaust Museum in Amsterdam

National Holocaust Museum is built in memory of the murder of 6 million Jews and 104,000 victims from the Netherlands. It is currently situated in the former Reformed Kweekschool at the Plantage Middenlaan, which is an important place of memory, resistance and, salvation. (Schrijver & Bijvoet).

The floor plan of the museum is shown in Figure 2.8. The front four-story building is connected with the back building by the corridor where visitors can see a patio. There are two exhibition rooms on the ground floor of the front building. The right one is used as the study object of the thesis. If visitors turn right and go straight after entering, a small lecture room where the documentary is played is seen. There are still some collections preserved in the back building where some flexible walls are displayed.

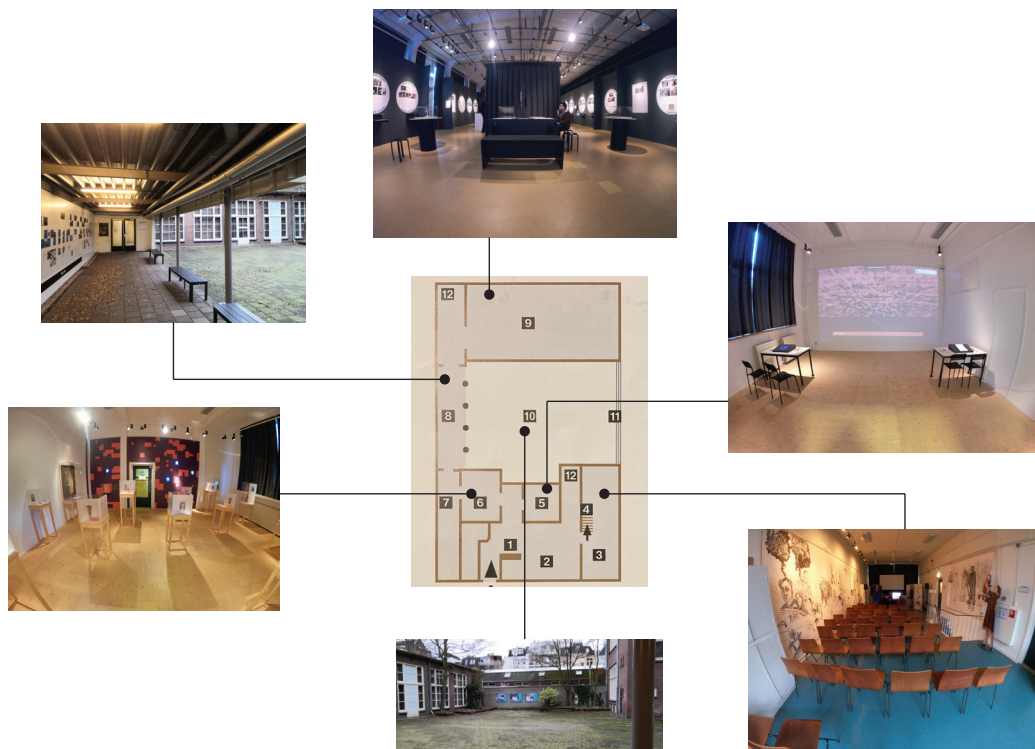


Figure 2.8: *Floor plan of the National Holocaust Museum in Amsterdam*

In terms of construction and climate system, the facade is made of masonry, and the window is made of single glazing, which is not well-insulated. Only radiators are installed in some rooms, and no mechanical ventilation is found in the front building.



Figure 2.9: *The facade of the front building (left). Details on the window (right).*

2.5 Conclusions

The previous research illustrated that the hygroscopic materials used on the surface of construction contribute to energy savings in museums. Moreover, the ventilation flow rate can be minimized to 0.98^{-1} with these materials on the finishing of the walls, ceiling, and floor. The investigation of the silica gel, as a kind of high capacity hygroscopic materials, shows that the RH can be stabilized between 45% and 55% with 4kg/m^2 ArtSorb silica gel used in the display case. Therefore, it is valuable to study whether it can be used on the level of the room and its effect on the hygrothermal performance in the exhibition space and energy demand.

The theory about combined heat conduction and moisture diffusion in the porous materials was completely researched in the past. So, the combined advective heat and moisture transfer in the silica gel needs to study in this thesis.

By visiting the National Holocaust Museum, it is observed that the quality of the facade is not good enough to have a stable indoor climate. Therefore, a more insulated building envelope with more precise control systems is required to achieve climate class A1 in the exhibition space.

3

Feasibility Study

3.1 Description of Model 1.0

3.2 Definition of Variables

3.3 Division of Groups

3.4 Simulation Results

3.5 Analysis of Parameters

3.6 Conclusions

3 Feasibility Study

In order to check the capability of the silica gel. A simple model followed with sensitivity analysis will be introduced in this chapter. Firstly, the model is described based on the mass balance equation. Then four independent parameters are defined for analysis. Finally, Matlab is used to simulate the different scenarios for analysis.

3.1 Description of Model 1.0

For simplification, the thermal condition is eliminated. The room is ventilated by the constant airflow with constant humidity ratio. Only the mass of air and silica gel are considered inside the room, and they are combined into one node based on thermal dynamic equilibrium as Figure 3.1 shows. The moisture loads are mainly produced by people, which follows the periodic function.

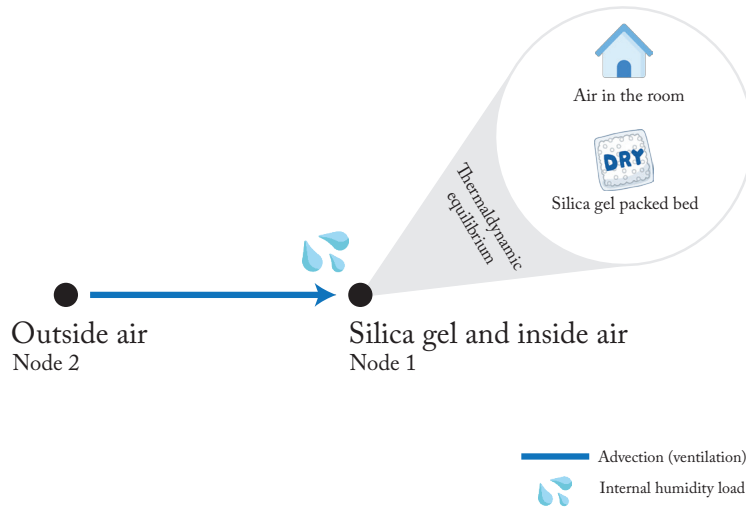


Figure 3.1: Assumption and mass transfer network of model 1.0

Both air and silica gel in the room contain moisture, and the mass balance equation can be written as:

$$\frac{d(m_a x_r + m_g x_g)}{dt} = \dot{m}(x_s - x_r) + G_v(t) \quad (3.1)$$

\dot{m} is the mass flow rate [kg/s]. m_a is the mass of air [kg]. m_g is the mass of silica gel [kg]. x_r is the humidity ratio of air in the room. x_g is the humidity ratio of the silica gel. x_s is the humidity ratio of supply air. $G_v(t)$ is the internal humidity load [kg/s].

Only one variable in the mass balance equation can be solved, so the formula is rewritten based on the correlation of the humidity ratio of silica gel and air. It is assumed that the moisture isotherms of silica gel and air are linear under 20 °C in Figure 3.2.

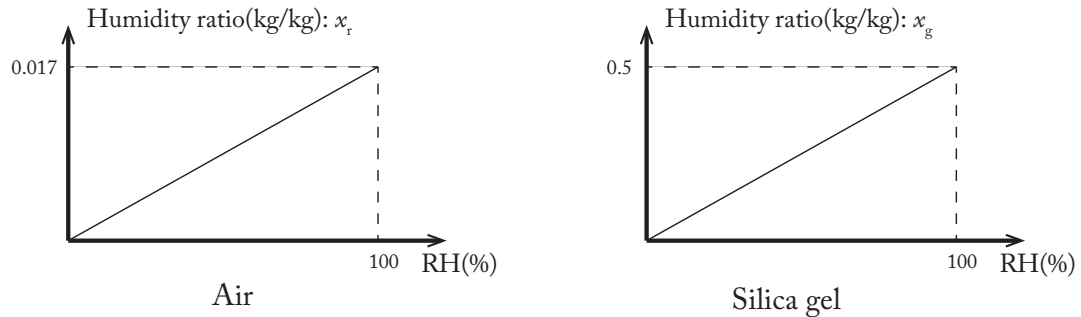


Figure 3.2: *The simplified moisture sorption isotherm of air and silica gel*

So, the relation between the humidity ratio of air and silica gel can be expressed:

$$x_g = \frac{x_r}{c} \quad (3.2)$$

$$c = \frac{x_{r, sat}}{x_{g, sat}} = \frac{0.017}{0.5} = 0.034 \quad (3.3)$$

Where c is the correlation factor between the humidity ratio of air and silica gel. $x_{r, sat}$ is the humidity ratio of air at saturation. $x_{g, sat}$ is the humidity ratio of silica gel at saturation. Now the humidity ratio on both sides of the equation can be expressed as one variable.

$$(m_a + \frac{m_g}{c}) \frac{dx_r}{dt} = \dot{m}(x_s - x_r) + G_v(t) \quad (3.4)$$

3.2 Definition of Variables

3.2.1 Dependent Variables

There are four independent variables and two dependent variables in the analysis, and independent variables are as follows:

1. Amount of silica gel
2. Ventilation flow rate
3. Period
4. Internal humidity load

3.2.1.1 Amount of Silica Gel

It is assumed that the silica gel beads are in the package and evenly spread with the sufficiently large surface area in the exhibition room, which ensures that there is excellent moisture transfer between air and silica gel. As Table 3.1 shows, the unit is kilogram per floor area and it is written in the form of the volume of silica gel in the Matlab model.

Table 3.1: *Amount of silica gel*

Amount of silica gel				Unit
0	2.5	5	10	kg/m ²
0	77.575	155.15	310.3	kg
0	0.129	0.259	0.517	m ³

3.2.1.2 Ventilation Flow Rate

The ventilation rate only represents the mechanical ventilation. The exhibition room always has a continuous ventilation rate with a constant relative humidity ratio. As Table 3.2 shows, the unit is liter per second per floor area, and it is written in the form of the mass flow rate in the Matlab model.

Table 3.2: *Ventilation flow rate*

Ventilation flow rate				Unit
0.5	1	2	4	L/s/m ²
0.019	0.037	0.074	0.149	kg/s

3.2.1.3 Internal Humidity Load

Moisture loads are produced by people in this model. Occupancy of 8 m²/person, 4 m²/person, and 2 m²/person are selected. The moisture production rate of one person indoor on average is 0.4 pounds per hour, which is equal to 5×10^{-5} kilogram per second. With the occupancy and floor area, the moisture production rate of three kinds of occupancy in the exhibition room is calculated, respectively in Table 3.3.

Table 3.3: *Humidity load*

Humidity load			Unit
0.625	1.25	2.5	$\times 10^{-5}$ kg/s/m ²
19.394	38.788	77.575	$\times 10^{-5}$ kg/s

3.2.1.4 Period

The moisture production rate does not keep the same in reality because of the change in occupancy. So it is assumed that the occupancy follows the simple periodic function, which simulates two scenarios with a fixed number of people and no person in the room, and it is the same with the moisture production rate in Figure 3.3. The period of 0.25h, 1h, and 4h are selected in Table 3.4.

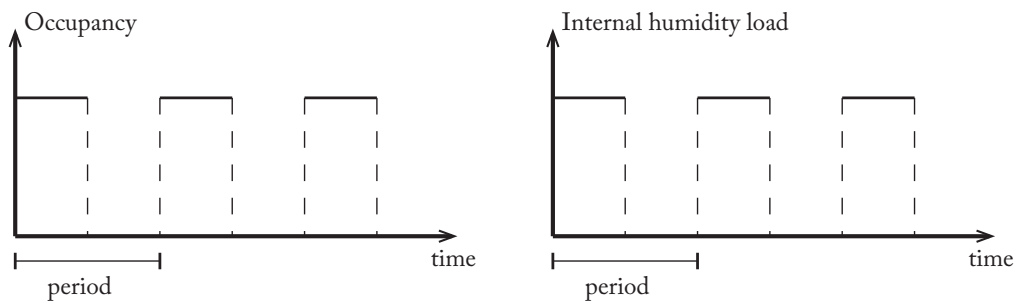


Figure 3.3: *Periodic moisture production*

Table 3.4: *Period*

Period			Unit
0.25	1	4	h
900	3600	14400	s

3.2.2 Dependent Variables

The dependent variables are average relative humidity (\overline{RH}) and the fluctuation of relative humidity (ΔRH) when the system is in the equilibrium.

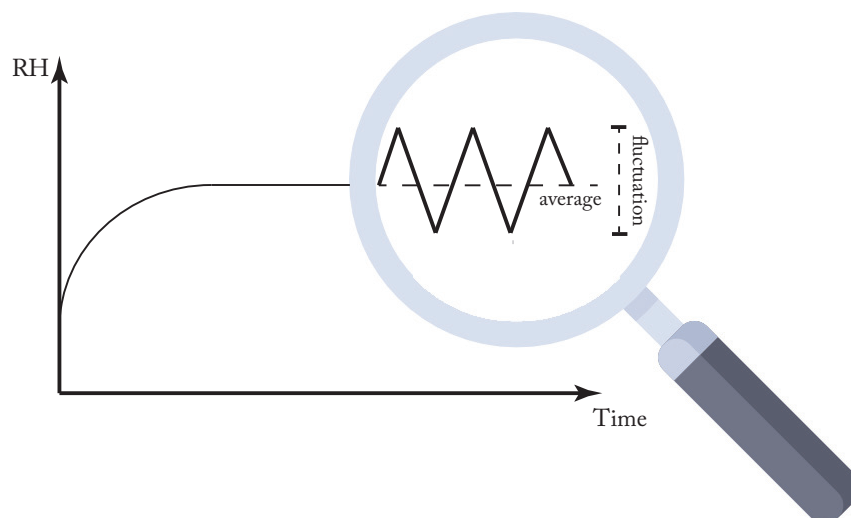


Figure 3.4: *The illustration of dependent variables*

3.3 Division of Groups

According to Table 3.1, Table 3.2, Table 3.3, and Table 3.4, there are 144 kinds of combination of variables which are divided into four groups based on the amount of silica gel, as Figure 3.5 shows. The main variable is the amount of silica gel, and there will be no silica gel in the control group, namely group one.

Table 3.5: *Division of groups*

Group	Amount of silica gel (kg/m ²)
1	0
2	2.5
3	5
4	10

As Figure 3.5 shows, each group has 36 combinations, and the scenarios are simulated by changing the ventilation rate, moisture production rate, and the period within the group.

Group 1/2/3/4

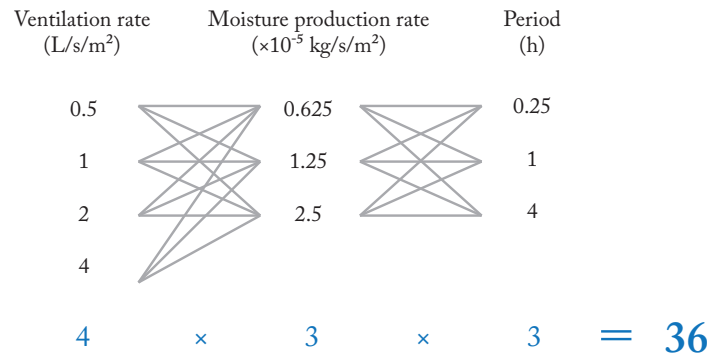


Figure 3.5: *The combination of variables for each group*

3.4 Simulation Results

144 simulation results are summarized in the figures (3.6 - 3.21), and more specific results about every combination are written in the appendix. Figures illustrate how the relative humidity in four groups vary with the change of moisture production rate and period under the condition of different ventilation rate. The left and right sides of every figure show the fluctuation and average value, respectively. Since the model is relatively simple, some combinations give unrealistic values that show the relative humidity is above 100% due to the lack of boundary conditions in this simple model. Since the aim of this model is to estimate the buffering effect mathematically instead of simulating the real scenarios, the data above 100% is still used for analysis.

3.4.1 Group 1: 0 kg/m² Silica Gel

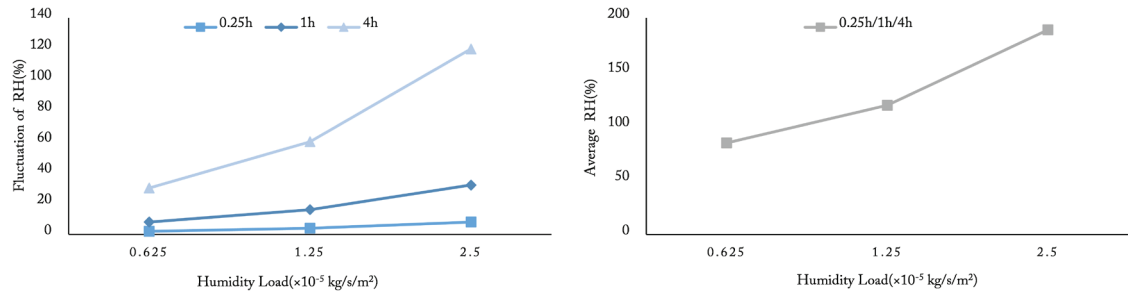


Figure 3.6: 0 kg/m² silica gel, ventilation rate=0.5 L/s/m²

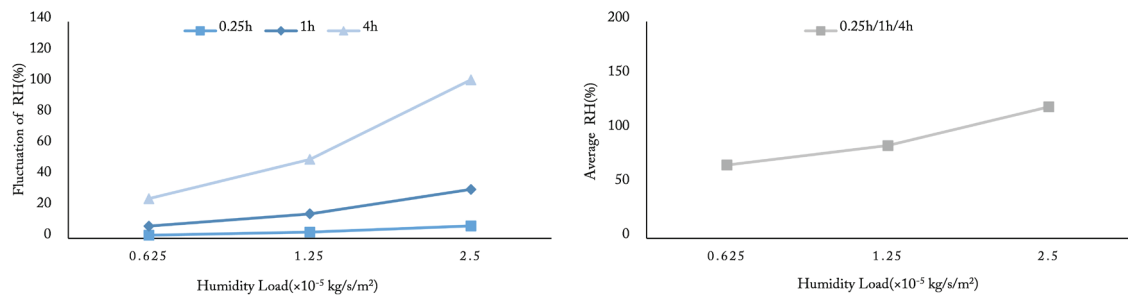


Figure 3.7: 0 kg/m² silica gel, ventilation rate=1 L/s/m²

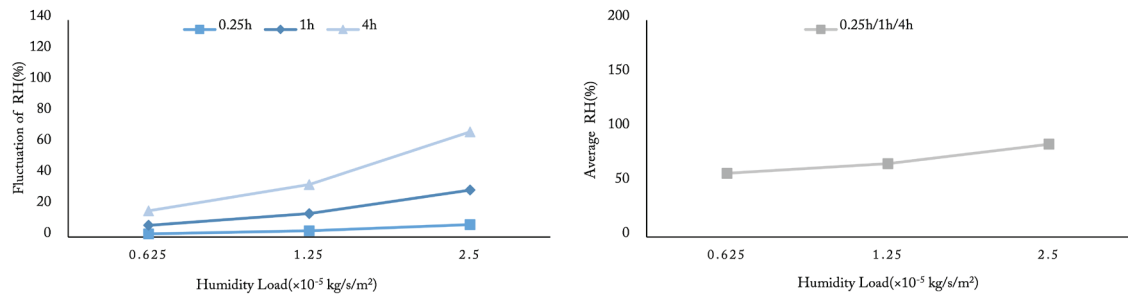


Figure 3.8: 0 kg/m² silica gel, ventilation rate=2 L/s/m²

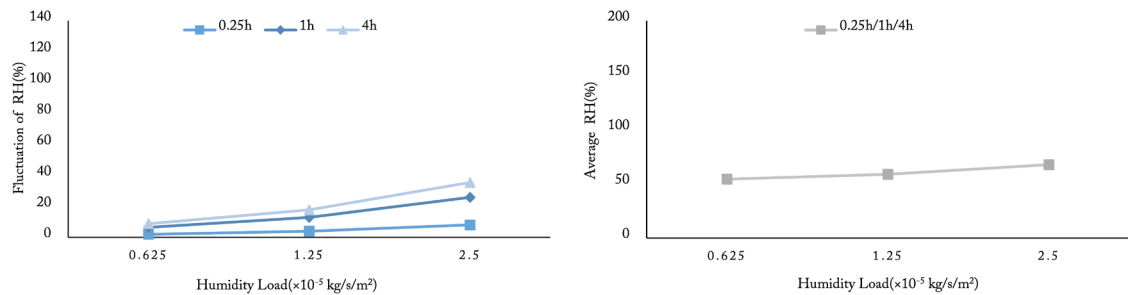


Figure 3.9: 0 kg/m² silica gel, ventilation rate=4 L/s/m²

3.4.2 Group 2: 2.5 kg/m² Silica Gel

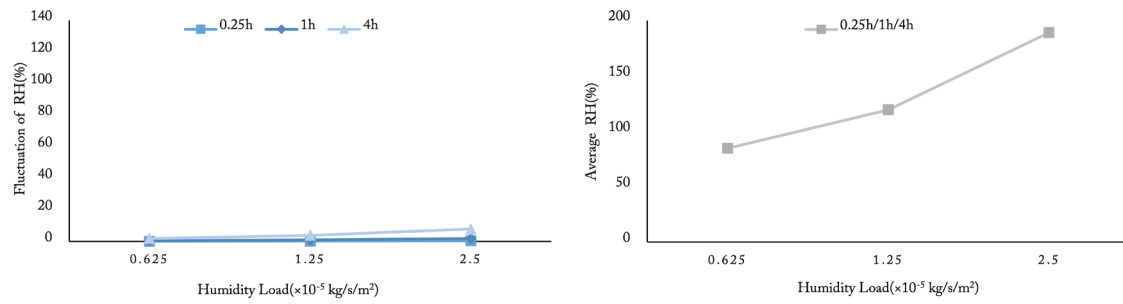


Figure 3.10: 2.5 kg/m² silica gel, ventilation rate=0.5 L/s/m²

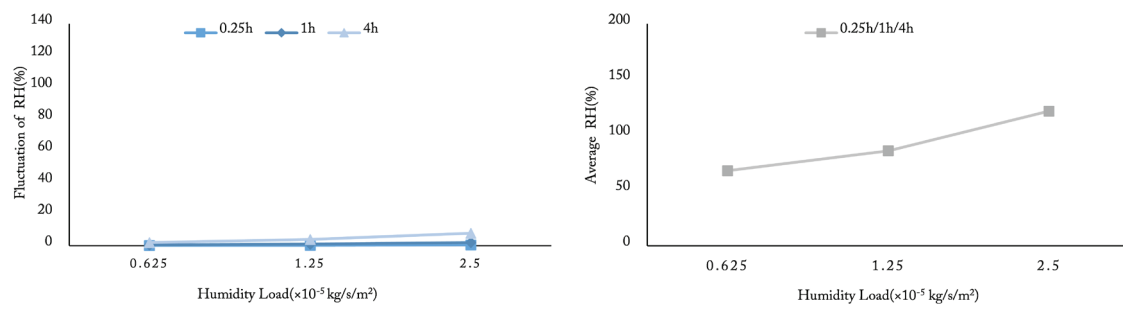


Figure 3.11: 2.5 kg/m² silica gel, ventilation rate=1 L/s/m²

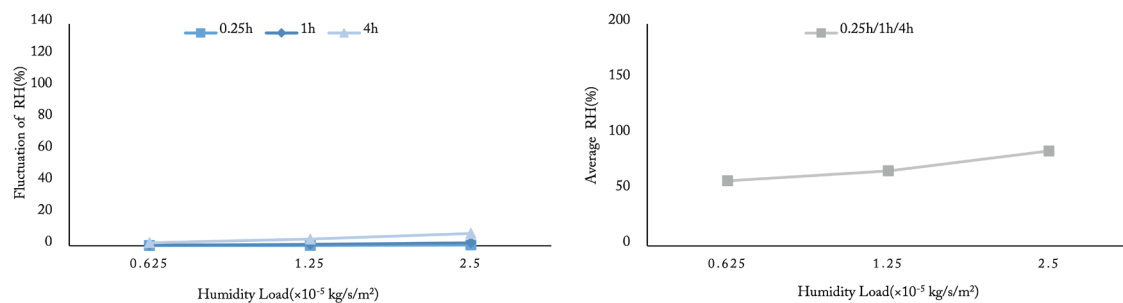


Figure 3.12: 2.5 kg/m² silica gel, ventilation rate=2 L/s/m²

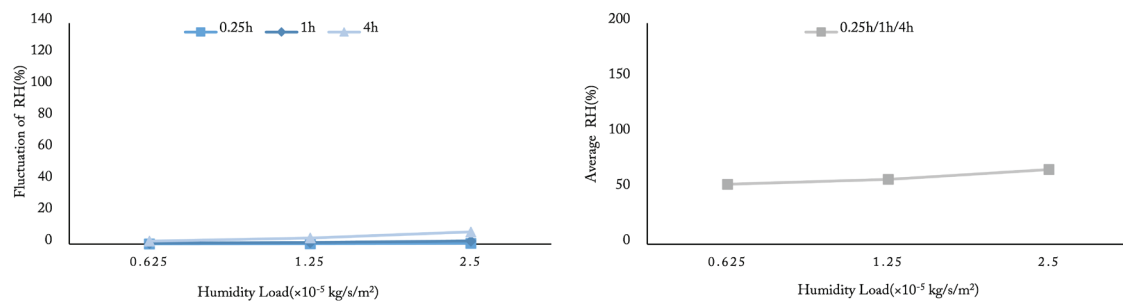


Figure 3.13: 2.5 kg/m² silica gel, ventilation rate=4 L/s/m²

3.4.3 Group 3: 5 kg/m² Silica Gel

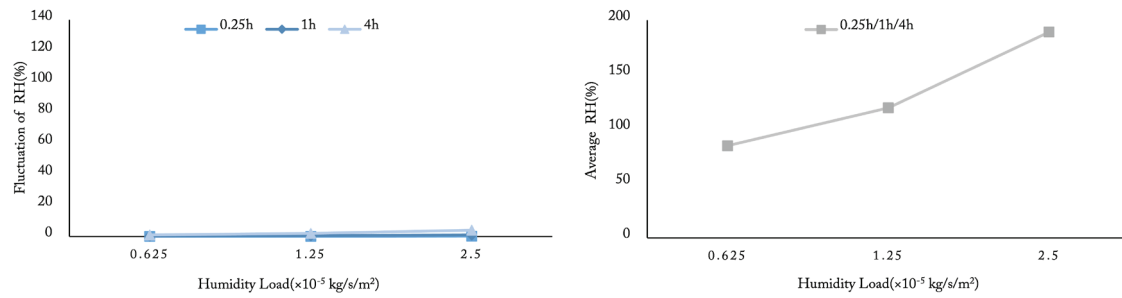


Figure 3.14: 5 kg/m² silica gel, ventilation rate=0.5 L/s/m²

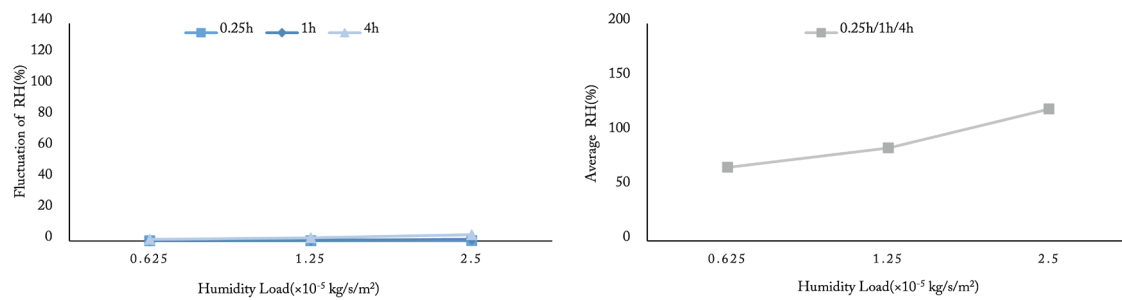


Figure 3.15: 5 kg/m² silica gel, ventilation rate=1 L/s/m²

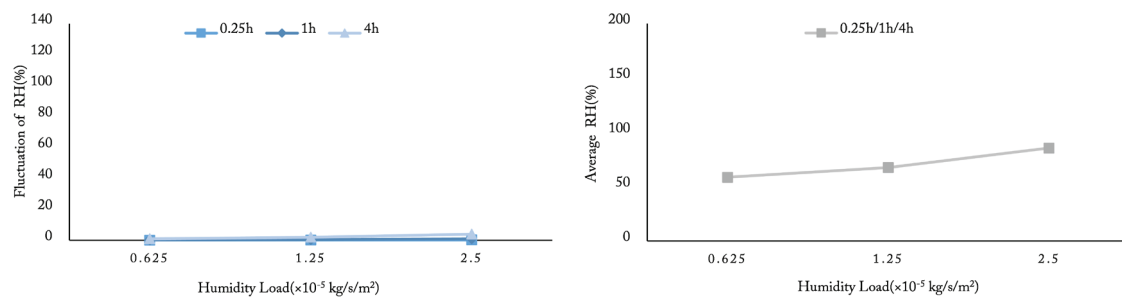


Figure 3.16: 5 kg/m² silica gel, ventilation rate=2 L/s/m²

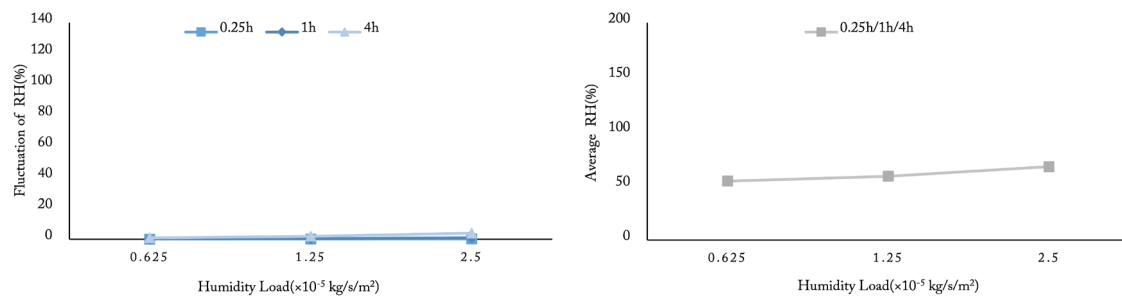


Figure 3.17: 5 kg/m² silica gel, ventilation rate=4 L/s/m²

3.4.4 Group 4: 10 kg/m² Silica Gel

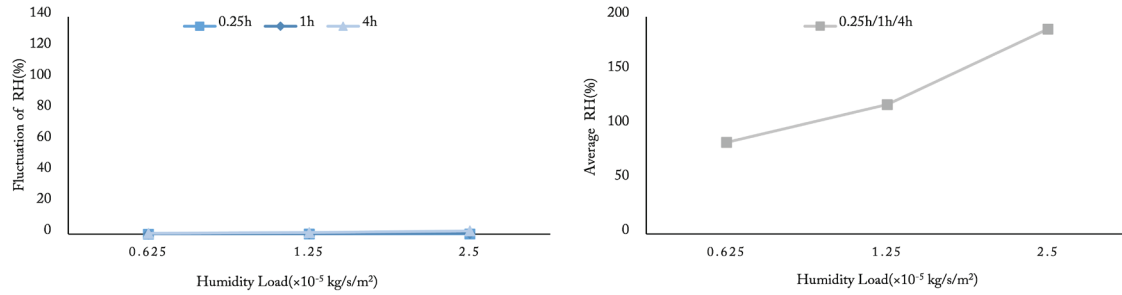


Figure 3.18: 10 kg/m² silica gel, ventilation rate=0.5 L/s/m²

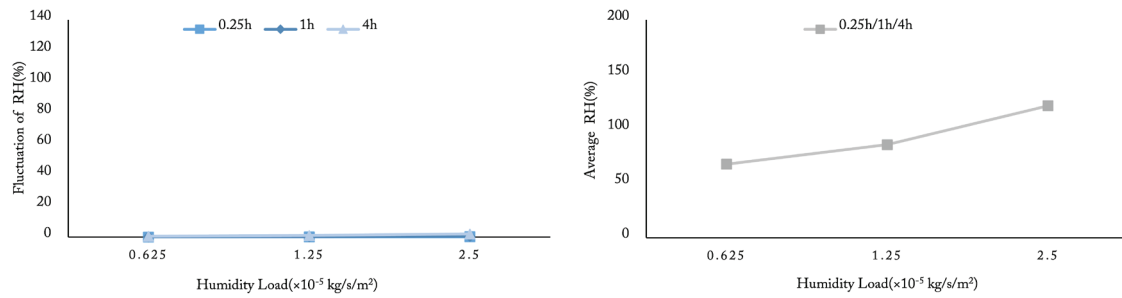


Figure 3.19: 10 kg/m² silica gel, ventilation rate=1 L/s/m²

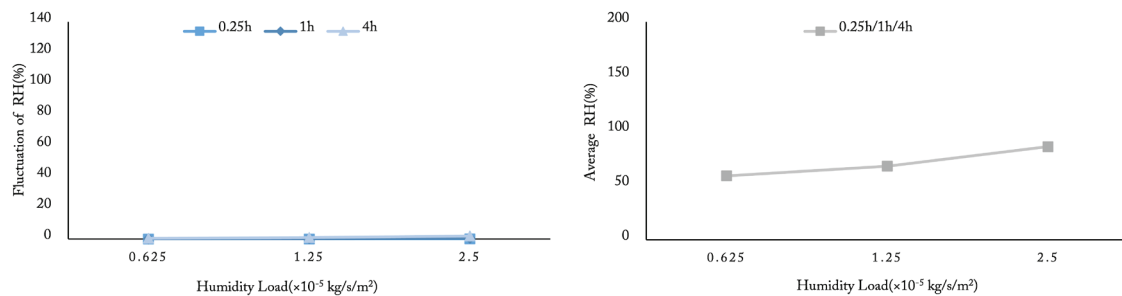


Figure 3.20: 10 kg/m² silica gel, ventilation rate=2 L/s/m²

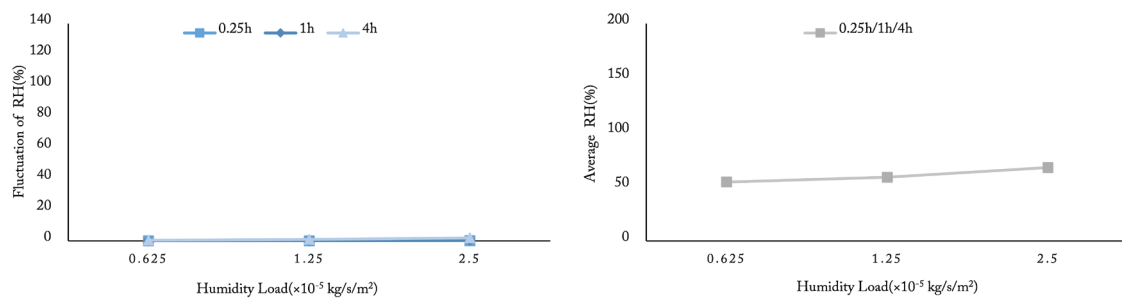


Figure 3.21: 10 kg/m² silica gel, ventilation rate=4 L/s/m²

3.5 Analysis of Parameters

3.5.1 Amount of Silica Gel

The average \overline{RH} and ΔRH of every group are calculated in Table 3.6 and Table 3.7, and the silica gel shows the excellent buffering effect which reduces the fluctuation of relative humidity sufficiently as it is expected. The fluctuation decreases to 1.72% when 2.5 kg/m^2 silica gel is used, compared with the scenario when there is no silica gel, and it is considered as the optimal amount. While the silica gel has no influence on the average relative humidity.

Table 3.6: *Average ΔRH of every group*

Group	ΔRH (%)
1	16.80
2	1.72
3	0.88
4	0.45

Table 3.7: *Average \overline{RH} of every group*

Group	\overline{RH} (%)
1	70.03
2	70.03
3	70.03
4	70.03

3.5.2 Ventilation Flow Rate

The ventilation rate plays a key role in the reduction of both fluctuation and average values of relative humidity when there is no silica gel in the room. With the application of silica gel, the ventilation rate only has a negligible reduction effect on the fluctuation. However, it still has an impact on the decrease of average relative humidity. As Figure 3.22 shows, ventilation is more capable of reducing the average relative humidity when the moisture production is higher ($1.25 \times 10^{-5} \text{ kg/s/m}^2$ and $2.5 \times 10^{-5} \text{ kg/s/m}^2$).

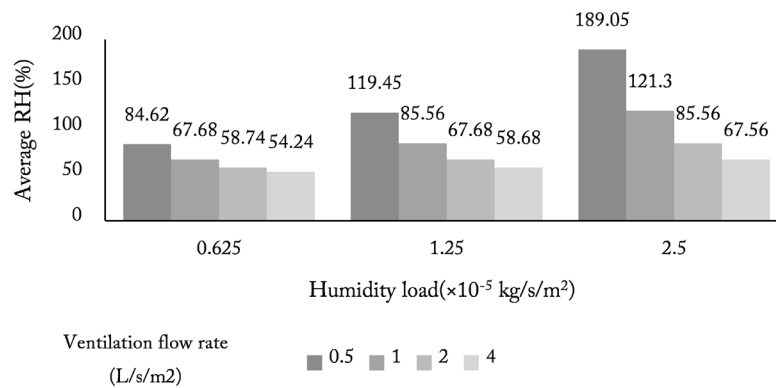


Figure 3.22: *The reduction effect on average relative humidity with different ventilation and moisture production rate*

3.5.3 Internal Humidity Load

Both fluctuation and average values go up with the rise of moisture production rate, and they show a faster upward trend in the higher range of moisture production rate. With the amount of silica gel increasing, the fluctuation humidity load hardly rises even if the humidity load becomes five times larger than the smallest value.

3.5.4 Period

The left side of the figures in the last section shows that the fluctuation of relative humidity increases by around four times with the fourfold increase of period. However, it does not affect the average relative humidity due to the fact that three curves always coincide in the right side of figures (3.6 - 3.21)

3.6 Conclusions

The feasibility study shows that silica gel is capable of stabilizing the relative humidity. Its buffering effect is also influenced by other independent variables. Based on the analysis in the last section, the application of silica gel is able to reduce the fluctuation of relative humidity from 16.80% to 1.72% with 2.5 kg/m² silica gel. With the increase in amount of silica gel, the influence does not improve a lot. The optimal amount of silica gel is equal to around 0.1% of room volume. As for the area of one exhibition room (30.19m²) in the National Holocaust Museum, 0.126m³ silica gel can be used to stabilize the relative humidity. Besides, it shows that there is potential for minimizing ventilation rate with the assistant of silica gel. However, it is still necessary to use mechanical ventilation to get the desired average relative humidity. It suggests that the combination of two measurements will give an ideal relative humidity value in the exhibition space.

4

Model Development

4.1 Description of Model 2.0

4.2 Description of Model 3.0

4.3 Summary of Two Models

4 Model Development

In the last chapter, model 1.0 shows that silica gel can stabilize the relative humidity effectively. It is unknown whether it is still effective when more realistic thermal conditions are included. In this chapter, two extended models are created. Both of them consist of the thermal part, the hygric part, and the air handling unit part.

4.1 Description of Model 2.0

The model of the exhibition room with the silica gel packed bed is made of thermal part, hygric part, and AHU part. The finite difference method is used for dynamic simulation. In every step simulation, the energy balance is solved to get the temperature and mass balance is solved to get vapor density, then the saturation vapor pressure at a certain temperature is calculated, which couples two models to calculate the relative humidity in the room.

4.1.1 Thermal Part

One thermal room model was developed and validated in previous research (van Unen, 2019), and it was referred and modified to match the existing case. There are 27 nodes in this model, and they are numbered in Figure 4.1. All the construction is modeled by node 1 to 24, and each element contains four nodes that represent three layers. In terms of the facade, windows are not modeled as independent nodes, and only the wall is taken into account since the thermal mass of glazing is relatively small. But the solar radiation through the window is still considered because it quite affects the air temperature. The air in the room and silica gel packed bed are combined into node 25, which assumes their temperature is always the same. Node 26 and 27 are two fixed nodes that model the air from AHU and outside, respectively.

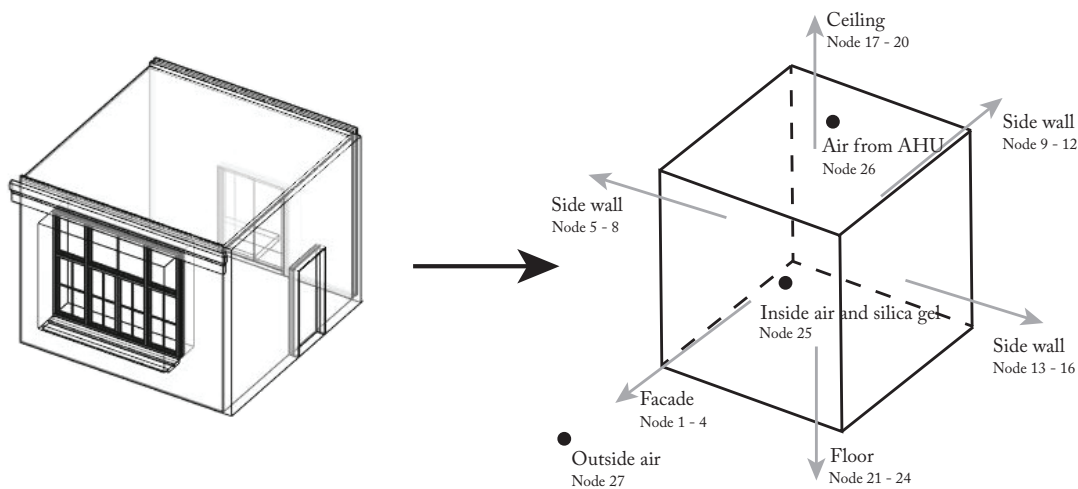


Figure 4.1: Definition of construction and nodes in the thermal

Figure 4.2 illustrates the heat transfer between each node with different lines, which includes conduction, radiation, and convection. The façade is taken as an example to show the connection with other construction and air, and a similar heat transfer network is omitted in the diagram. In addition, the heat from installation and all the internal heat loads are only added to the inside air node. The dependent variable is the temperature.

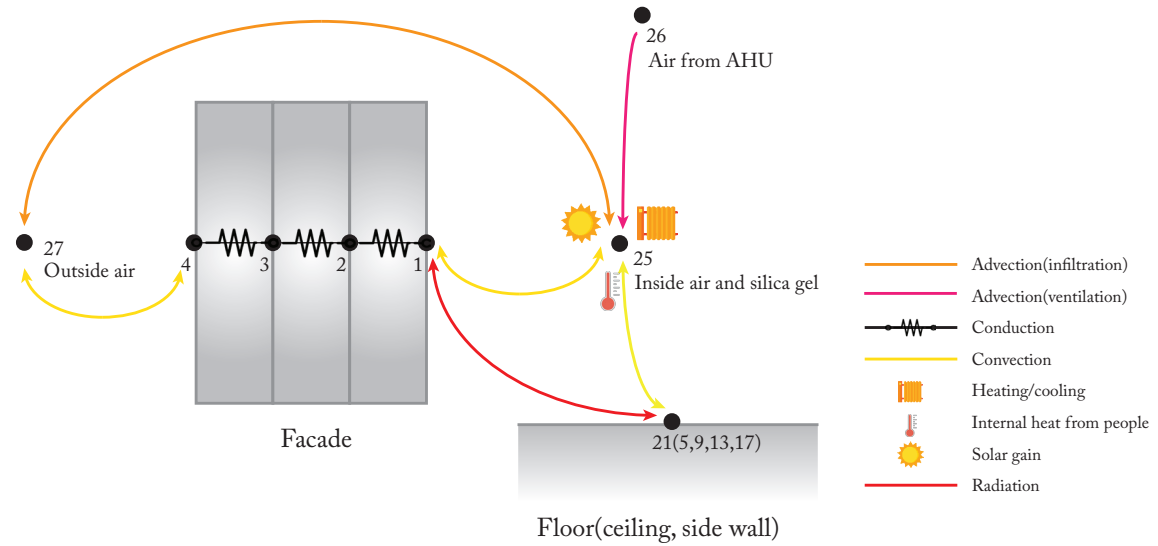


Figure 4.2: Heat transfer network of model 2.0

According to the heat transfer diagram, node 25 is taken as an example, and its energy balance can be written as:

$$\begin{aligned} \rho_a V_r c_a \frac{dT_{25}}{dt} = & \alpha_c A_1 (T_1 - T_{25}) + \alpha_c A_5 (T_5 - T_{25}) + \alpha_c A_{13} (T_{13} - T_{25}) + \alpha_c A_{17} (T_{17} - T_{25}) \\ & + \alpha_c A_{21} (T_{21} - T_{25}) + \rho_a Q_{AHU} c_a (T_{26} - T_{25}) + \rho_a Q_{inf} c_a (T_{26} - T_{25}) + Q_{add}(t) \\ & + Q_{sol}(t) + Q_{per}(t) \end{aligned} \quad (4.1)$$

Where:

A_i is the inside surface of construction ($i = 1, 5, 9, 13, 17, 21$) [m^2].

T_i is the temperature of node ($i = 1, 5, 9, 13, 17, 21$) [m^2].

c_a is the specific heat capacity of dry air [$J/(kg \cdot K)$].

ρ_a is the density of dry air [kg/m^3].

V_r is the volume of the room [m^3].

α_c is the convection coefficient [W/m^2K].

Q_{inf} is the volumetric flow rate of infiltration [m^3/s].

Q_{AHU} is the volumetric flow rate of ventilation [m^3/s].

$Q_{per}(t)$ is the heat gain from people [W].

$Q_{add}(t)$ is the heating or cooling energy [W].

$Q_{sol}(t)$ is the solar gain [W].

There are heating and cooling control in the room all the time, and the setpoint of the thermostat for heating and cooling is 20°C and 24°C, respectively.

4.1.2 Hygric Part

The silica gel packed bed is assumed in thermodynamic equilibrium, which means all the moisture transfer inside beads and void space is eliminated. Thus, the silica gel packed bed is simplified as one node.

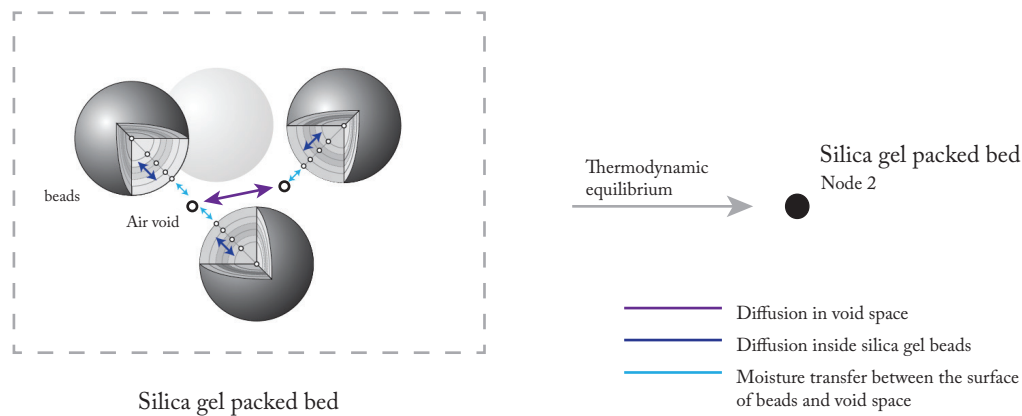


Figure 4.3: *Thermodynamic equilibrium in the packed bed*

Moisture transfer between construction and inside air is eliminated due to the fact that advection dominates mass transfer in the hygric model. The whole hygric room model is depicted in Figure 4.4. There is infiltration between outside and inside, and ventilation is provided by AHU, and moisture is also transferred between the packed bed and air in the room.

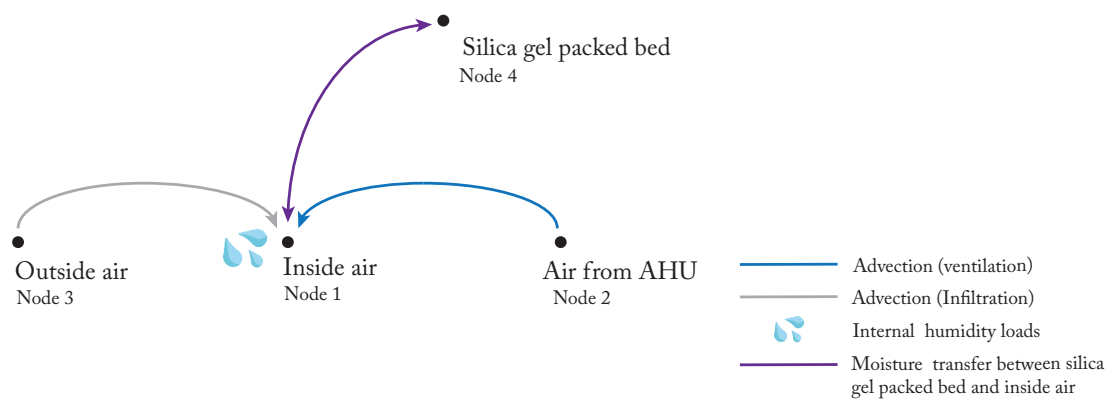


Figure 4.4: *Mass transfer network of model 2.0*

The dependent variable in the hygric model is the vapor density of air. And mass balance equations of node one and four are written based on the mass transfer network.

4.1.2.1 Node one

$$V_r \frac{\partial \rho_{v,a}}{\partial t} = \beta_c (\rho_{v,g} - \rho_{v,a}) + G_{AHU}(t) + G_{inf}(t) + G_v(t) \quad (4.2)$$

Where $\rho_{v,a}$ is the vapor density of air in the room [kg/m³]. β_c is the moisture transfer coefficient between the air in the packed bed and in the room [m/s]. $\rho_{v,g}$ is the vapor density of packed bed [kg/m³]. $G_{AHU}(t)$ is the advection effect by ventilation [kg/s]. $G_{inf}(t)$ is the advection effect by infiltration [kg/s]. $G_v(t)$ is the humidity load [kg/s]. V_r is the volume of the room [m³].

4.1.2.2 Node four

$$(1 - \varepsilon) V_g \frac{\partial w_g}{\partial t} = \beta_c (\rho_{v,a} - \rho_{v,g}) \quad (4.3)$$

Where w is the moisture content of the silica gel [kg/m³]. ε is the porosity of the packed bed. V_g is the volume of the packed bed [m³].

The relative humidity can be simply calculated by the ratio of vapor density to vapor density at saturation:

$$\phi \approx \frac{\rho_{v,g}}{\rho_{sat,g}(T)} \quad (4.4)$$

Since silica gel packed bed can be considered as hygroscopic materials. So, the time derivative of the moisture content on the left side of the equation can be written as:

$$\frac{\partial w_g}{\partial t} = \frac{\partial w_g}{\partial \phi} \frac{\partial \phi}{\partial t} = \xi \frac{\partial \phi}{\partial t} = \xi \frac{\partial (\frac{\rho_{v,g}}{\rho_{sat,g}(T)})}{\partial t} \quad (4.5)$$

After derivation:

$$\frac{\partial w_g}{\partial t} = \xi \left(\frac{1}{\rho_{sat,g}(T)} \frac{\partial \rho_{v,g}}{\partial t} - \frac{\rho_{v,g}}{\rho_{sat,g}^2(T)} \frac{\partial \rho_{sat,g}(T)}{\partial t} \right) \quad (4.6)$$

ξ is the moisture capacity of silica gel [kg/m³], which is defined as the slope of sorption isotherm of silica gel. $\rho_{sat,g}(T)$ is the density of water vapor in the saturation condition at temperature T [kg/m³].

Since the hygric model should be coupled with the thermal model, the Clausius-Clapeyron equation is used to calculate the equilibrium vapor pressure at a certain temperature.

$$\frac{dp_{sat(T)}}{dT} = \frac{L_{lv}}{R_v T^2} p_{sat(T)} \quad (4.7)$$

After derivation:

$$\frac{d\rho_{sat(T)}}{dT} = \frac{d\rho_{sat(T)} L_{lv}}{R_v T^2} - \frac{\rho_{sat(T)}}{T} \quad (4.8)$$

L_{lv} is the specific latent heat of vaporization of water [J/kg]. R_v is the gas constant of water vapor [J/(kg.K)]. $\rho_{sat(T)}$ is the density of water vapor in the saturation condition at temperature T [kg/m³].

By combining equation 4.3, 4.5, and 4.7, the mass balance of silica gel packed bed can be written as:

$$(1 - \varepsilon) V_g \xi \frac{1}{\rho_{sat,g(T)}} \left(\frac{\partial \rho_{v,g}}{\partial t} - \rho_{v,g} \left(\frac{L_{lv}}{R_v T} - \frac{1}{T} \right) \frac{\partial T}{\partial t} \right) = \beta_c (\rho_{v,a} - \rho_{v,g}) \quad (4.9)$$

4.1.2.3 Integrated node one

To simplify the model, it is assumed that the moisture transfer between the air and the packed bed is extremely fast, so $\rho_{v,a} = \rho_{v,g}$. Then the moisture capacity of silica gel packed bed can be added to that of air in the room, the term in equation 4.9 can be estimated as $\frac{L_{lv}}{R_v T} - \frac{1}{T} \approx 0.06$, and equation 4.2 and 4.9 can be combined:

$$\left(V_r + \frac{(1 - \varepsilon) V_g \xi}{\rho_{sat,g(T)}} \right) \frac{\partial \rho_{v,a}}{\partial t} = 0.06 \frac{(1 - \varepsilon) V_g \xi}{\rho_{sat,g(T)}} \rho_{v,a} \frac{\partial T}{\partial t} + G_{AHU}(t) + G_{inf}(t) + G_v(t) \quad (4.10)$$

With the integration of node one and four, the hygric model is simplified as Figure 4.5. Only node one is a free node which represents inside air and the packed bed.

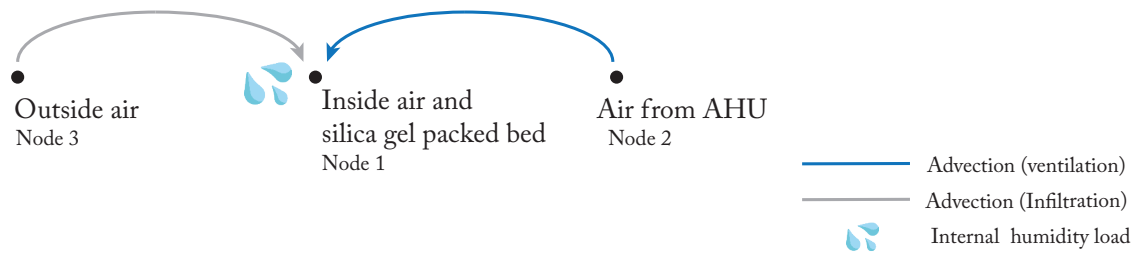


Figure 4.5: Simplified mass transfer network of model 2.0

4.1.3 AHU Part - Humidity Control

For simplification, thermal conditions are eliminated in the air handling unit model, the temperature of supply air is 20°C. Figure 4.6 shows that relative humidity is controlled by the enthalpy wheel, humidifier and dehumidifier in the air handling unit.

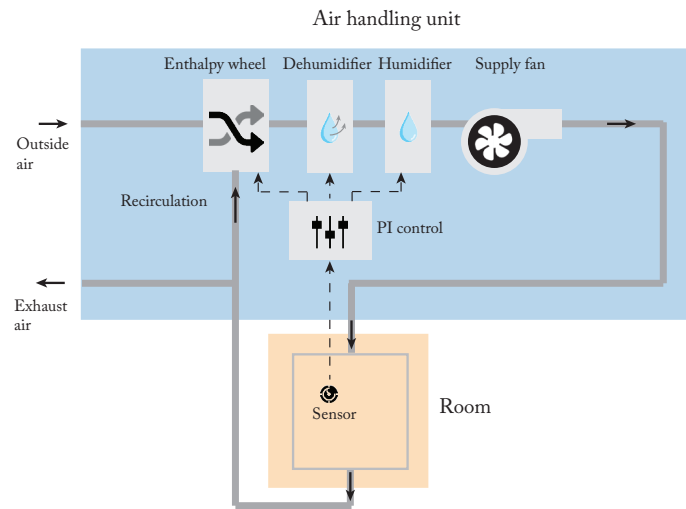


Figure 4.6: *Simplified AHU model*

4.1.3.1 Signal Generation

According to the climate class A1 requirement, seasonal change of RH is $\pm 10\%$ around the setpoint. While short-term fluctuation range of RH is $\pm 5\%$ around the setpoint. For instance, the RH is allowed to vary from 45% to 55% with the setpoint of 50% in spring. As the Figure 4.7 shows, the PI controller is used to calculate the difference between RH in the room and upper or lower limit, then converts it into the difference of humidity ratio, which is added to humidity ratio of room (x_r) to get the desired humidity ratio (x_{set}), which is also the humidity ratio of supply air (x_s). If the RH is lower than 45%, the signal will pass the upper controller and calculate the positive difference value for humidification. While signal will go via lower the controller to calculate the negative difference value for dehumidification likewise in the case of RH above 55%. When the RH is between 45% and 55%, the PI controller will take no actions.

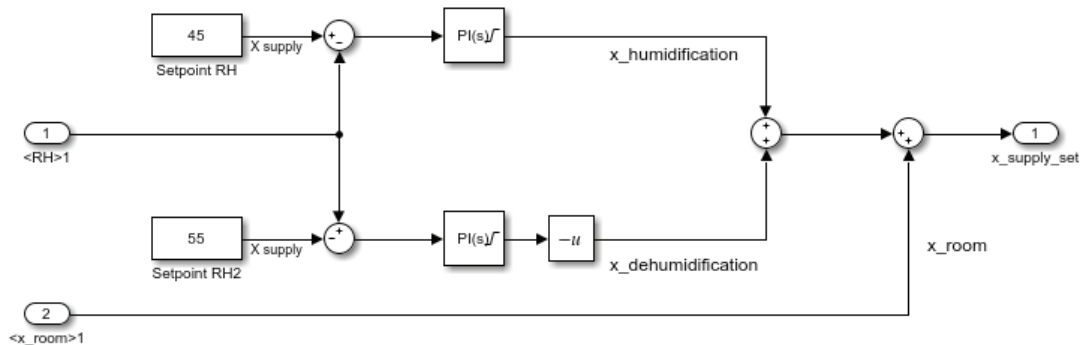


Figure 4.7: *Humidity control components in Simulink*

4.1.3.2 Enthalpy Wheel

Firstly, the enthalpy wheel is used to control the RH by mixing the outside air and returning air from the room, and the control variable is the working efficiency(η), which ranges from 0 to 70%. To determine its value, two different scenarios are discussed in Table 4.1 and Table 4.2.

In the humidification scenario, the efficiency of the enthalpy wheel can be defined as the function of the outside humidity ratio. When $x_e < x_r$, the enthalpy wheel should work with maximum efficiency since the outside air is drier than the inside air, which generates the mixed air with the highest humidity ratio. When $x_r < x_e < x_{sat}$, the enthalpy wheel does not need work because the outside air is more humid than the inside air. Without mixing with returning air, the inside air can be humidified by outside air naturally, which is the optimal humidification. When $x_e > x_{sat}$, the enthalpy wheel should start work again to prevent the inside air from excessive humidification by reducing the humidity ratio of mixed air. η increases with the increase of x_e and the maximum value is η_{max} .

Table 4.1: Working efficiency of enthalpy when the room needs humidification

x_e	η
$x_e \leq x_r$	η_{max}
$x_r < x_e \leq x_{set}$	0
$x_{set} < x_e \leq \frac{\eta_{max}(x_e - x_{set})}{x_e - x_r}$	$\frac{x_e - x_{set}}{x_e - x_r}$
$x_e > \frac{\eta_{max}(x_e - x_{set})}{x_e - x_r}$	η_{max}

Opposite cases occur in the dehumidification scenario. When $x_e > x_r$, the enthalpy wheel should work with the maximum efficiency to lower down the humidity ratio of mixing air as much as possible. When $x_e < x_r$, the room air is dehumidified naturally by the outside air without the enthalpy wheel. If x_e keeps dropping and becomes lower than x_{set} , the enthalpy wheel starts working again to prevent the mixing air from over dehumidification, and its efficiency increases with the decrease of the humidity ratio of outside air.

Table 4.2: *Working efficiency of enthalpy when the room needs dehumidification*

x_e	x_e
$x_e \leq \frac{\eta_{max}(x_e - x_{set})}{x_e - x_r}$	η_{max}
$\frac{\eta_{max}(x_e - x_{set})}{x_e - x_r} < x_e \leq x_{sat}$	0
$x_{set} < x_e \leq x_r$	$\frac{x_e - x_{set}}{x_e - x_r}$
$x_e > x_r$	η_{max}

4.1.3.3 Humidifier and Dehumidifier

If x_{set} cannot be reached with the maximum working efficiency of the enthalpy wheel, the humidifier or dehumidifier will be activated. Δx is defined as the difference between humidity ratio of air that goes into and out the device, and the equation to calculate it can be written as:

$$\Delta x = x_{set} - x_e - \eta(x_r - x_e) \quad (4.11)$$

A positive value means the humidification, and a negative value means dehumidification.

4.1.3.4 Energy Consumption

The energy consumption of humidification and dehumidification can be estimated based on the difference of enthalpy. Since the temperature is the same, the difference of enthalpy is equal to the difference of humidity ratio that times the latent heat of vaporization. The equation of energy consumption can be written as:

$$E_{hum} = \int (\dot{m} \Delta x L_{lv} \times COP_{hum}) dt \quad (4.12)$$

$$E_{dehum} = \int (\dot{m} \Delta x L_{lv} \times COP_{dehum}) dt \quad (4.13)$$

Where $COP_{hum} = 1$ is the coefficient of performance of the humidifier. $COP_{dehum} = 1.3$ is coefficient of performance of dehumidifier with a heat pump system.

The energy consumption of the fan can be estimated based on the pressure drop and ventilation flow rate. The power of fan is estimated as:

$$P_{fan} = \frac{\Delta p Q_{AHU}}{\eta_{fan}} \quad (4.14)$$

Where P_{fan} is the power of fan [W]. η_{fan} is the working efficiency of the fan. Δp is the pressure drop [Pa].

4.2 Description of Model 3.0

Model 3.0 is developed based on model 2.0. The main difference is that the silica gel and inside air are modeled as individual nodes and the former is divided into a couple of nodes that represent the packed bed in a cylinder container. And the recirculation flow is taken from the top of the container. The AHU part is the same as that in model 2.0.

In Figure 4.8 and Figure 4.10, ten nodes are defined to model the container in view of simulation accuracy and speed, and they are numbered from I to X. Two fixed nodes are air from AHU and outside with serial number XI and XII, respectively. The node number of construction and inside air is still sorted by Arabic numerals in consistence with model 2.0.

4.2.1 Thermal Part

In the cylinder container, advection dominates the heat transfer in the longitudinal direction. So, the conduction effect is discarded. It is assumed that 1-D heat transfer and advection are modeled in the upwind scheme.

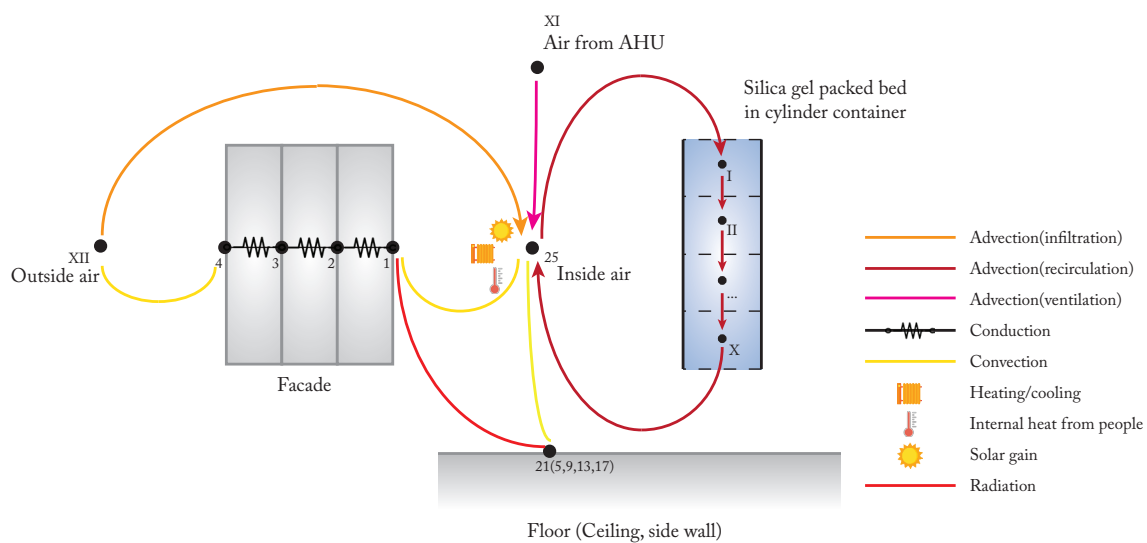


Figure 4.8: Heat transfer network of model 3.0

The heat storage in the pore space is eliminated since it is negligible compared with heat storage in the silica gel beads. The node X is taken as an example to write the energy balance equation:

$$(1 - \epsilon)(\rho_g c_g + c_l w_g) V_c \frac{\partial T_X}{\partial t} = Q_{re}(\rho_a c_a T_{IX} + \rho_{sat(T_{IX})} \phi_{IX} (L_{lv} + c_v T_{IX})) - Q_{re}(\rho_a c_a T_X + \rho_{sat(T_X)} \phi_X (L_{lv} + c_v T_X)) \quad (4.15)$$

Where $(1 - \epsilon)(\rho_g c_g + c_l w_g) V_c$ is the heat capacity of silica gel beads and it consists of heat capacity of beads and liquid water [J/K], and V_c is the volume of one control volume [m³]. Q_{re} is the volumetric flow rate of recirculation [m³]. The airflow consist of dry air and water vapor. So, $Q_{re} \rho_a c_a T_i$ represents the heat from the dry air of node i (i = I, II, ... X) [J/s]. $\rho_{sat(T_i)} \phi_i (L_{lv} + c_v T_i)$ is the heat from water vapor of node i [J/s], and it also includes the latent heat of vaporization, and the density of water is approximately calculated by $\rho_{sat(T_i)} \phi_i$.

In terms of air in the room, only heat storage of dry air and water vapor are considered, but latent heat is not considered in the room. Furthermore, all the heat load is added to the air node. The equation is:

$$(\rho_a c_a + \rho_v c_v) V_r \frac{\partial T_{25}}{\partial t} = Q_{re}(\rho_a c_a T_X + \rho_{sat(T_X)} \phi_X c_v T_X) - Q_{re}(\rho_a c_a T_{25} + \rho_{sat(T_{25})} \phi_{25} c_v T_{25}) + Q_{AHU}(\rho_a c_a T_{XI} + \rho_{v,XI} c_v T_{XI}) - Q_{AHU}(\rho_a c_a T_{25} + \rho_{v,25} c_v T_{25}) + Q_{inf}(\rho_a c_a T_{XII} + \rho_{v,XII} c_v T_{XII}) - Q_{inf}(\rho_a c_a T_{25} + \rho_{v,25} c_v T_{25}) + Q_{sol}(t) + Q_{per}(t) + Q_{add}(t) + Q_{convection}(t) \quad (4.16)$$

Where

$(\rho_a c_a + \rho_v c_v) V_r$ is the heat capacity of air in the room [J/K].

$Q_{re}(\rho_a c_a T_X + \rho_{sat(T_X)} \phi_X c_v T_X) - Q_{re}(\rho_a c_a T_{25} + \rho_{sat(T_{25})} \phi_{25} c_v T_{25})$ is the heat transfer by recirculation [J/s].

$Q_{AHU}(\rho_a c_a T_{XI} + \rho_{v,XI} c_v T_{XI}) - Q_{AHU}(\rho_a c_a T_{25} + \rho_{v,25} c_v T_{25})$ is the heat transfer by ventilation [J/s].

$Q_{inf}(\rho_a c_a T_{XII} + \rho_{v,XII} c_v T_{XII}) - Q_{inf}(\rho_a c_a T_{25} + \rho_{v,25} c_v T_{25})$ is the heat transfer by infiltration [J/s].

$Q_{convection}(t)$ is the heat transfer by convection [J/s].

4.2.2 Hygric Part

As it is mentioned above, the cylinder container is divided into ten control volumes that are also regarded as representative elementary volume (REV), and it is assumed thermal dynamic equilibrium in the control volume. In other words, the moisture transfer inside silica gel beads is not considered, and the sorption isotherm is defined as the relationship between the relative humidity of pore space and the amount of moisture its surrounding beads. For simplification, both the sorption and desorption isotherm are assumed as a linear function with a slope of 350 instead of modeling polynomial function with the hysteresis.

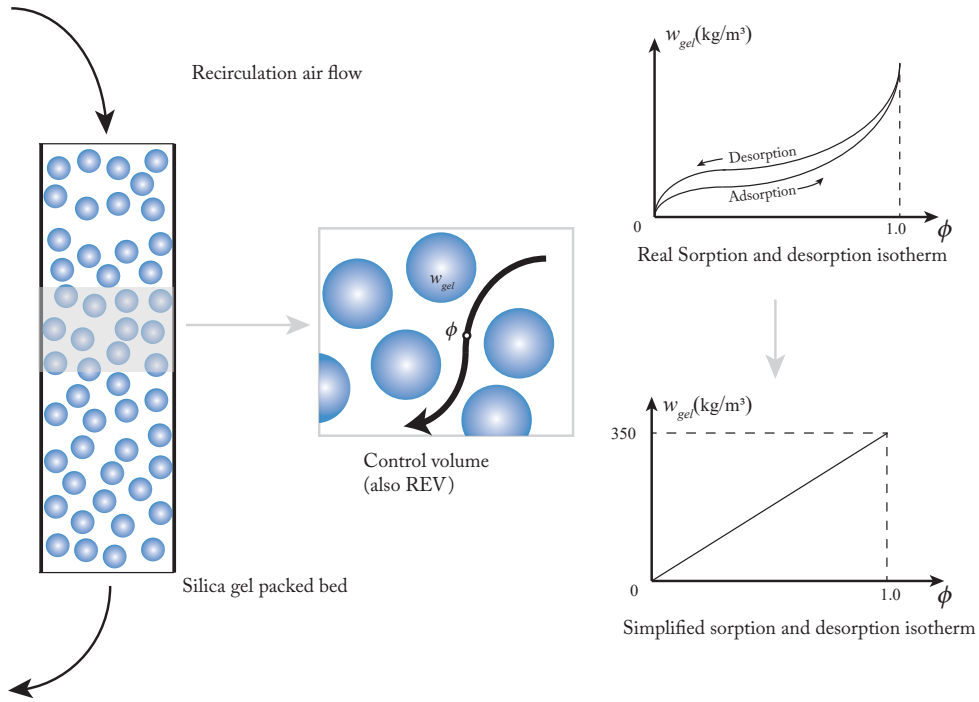


Figure 4.9: Definition of control volumes and the simplification of moisture sorption isotherm

It is still assumed that advection dominates the mass transfer in the hygric model. And moisture transfer between construction and air and diffusion between control volumes of silica gel are eliminated. The dependent variable in the packed bed is the relative humidity (ϕ). The node X is taken as an example to write the mass balance equation:

$$\xi V_c \frac{\partial \phi_X}{\partial t} = Q_{re} (\rho_{sat(T_{IX})} \phi_{IX} - \rho_{sat(T_X)} \phi_X) \quad (4.17)$$

Where the ξ is the moisture capacity of silica gel [kg/m^3], which is defined as the slope of sorption isotherm, and the density of water vapor is still approximately calculated by $\rho_{sat(T_i)} \phi_i$.

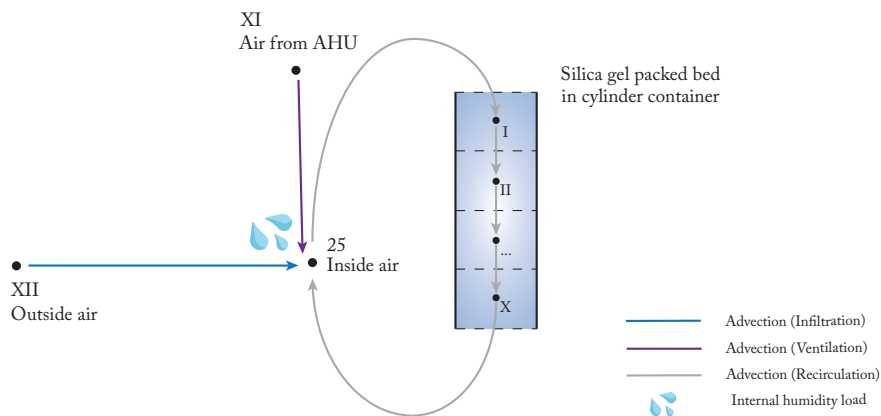


Figure 4.10: Mass transfer network of model 3.0

The density of water vapor is used as the dependent variable in the mass balance of air in the room. And the equation is:

$$V_r \frac{\partial \rho_{v,25}}{\partial t} = Q_{re}(\rho_{sat(T_X)} \phi_X - \rho_{v,25}) + Q_{AHU}(\rho_{v,XI} - \rho_{v,25}) + Q_{inf}(\rho_{v,XII} - \rho_{v,25}) + G_v(t) \quad (4.18)$$

Where

$Q_{re}(\rho_{sat(T_X)} \phi_X - \rho_{v,25})$ is the mass transfer by recirculation [kg/s].

$Q_{AHU}(\rho_{v,XI} - \rho_{v,25})$ is the mass transfer by ventilation [kg/s].

$Q_{inf}(\rho_{v,XII} - \rho_{v,25})$ is the mass transfer by infiltration [kg/s].

$G_v(t)$ is internal humidity load [kg/s].

4.3 Summary of Two Models

The simulated elements and their nodes of both model 2.0 and 3.0 are summarized in Table 4.3.

Table 4.3: Summary of model 2.0 and 3.0

	Model 2.0		Model 3.0	
Thermal part	Construction	Node 1 - 24	Construction	Node 1 - 24
	Air in the room	Node 25	Air in the room	Node 25
	and silica gel			
	Air from AHU	Node 26	Air from AHU	Node XI
	Outside air	Node 27	Outside air	Node XII
			Silica gel packed bed	Node I - X
Hygic part	No construction		No construction	
	Air in the room	Node 25	Air in the room	Node 25
	and silica gel			
	Air from AHU	Node 26	Air from AHU	Node XI
	Outside air	Node 27	Outside air	Node XII
			Silica gel packed bed	Node I - X
AHU			PI control Enthalpy wheel Humidifier Dehumidifier Fan	

5

Model Verification and Validation

5.1 Introduction

5.2 Design Builder Model

5.3 Model Comparison

5.4 Testing of Model 3.0

5.5 Conclusions

5 Model Verification and Validation

This chapter focuses on the first sub-question: How accurate the developed models are. Four validation techniques are introduced in section 5.1. Based on this customized case, comparative testing is applied with Design Builder as comparative software used to validate the model 2.0 and model 3.0. It is proved that model 3.0 is accurate enough, and the preliminary testing is done on it to check whether its output corresponds to the expectation and the previous assumption is correct, which is as a supplement for validation.

5.1 Introduction

Simulation models are used to make decisions in the design phase. So, the correctness and accuracy of results are the main concern, which is addressed by model verification and validation. Model verification is the process of ensuring the implementation of the computerized model is correct. While model validation is the process of ensuring the range of accuracy is acceptable concerning its application (Sargent, 2013).

In practice, verification and validation are usually combined in the model development process. A simplified version of this process was described by Sargent (1981) in Figure 5.1. Conceptual model validation is to confirm the assumptions, theories, and equations are reasonable enough to support the purpose of the conceptual model. Computerized model verification is to check whether the programming and implementation are correct. Operational validation is to determine whether the results of the model have an acceptable range of accuracy corresponding to its purpose of the application. Data validity is to ensure the data can support the modeling, testing, and experiments sufficiently and correctly.

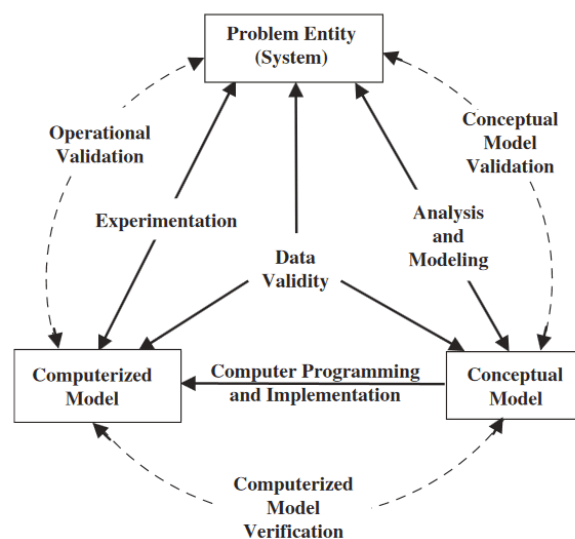


Figure 5.1: The simplified version of the model development process (Sargent, 1981)

Model validation is to demonstrate that the simulation model can represent the actual system reasonably, and four validation techniques are summarized by Hillston (2003):

Expert intuition: an “expert” in the field of the system examines the model by inspecting the output and behavior of the model.

Real system measurements: it is the most reliable validation approach. The output of the model is compared with measurement in the real system, such as testing in a laboratory and measurement in the building.

Theoretical results/analysis: the model can be validated by comparing its results with a simple network model with the known same system.

Comparative testing: the output of the model is compared with that of another validated model

Among these four techniques, measurement in the National Holocaust Museum is not possible since it is closed. In addition, a simple network model with a known system cannot be found to compare. Comparative testing is chosen to validate the model implemented in Matlab/Simulink, and Design Builder is selected as the comparative software since it is user-friendly software with EnergyPlus as an engine to generate performance data (Design Builder, 2009).

5.2 Design Builder Model

One room model is created to simulate the exhibition room with silica gel present. The construction and thermal conditions are easily made consistent with that in the Matlab/Simulink model. So, it is not discussed in this section. The most crucial part is to model the silica gel in Design Builder. Since it is not possible to model a cylinder with airflow going through, an alternative is to add extreme thin partitions made of silica gel with large surface area, which results in excellent contact with air in the room. And the total volume of partitions is equal to that of the cylinder.

It is found that the ratio of the amount of silica gel to room volume is 0.1% in chapter 3. In Figure 5.2, the thickness of partitions is set as 0.001m. If 0.126m³ silica gel is applied in the room with a height of 4.6m, the total length of partitions is around 27m. However, multiple zones are created if partitions are built in Design Builder. The solution is to make partitions as far as possible to the facade, splitting the room into one large zone and one small zone. The large zone can be regarded as the exhibition room, and the small zone is not analyzed.

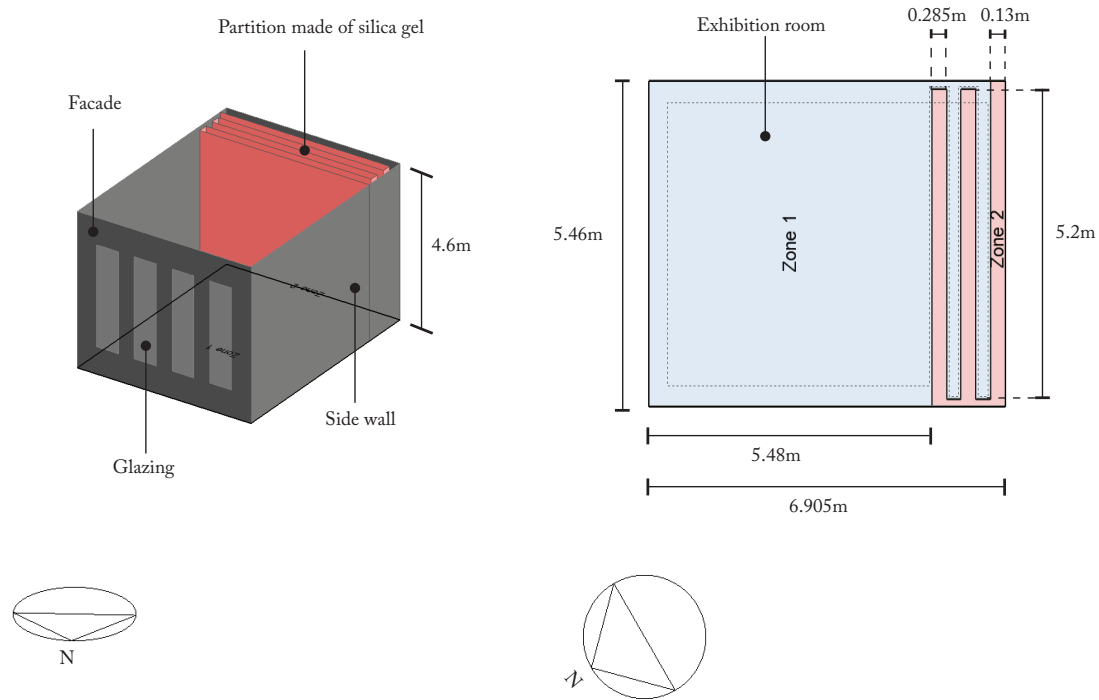


Figure 5.2: Illustration of Design Builder model

Moisture transfer can be simulated by HAMT(Combined Heat and Moisture Transfer) algorithms in Design Builder. The slope of sorption isotherm is simply defined as 350, and diffusion is also discarded, which is consistent with that in the Matlab/Simulink model.

5.3 Model Comparison

5.3.1 Simulation Conditions

Three simple scenarios with different complexity are analyzed to calibrate model 2.0 and 3.0 by comparing with Design Builder model. The simulation conditions are described in Table 5.1. Firstly, the most simple scenario a1 is defined. The room is mechanically ventilated with the air exchange rate of 1h^{-1} , and there is no occupancy in the room. In scenario a2 and a3, the scenarios become more complicated with the addition of occupancy and humidity control.

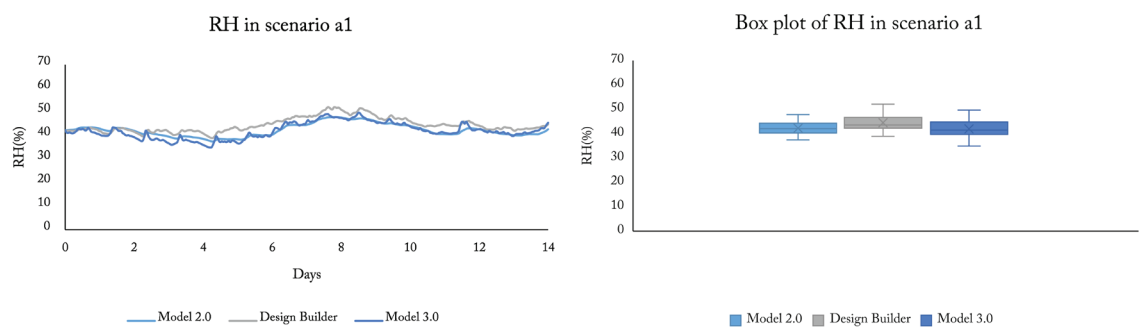
It is defined that the occupancy is always 0.27 people/m^2 between 11 am and 5 pm, and the air exchange rate keeps the same. The aim is just to compare the effect of occupancy in three models instead of simulating the real conditions. Besides, the humidity control part is compared in scenario a3 with the same setpoint setting in all the models. More specifically, the humidification switches on when RH is below 45%, while the dehumidification switches on when RH is above 55%.

Table 5.1: *Summary of scenarios*

Scenarios	a1	a2	a3
Climate data	NEN5060_2018		
Period	16th - 30th in April		
Amount of silica gel	0.126m ³		
Air exchange rate	1h ⁻¹	1h ⁻¹	1h ⁻¹
Occupancy	-	11:00 am - 5 pm: 0.27 people/m ²	11:00 am - 5 pm: 0.27 people/m ²
Humidity Control	-	-	Humidification setpoint: 45% Dehumidification setpoint: 55%

5.3.2 Comparison of Results

The relative humidity of the three models is compared in Figure 5.3, Figure 5.4, and Figure 5.5. For each figure, relative humidity varying over time is shown in the left part where the extent to which curves coincide with each other is observed. At the same time, the hourly data is collected to make the box plot in the right part where the fluctuation of relative humidity is compared.

**Figure 5.3:** *Comparison of RH in scenario a1*

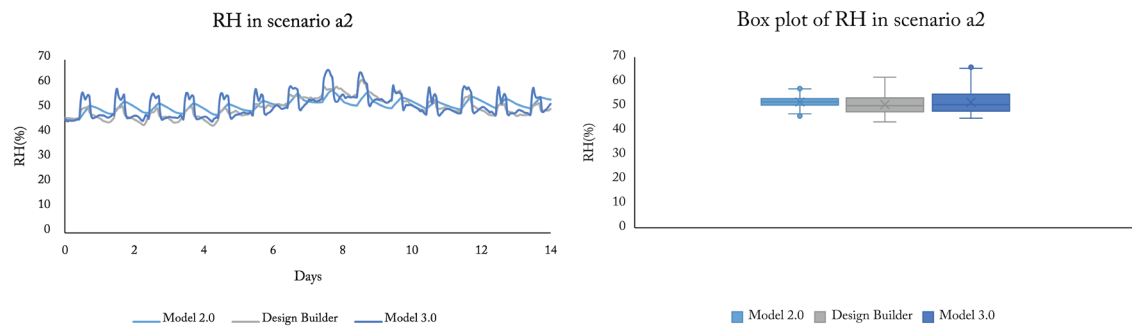


Figure 5.4: Comparison of RH in scenario a2

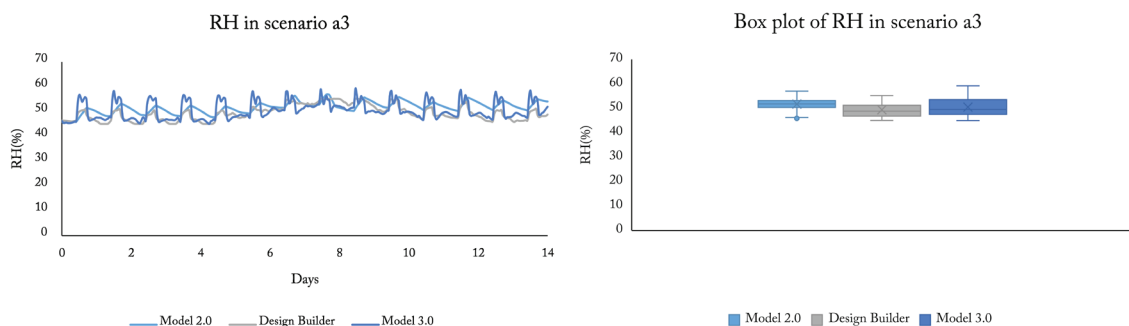


Figure 5.5: Comparison of RH in scenario a3

The accuracy of model 2.0 and 3.0 are discussed in both comparison of results and modeling principle.

By observing the left part of each figure, it indicates that the results of model 3.0 coincide with that of Design Builder more than that of model 2.0 since the shortest fluctuation time of the former two is very similar. While the line of model 2.0 is more smooth with longer fluctuation time. In terms of the right part of each figure, it is not obvious which model matches more with Design Builder model in scenario a1. By comparing the results in the right part in scenario a2 and a3, there are similarities between model 3.0 and Design Builder model in terms of the distribution of data, namely the interquartile range.

In terms of the fluctuation range, all the data are summarized in Table 5.2. It shows that the range in model 3.0 is closer to that in Design Builder model than that in model 2.0, except scenario a3. In scenario a1, the fluctuation range in model 3.0 and Design Builder model is 13.20% and 14.71%, respectively, which prove the combination of moisture and heat transfer is accurately simulated in model 3.0. The effect of occupancy and humidity control is estimated by calculating the difference in fluctuation range between scenarios. It is observed that the increment on fluctuation affected by humidity load from occupancy in model 3.0 is more convincing than that in model 2.0 with negative values. The ideal humidity control in Design Builder model results in a larger decrement on the fluctuation.

Table 5.2: *Comparison of fluctuation of RH in scenario a1, a2, and a3*

	Model 2.0	Design Builder	Model 3.0
Scenario a1	10.37%	13.20%	14.71%
Scenario a2	10.29%	18.36%	20.04%
Scenario a3	10.76%	10.17%	14.22%
Increment with the effect of occupancy (a2 - a1)	-0.08%	5.16%	5.33%
Decrement with the effect of humidity control (a2 - a3)	-0.47%	8.19%	5.82%

In spite of excellent contact between the air and the silica gel in all three models, the modeling principle is different, which results in a small difference. In model 2.0, silica gel and air are combined into one node, which means the moisture capacity of silica gel is directly added to the air, and they have the same temperature as well. In Design Builder model, silica gel is made into partitions with a large surface area of 126 m², which ensures sufficient moisture exchange between air and silica gel. In model 3.0, silica gel is put in the cylinder container where a large recirculation flow rate goes through, and moisture transfer is achieved by the advection effect. In short, it infers that the descending order of extent of contact between the silica gel and the air is: model 2.0, Design Builder model, and model 3.0. This also is reflected in the comparison of results in scenario a1 and a2 since the fluctuation range is smallest in model 2.0 and largest in model 3.0. Although there is less fluctuation in model 2.0, it corresponds to neither theory nor practice. Because it is impossible that silica gel and the air are combined into an entirety and their thermal conditions are always the same. While silica gel packed bed in the container with recirculation flow going through is more realistic.

Therefore, model 3.0 is more accurate than model 2.0 because of similarity with Design Builder model. In addition, model 3.0 is more realistic than 2.0 because it simulates the real conditions that can be achieved in practice.

5.4 Testing of Model 3.0

Although model 3.0 shows its accuracy in section 5.3. It is preferable to do simple testing before doing the complete simulation, which is helpful to check whether the assumption is correct, and the model can simulate what is expected.

5.4.1 Estimation of Magnitude of Moisture Transfer between Construction and Air

Since the moisture transfer between construction and air is eliminated in both model 2.0 and 3.0, the estimation of its magnitude is compared with that of the advection effect to prove the previous assumption is reasonable.

The vapor flux can be calculated based on the pressure difference between air and construction, which is illustrated in Figure 5.6, and the equation is:

$$g = \beta_p (p_e - p_s) \quad (4.19)$$

Where β_p is the surface vapor transfer coefficient, and it is equal to 2.0×10^{-8} s/m as for the inside conditions. p_e is the vapor pressure in the air [Pa]. p_s is the vapor pressure on the surface of construction [Pa].

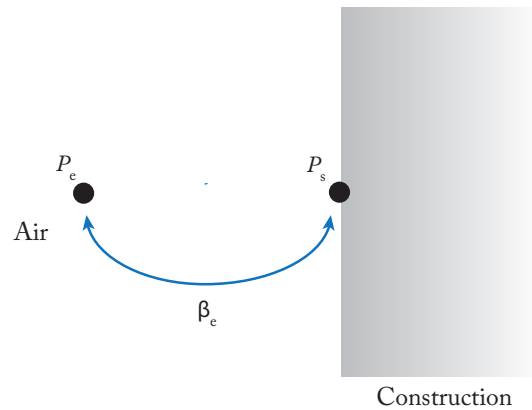


Figure 5.6: *Moisture transfer between construction and air*

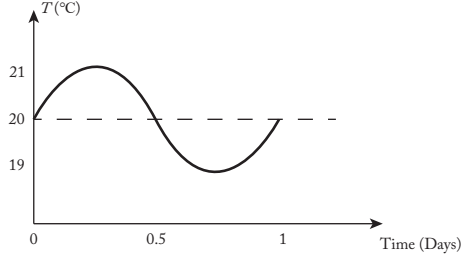
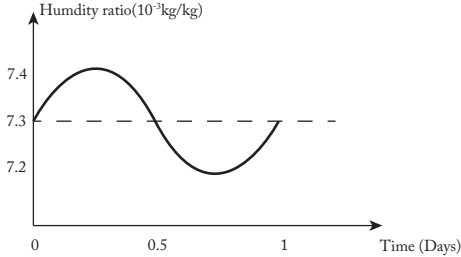
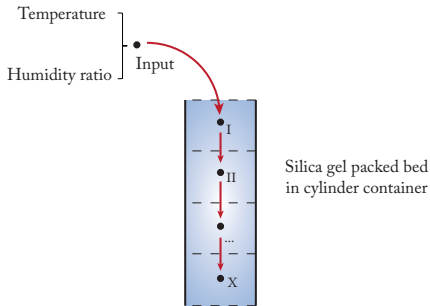
It is assumed that the relative humidity of both air and the surface of construction is 50% initially. If there is a 1% change on the RH of air and the RH of the surface still keeps the same, and the pressure difference is around 23 Pa. By applying equation 4.19, the vapor flux is 4.6×10^{-7} kg/m²s. The total surface area of one exhibition room is around 135.45 m². So, the mass flow rate between construction and air is 6.23×10^{-5} kg/s.

To compare the magnitude, the moisture transfer by recirculation is calculated based on model 3.0, and the value is 7.3×10^{-4} kg/s. It is estimated that the recirculation effect is ten times larger than that of moisture transfer between construction and air. So, the elimination of construction in the hygric part in chapter 4 is reasonable.

5.4.2 Hygrothermal Performance of Packed Bed

The silica gel packed bed model is the most important part of model 3.0. It is preferable to check whether its output that of the node X corresponds to physical phenomenons by giving simple sine-wave input of temperature and humidity ratio separately. The period of both sine functions is one day.

Table 5.3: *Input variables of the packed bed*

	Scenario b1	Scenario b2
Temperature		20°C
Humidity ratio	$7.3 \times 10^{-3} \text{ kg/kg}$	
		

In scenario b1, the input temperature follows the sine function with the period of one day, and the value fluctuates from 19°C to 21°C in Figure 5.7. The input humidity ratio is 7.3×10^{-3} , corresponding to the RH of air is 50% at 20°C. The output results are shown in Figure 5.8, Figure 5.9, and Figure 5.10. It indicates that the temperature varying has a large influence on the fluctuation of RH. The largest range occurring at the top of the container is between 47.3% and 53.2%. While node X at the bottom has the smallest range, which is from 48.0% to 52.1%. The packed bed is heated up when the input temperature increases. Moreover, the closer to the bottom the node is, the less energy it can get. The amount of increase in temperature of node X is the smallest, and there is less evaporation of water in silica gel beads, which causes the least reduction in the RH and highest humidity

ratio among all the nodes. Similarly, its increment is also the smallest when the input temperature decreases. Besides, the dynamic equilibrium is reached after one day when temperature varies by observing the first wave us different from the rest six waves in the three output diagrams.

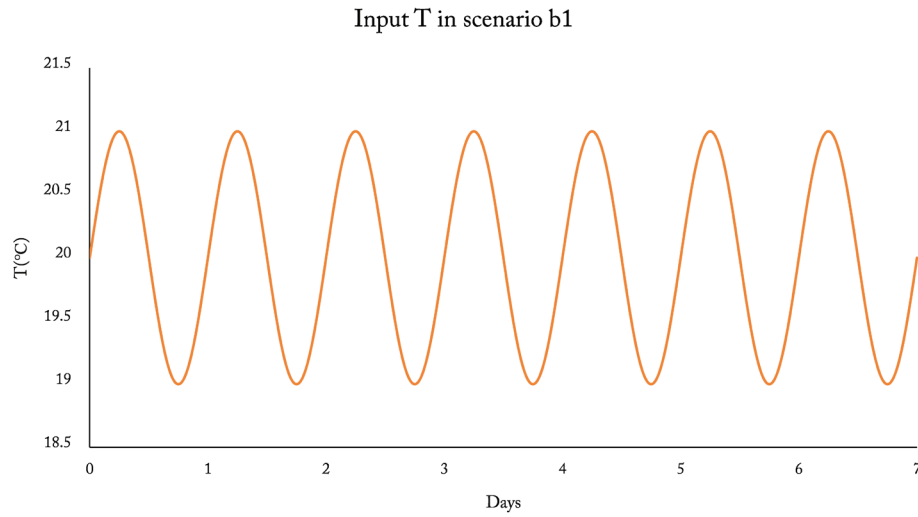


Figure 5.7: *Input T in scenario b1*

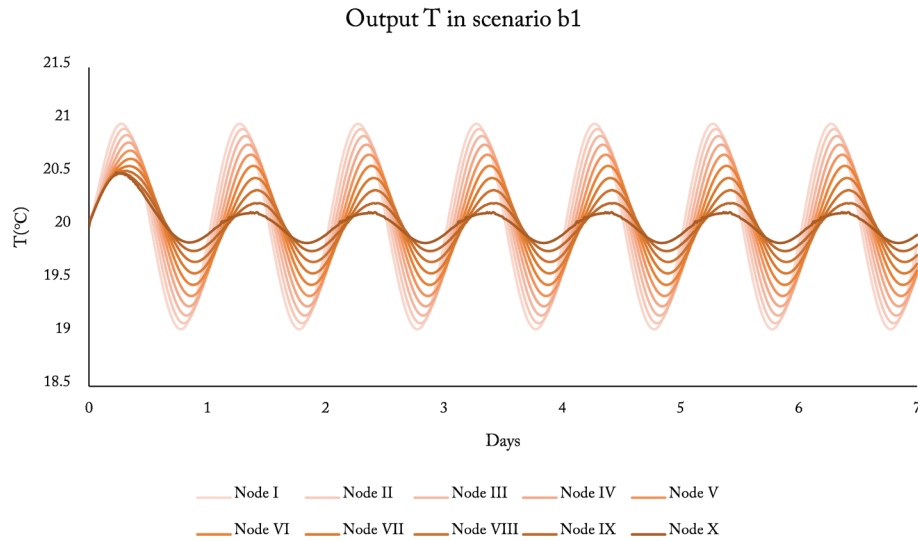


Figure 5.8: *Output T in scenario b1*

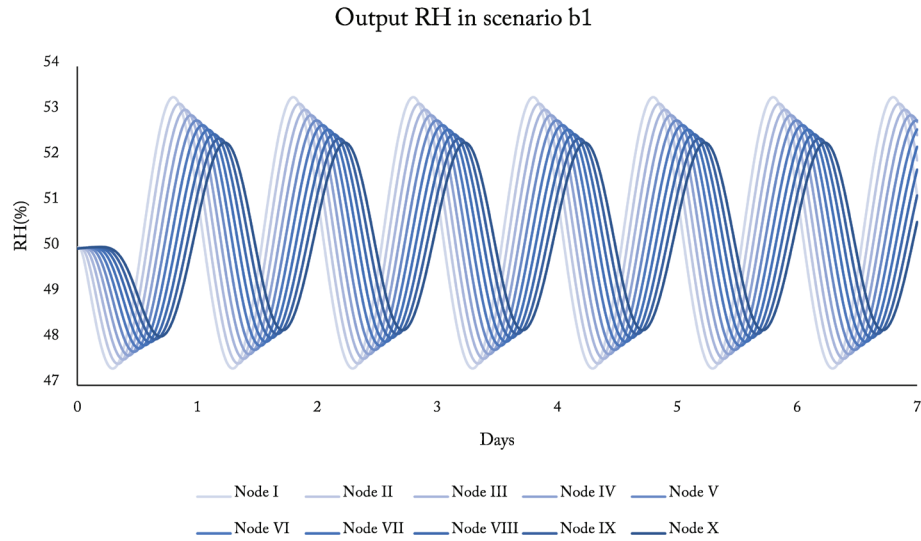


Figure 5.9: *Output RH in scenario b1*

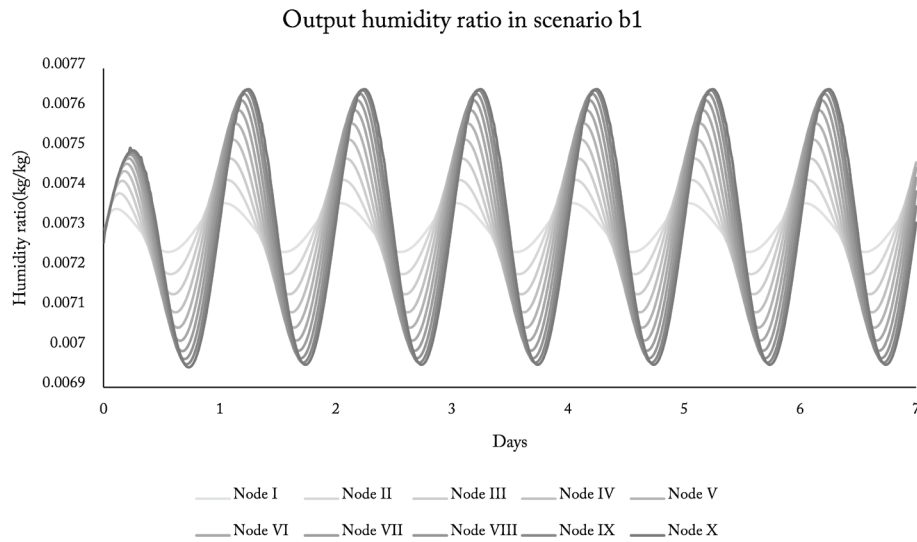


Figure 5.10: *Output humidity ratio in scenario b1*

In scenario b2, the input humidity follows the sine function with the period of one day, and the value fluctuates from 7.2×10^{-3} to 7.4×10^{-3} , corresponding to that the RH is between 49% and 51% at 20°C. The input temperature is 20°C. The output results are shown in Figure 5.12, Figure 5.13, and Figure 5.14. The silica gel packed bed is effective to stabilize relative humidity. Compared with the range of input RH, the output value decreases by half. Besides, the RH varying does not have a large influence on the temperature.

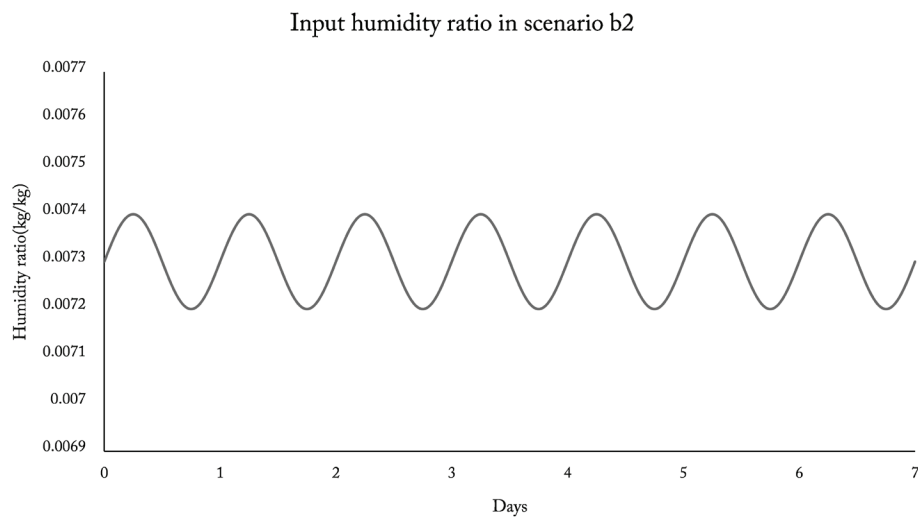


Figure 5.11: *Input humidity ratio in scenario b2*

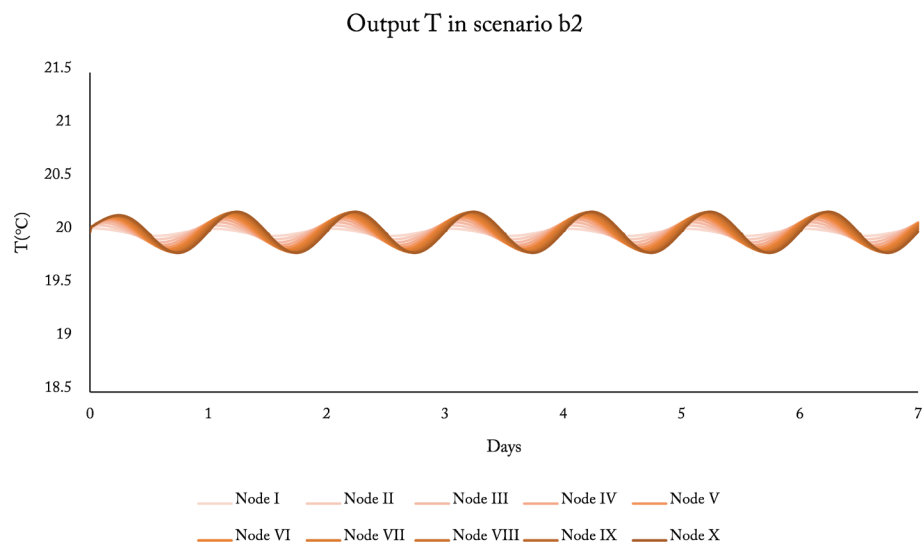


Figure 5.12: *Output T in scenario b2*

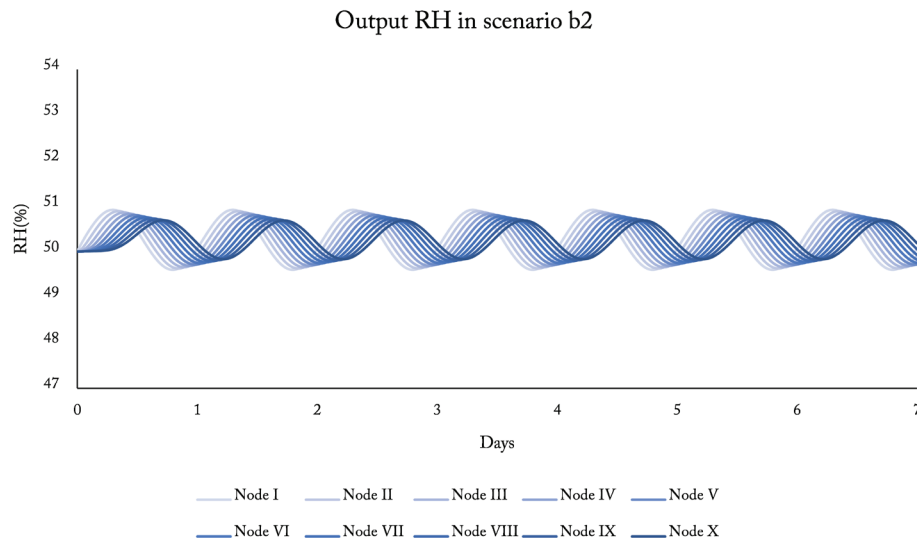


Figure 5.13: *Output RH in scenario b2*

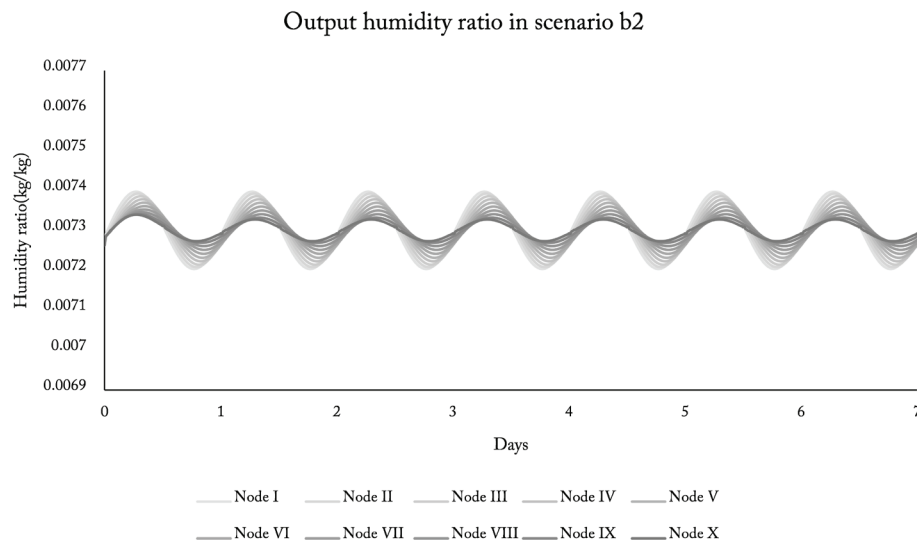


Figure 5.14: *Output humidity ratio in scenario b2*

Therefore, the hygrothermal performance of the packed bed follows the basic physical phenomenon. The buffering effect is significant when the outside relative humidity changes. However, temperature varying has an adverse impact on the moisture buffering effect. So, the fluctuation of the temperature of the inlet recirculation flow should be avoided.

5.5 Conclusions

Model 2.0 and 3.0 are compared with Design Builder model, and it is concluded that model 3.0 is superior to model 2.0 in the aspects of accuracy and degree of matching reality. Besides, the elimination of moisture transfer between construction and air is proved since its effect is only one-tenth of that of recirculation. A preliminary analysis of the packed bed is carried, which shows the fluctuation of RH decreases by half when the outside temperature is constant.



Simulation Conditions

6.1 Renovation Design of the National Holocaust Museum

6.2 Definition of Scenarios in One Room

6.3 Definition of Scenarios in the Whole Building

6.4 Simulation Setting in Matlab/Simulink

6 Simulation Conditions

Firstly, the renovation design of the National Holocaust Museum is described. Secondly, simulation scenarios are defined in both one exhibition room and the whole building. The variables of scenarios are the presence or absence of silica gel, the number of visitors, the ventilation flow rate, and the setpoint of humidity control.

6.1 Renovation Design of the National Holocaust Museum

As mentioned in chapter 2, the National Holocaust Museum is situated on Plantage Middenlaan in Amsterdam. As Figure 6.1 shows, the new design consists of a previous historic building, the temporary exhibition space, the auditorium, and the patios. A three-story historic building and a four-story building are in the front of the whole complex, facing the street. Its south facade with expressive brick and masonry is well integrated with other historic buildings on the street. Moreover, the new main entrance is also on the south facade. The new auditorium and temporary exhibition space are behind the historic building. Space is made full of use with the flexible walls and slide-out screen, which is appropriate in different occasions. A patio and introduction room are along the boundary, and the previous creche is rebuilt to a garden with a bay window.

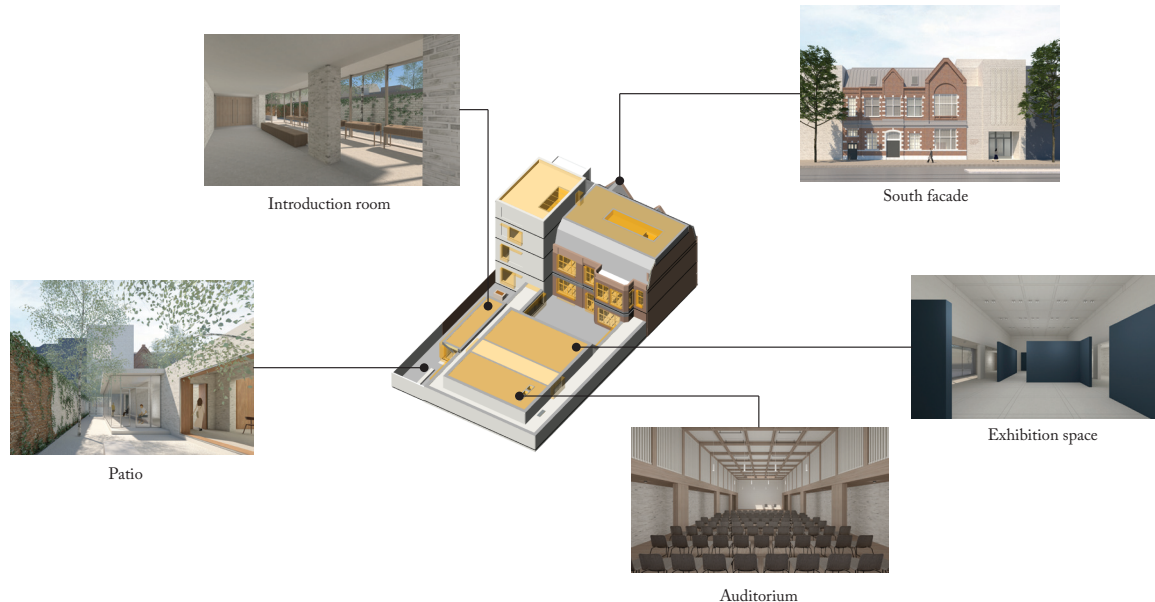


Figure 6.1: *The overview renovation design of the National Holocaust Museum (ABT & Winhov, 2020)*

The front building and one of its exhibition rooms are simulated objects. The south facade of the building is in direction 30° west of north. The room is located on the ground floor at the back of the building, and its façade is in direction 30° east of north.

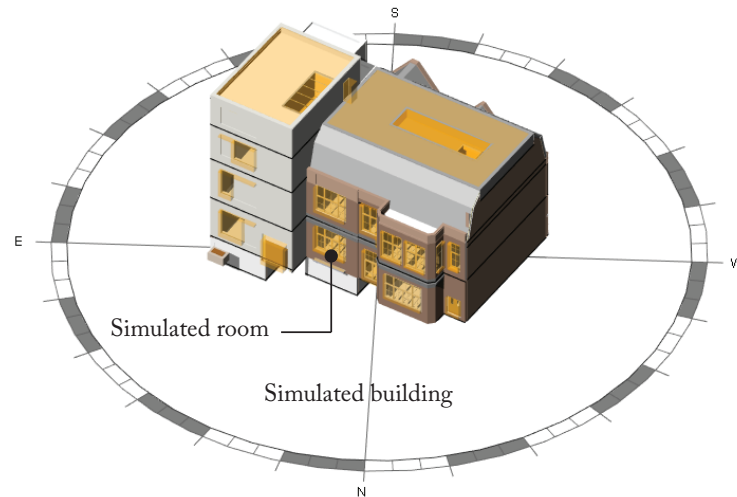


Figure 6.2: *Simulated objects (ABT & Winhov, 2020)*

6.2 Definition of Scenarios in One Room

The floor area of the exhibition room is 30.19m^2 , with a height of 4.6m . The thermal resistance of the façade $4.5\text{m}^2\text{K/W}$. Besides, the thermal transmittance of the double-glazing window is $1.65\text{ m}^2\text{K/W}$. The other detailed information is shown in section 11.6.5 and 11.6.6 of appendix E.

6.2.1 Outside Climate Conditions and Schedule

Climate data is collected from the NEN 5060 (NEN, 2018). In terms of the room model. Three scenarios in different seasons with one week individually are chosen. More specifically, one week is defined from 23th to 30th in April for spring, from 22th to 29th in July for summer, from 17th to 24th in December for winter. For each scenario, RH and energy consumption are studied in the case of silica gel present and absent. In addition, the scenario with the simulation period of one year is required. National Holocaust Museum follows the same schedule every day, and it is open between 11 am and 5 pm and closed at the rest time.

6.2.2 Occupancy

Usual visitor densities in the exhibition room are between 2.8 and 4.6 m^2 per person, and visitors put up with 1.8 m^2 per person in peaked time (Lord et al., 2002). However, the occupancy in the National Holocaust Museum is not that high. So, the occupancy was defined between 15 m^2 and 5 m^2 per person, and the number of people was calculated based on the floor area. It follows normal distribution every day, and the most popular time is usually around 2 pm. In addition, the occupancy varies from season to season. According to the tourism seasonality, there are more visitors in summer and fewer visitors in winter, compared with ones in spring or autumn (Wang, 2019), and the occupancy in different seasons is shown in Figure 6.3, Figure 6.4, and Figure 6.5.

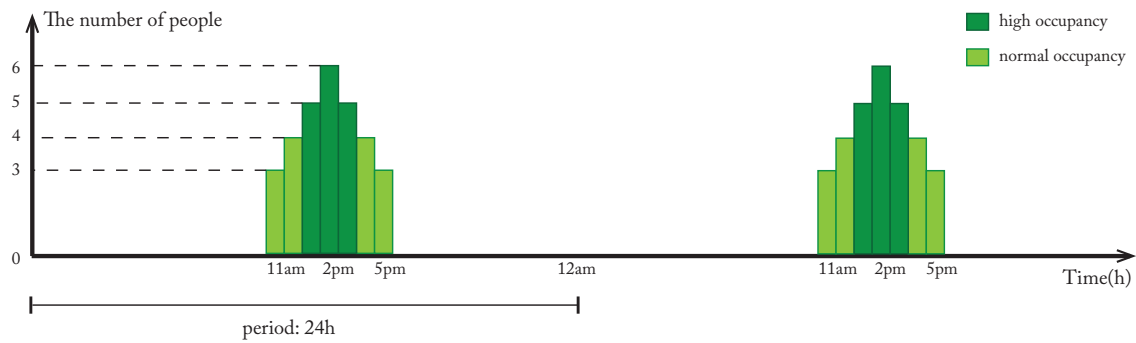


Figure 6.3: *Occupancy in one exhibition room in spring and autumn*

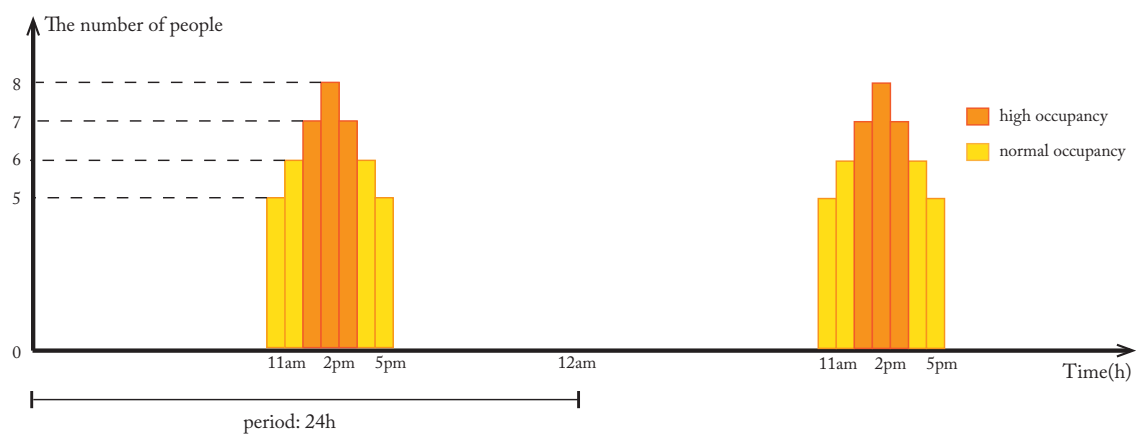


Figure 6.4: *Occupancy in one exhibition room in summer*

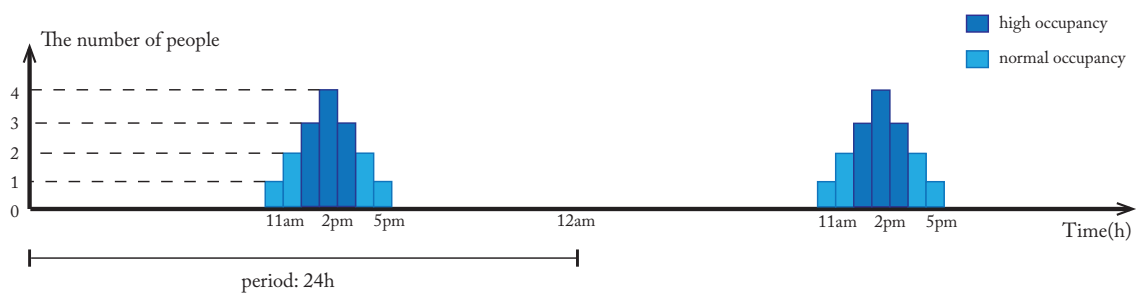


Figure 6.5: *Occupancy in one exhibition room in winter*

6.2.3 Internal Humidity Load

People and cloth drying are considered as the primary moisture source. Moisture production from light activity people is between 0.03 kg/h and 0.12 kg/h per person (Trechsel, 2001). 0.05 kg/h per person is used as the standard humidity load in this case. So, the humidity load is calculated in Figure 6.6, Figure 6.7, and Figure 6.8.

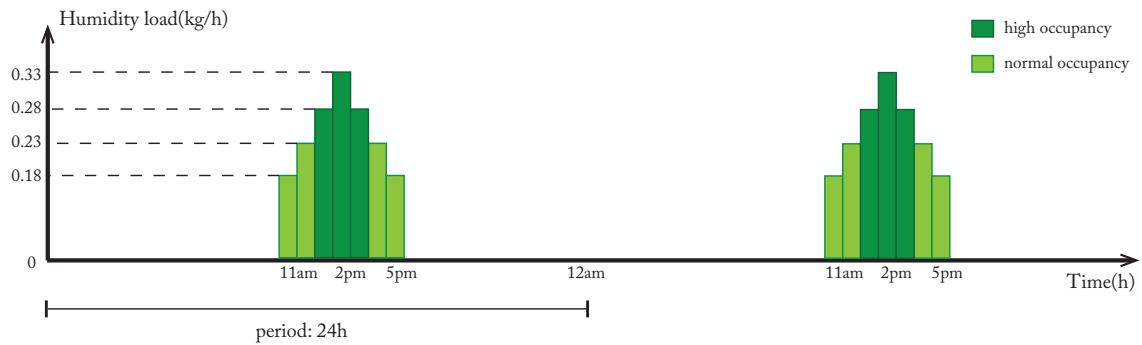


Figure 6.6: Internal humidity load in one exhibition room in spring and autumn

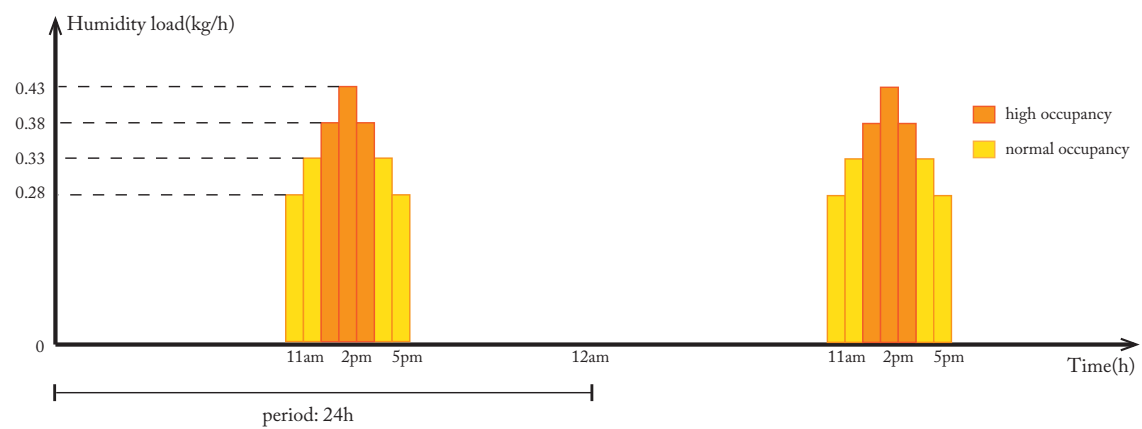


Figure 6.7: Internal humidity load in one exhibition room in summer

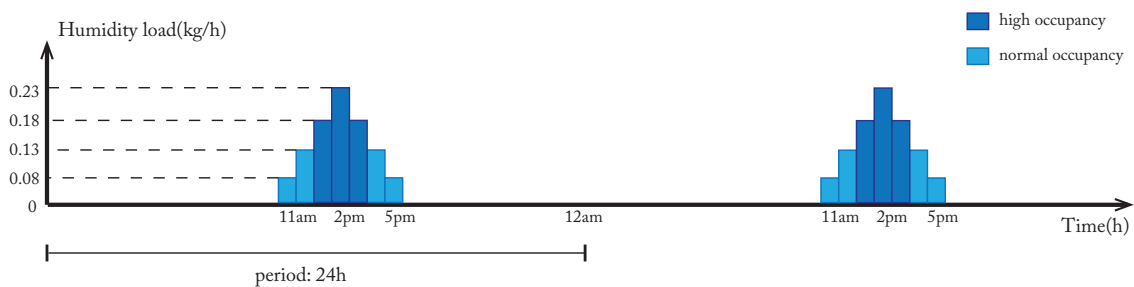


Figure 6.8: Internal humidity load in one exhibition room in winter

6.2.4 Ventilation and Infiltration

The ventilation rate can be determined based on the number of persons in the room, and the standard value is 12 L/s per person. The maximum supply capacity is 5 L/s per m² per floor area. If there is no occupancy, the ventilation rate is 0.5 L/s per m² of floor area. So, the ventilation rate is calculated according to the occupancy.

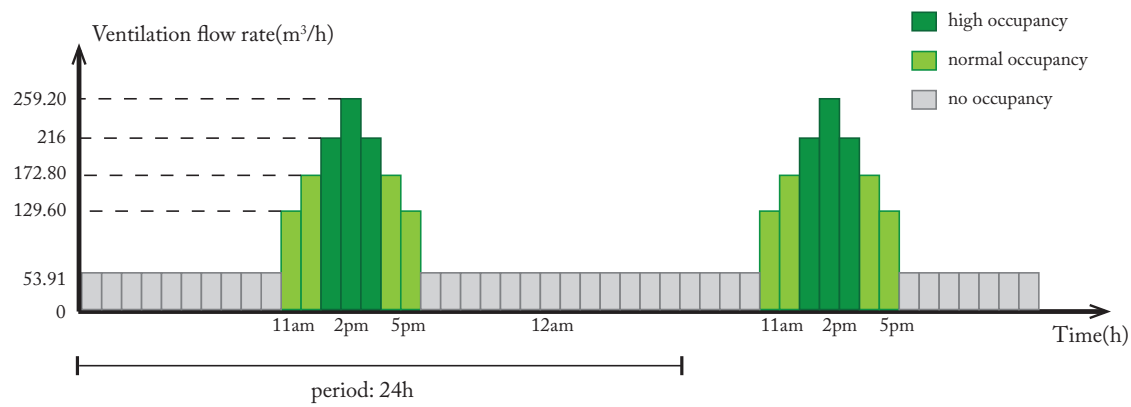


Figure 6.9: Ventilation flow rate in one exhibition room in spring and autumn

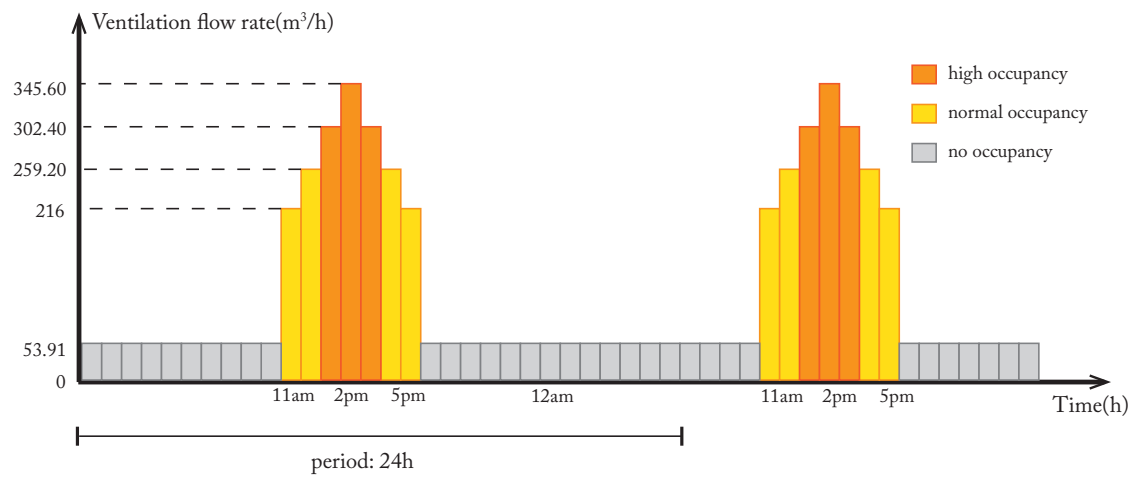


Figure 6.10: Ventilation flow rate in one exhibition room in summer

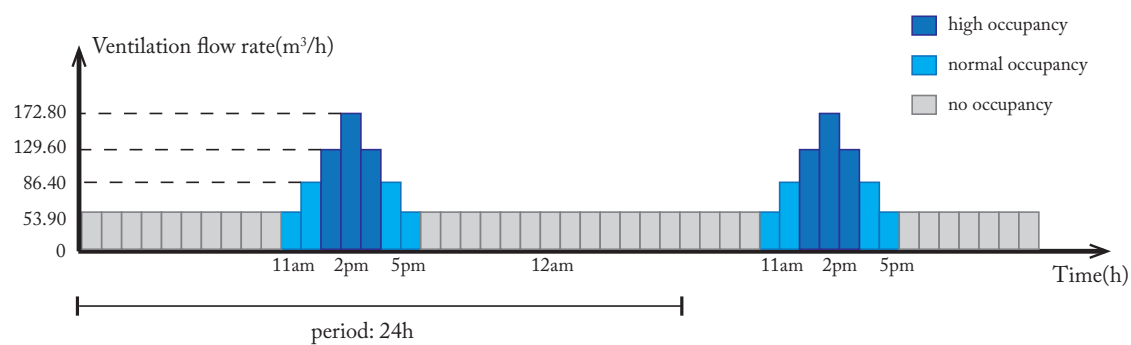


Figure 6.11: Ventilation flow rate in one exhibition room in winter

It is defined that RH setpoint in spring, summer, and winter is 50%, 60%, and 42%, respectively, and the acceptable range of RH in spring is between 45% and 55%, and the allowed range of RH in summer and winter is 55% - 65% and 37% - 47%. Infiltration is dominated by the advection effect, and the value is 0.1 dm³/s per m² floor area, which is equal to 10.85 m³/h.

6.2.5 Amount of Silica Gel

As it is mentioned at the beginning of section 6.2.1, each climate scenario is analyzed in the case of silica gel present and absent. According to the conclusion in chapter 3, 0.1 % of room volume is the optimal amount of silica gel. So, 0.126m^3 silica gel is used for analysis. The length of the packed bed is 1m, and the diameter of the cross section is 0.4m. Furthermore, it is concluded that the performance is the best when the mass flow rate of recirculation is 0.1 kg/s by trial and error method.

6.2.6 Summary of Conditions

Simulation conditions in one room with a period of one week are summarized in Table 6.1. The different variables among the climate scenarios are outside conditions, RH of supply air, and the humidity load. Spring, summer, and winter are numbered as c, d, and e, respectively. For each season, "1" means there is no silica gel in the room, and "2" means when the silica gel is applied. The yearly simulation scenario with and without silica gel is numbered as f1 and f2, which are shown in Table 6.2.

Table 6.1: *Summary of simulation scenarios in one room with a period of one week*

Scenarios		c1	c2	d1	d2	e1	e2
Amount of silica gel (m^3)		0	0.126	0	0.126	0	0.126
Period		Spring 23th - 30th, April		Summer 22th - 29th, July		Winter 17th - 24th, December	
Occupancy (person)		3 - 6		5 - 8		1 - 4	
Humidity load(kg/h)		0.18 - 0.33		0.28 - 0.43		0.08 - 0.23	
Ventilation	Flow (m^3/h)	53.91 - 259.20		53.91- 345.60		53.91 - 172.80	
	T ($^{\circ}\text{C}$)	20		20		20	
	RH	$50\% \pm 5\%$		$60\% \pm 5\%$		$42\% \pm 5\%$	
	Infiltration flow (m^3/h)	10.85		10.85		10.85	

Table 6.2: *Scenario f1 when there is no silica gel in the room a period of one year*

Scenario f1				
Amount of silica gel (m ³)		0		
Period		Mar - May(Spring) Sep - Nov(Autumn)	Jun - Aug(Summer)	Dec - Feb(Winter)
Occupancy (person)		3 - 6	5 - 8	1 - 4
Humidity load(kg/h)		0.18 - 0.33	0.28 - 0.43	0.08 - 0.23
Ventilation	Flow (m ³ /h)	53.91 - 259.20	53.91- 345.60	53.91 - 172.80
T (°C)		20	20	20
RH		50% ± 5%	60% ± 5%	42% ± 5%
Infiltration flow (m ³ /h)		10.85	10.85	10.85

Table 6.3: *Scenario f2 when there silica gel is applied in the room with a period of one year*

Scenario f2				
Amount of silica gel (m ³)		0.126		
Period		Mar - May(Spring) Sep - Nov(Autumn)	Jun - Aug(Summer)	Dec - Feb(Winter)
Occupancy (person)		3 - 6	5 - 8	1 - 4
Humidity load(kg/h)		0.18 - 0.33	0.28 - 0.43	0.08 - 0.23
Ventilation	Flow (m ³ /h)	53.91 - 259.20	53.91- 345.60	53.91 - 172.80
T (°C)		20	20	20
RH		50% ± 5%	60% ± 5%	42% ± 5%
Infiltration flow (m ³ /h)		10.85	10.85	10.85

6.3 Definition of Scenarios in the Whole Building

For simplification, the whole building can be modeled as one large room, with the area equal to the building's gross area, excluding the area where few people are present, such as the technical room, toilet, and dressing room. The room's height is assumed as an average of the story height, and it is around 4 m. Occupancy and the ventilation flow rate in the building are redefined in 6.3.2 and 6.3.3, respectively. Internal humidity load and infiltration rate are calculated based on the same standard value in 6.2.3 and 6.2.4, respectively.

6.3.1 Outside Climate Conditions and Schedule

Climate data is also collected from the NEN 5060 (NEN, 2018), which is the same as section 6.2.1. However, the simulation period of the building model is one year. Furthermore, two scenarios when the silica gel is present and absent are analyzed. It is still assumed that the National Holocaust Museum follows the same schedule every day, during the whole year and it is open between 11 am and 5 pm, and closed at other time. Special events and public holidays are not considered.

6.3.2 Occupancy

According to ABT's VO design, the maximum occupancy is 50 persons per floor (ABT & Winhov, 2019). Since only visitors mainly occupy the ground floor, first floor, and second floor. It is defined that maximum occupancy is 150 persons, which is the value at 2 pm every day in summer. Tourism seasonality is still considered. There are more visitors in summer and fewer visitors in winter, compared with ones in spring or autumn (Wang, 2019). Occupancy at other time decreases by 10 with a serial number starting with 150. The details are summarized in section 6.3.5.

6.3.3 Ventilation

The building model first simulates the scenarios when the silica gel is present and absent with the standard ventilation flow rate of 12 L/s per person. Moreover, the maximum total supply capacity of AHU is 8000 m³/h. In terms of study on reducing the ventilation flow rate when the silica gel is present, the minimum value to maintain the air quality in museums is 4.6 L/s per person (ASHRAE, 2013). The scenarios when the silica gel is present with 6 L/s and 9 L/s are chosen to compare with the scenario when the silica gel is absent with 12 L/s.

6.3.4 Amount of Silica Gel

It is calculated that 3.70m³ silica gel is needed in the whole building based on the volume of the simulated building and the recirculation flow rate is 3 kg/s.

6.3.5 Summary of Conditions

All the simulation scenarios in the building are summarized in tables(6.4 - 6.7).

Table 6.4: *Scenario g1 when there is no silica gel with 12 L/s/ per person ventilation rate*

Scenario g1				
Amount of silica gel (m ³)		0		
Period		Mar - May(Spring) Sep - Nov(Autumn)	Jun - Aug(Summer)	Dec - Feb(Winter)
Occupancy (person)		90 - 120	120 - 150	60 - 90
Humidity load(kg/h)		5.4 - 6.9	6.9 - 8.4	3.9 - 5.4
Ventilation	Flow (m ³ /h)	1661 - 4320	1661 - 6480	1661 - 3888
	T (°C)	20	20	20
	RH	50% ± 5%	60% ± 5%	42% ± 5%
Infiltration flow (m ³ /h)		332.21.	332.21	332.21

Table 6.5: *Scenario g2 when the silica gel is applied with 12 L/s per person ventilation rate*

Scenario g2				
Amount of silica gel (m ³)		3.70		
Period		Mar - May(Spring) Sep - Nov(Autumn)	Jun - Aug(Summer)	(Dec - Feb)Winter
Occupancy (person)		90 - 120	120 - 150	60 - 90
Humidity load(kg/h)		5.4 - 6.9	6.9 - 8.4	3.9 - 5.4
Ventilation	Flow (m ³ /h)	1661 - 4320	1661 - 6480	1661 - 3888
	T (°C)	20	20	20
	RH	50% ± 5%	60% ± 5%	42% ± 5%
Infiltration flow (m ³ /h)		332.21	332.21	332.211

Table 6.6: *Scenario when the silica gel is applied with 9 L/s per person ventilation rate*

Scenario h				
Amount of silica gel (m ³)		3.70		
Period		Mar - May(Spring) Sep - Nov(Autumn)	Jun - Aug(Summer)	(Dec - Feb)Winter
Occupancy (person)		90 - 120	120 - 150	60 - 90
Humidity load(kg/h)		5.4 - 6.9	6.9 - 8.4	3.9 - 5.4
Ventilation	Flow (m ³ /h)	1661 - 3888	1661 - 4860	1661 - 2916
	T (°C)	20	20	20
	RH	50% ± 5%	60% ± 5%	42% ± 5%
Infiltration flow (m ³ /h)		332.21	332.21	332.21

Table 6.7: *Scenario when the silica gel is applied with 6 L/s per person ventilation rate*

Scenario i				
Amount of silica gel (m ³)		3.70		
Period		Mar - May(Spring) Sep - Nov(Autumn)	Jun - Aug(Summer)	(Dec - Feb)Winter
Occupancy (person)		90 - 120	120 - 150	60 - 90
Humidity load(kg/h)		5.4 - 6.9	6.9 - 8.4	3.9 - 5.4
Ventilation	Flow (m ³ /h)	1661 - 2592	1661 - 3240	1661 - 1944
	T (°C)	20	20	20
	RH	50% ± 5%	60% ± 5%	42% ± 5%
Infiltration flow (m ³ /h)		332.21	332.21	332.21

6.4 Simulation Setting in Matlab/Simulink

All the variables are parameterized in Matlab script in order to change quickly and avoid mistakes.

All the equations are solved in solver ode23tb of Simulink, and the variable-step is taken. Output time with simulation period of one week and one year are 15 minutes and 1 hour, respectively.

6.5 Summary of Scenarios

Scenarios in the exhibition room are defined in section 6.2 and scenarios in the building are defined in section 6.3. They are summarized in Table 6.8, and only the simulation period, the amount of silica gel, and the ventilation flow rate are shown.

Table 6.8: The summary of all the simulation scenarios

Place	Scenario	Simulation period	Amount of silica gel (m ³)	Ventilation flow rate (L/s per person)
One exhibition room	c1	One week	0	12
	c2	One week	0.126	12
	d1	One week	0	12
	d2	One week	0.126	12
	e1	One week	0	12
	e2	One week	0.126	12
	f1	One year	0	12
	f2	One year	0.126	12
The whole building	g1	One year	0	12
	g2	One year	3.70	12
	i	One year	3.70	9
	h	One year	3.70	6

7

Simulation Results

7.1 Simulation of One Room

7.2 Simulation of the Whole Building

7.3 Design Concept of Humidity Control Device

7.4 Conclusions

7 Simulation Results

Based on the simulation conditions in chapter 6, the simulation is done in both the room model and the building model. The results are displayed separately in this chapter. The effect on relative humidity and how to design a humidity control device is studied in the room model. While the impact on energy demand and ventilation flow rate are analyzed in the building model.

7.1 Simulation of One Room

7.1.1 Results

Scenarios with a period of one week when the silica gel is present and absent are shown in one graph for each season in Figure 7.1, Figure 7.2, and Figure 7.3. The left is the relative humidity in the room, and the right is the temperature in the room.

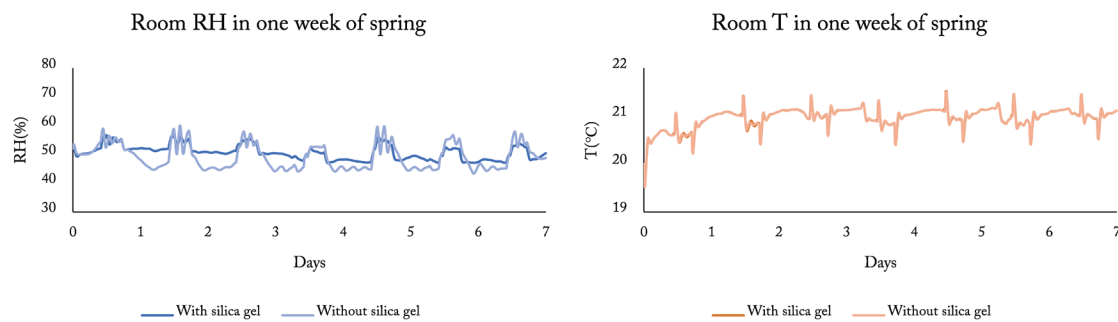


Figure 7.1: Relative humidity and temperature in scenario c1 and c2.

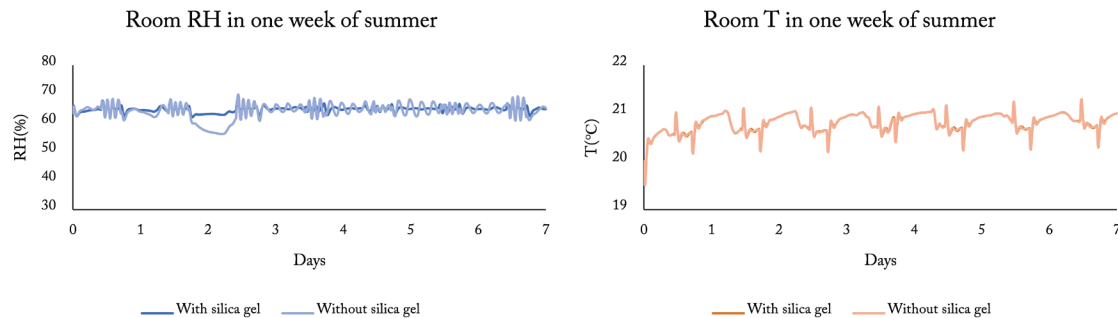


Figure 7.2: Relative humidity and temperature in scenario d1 and d2

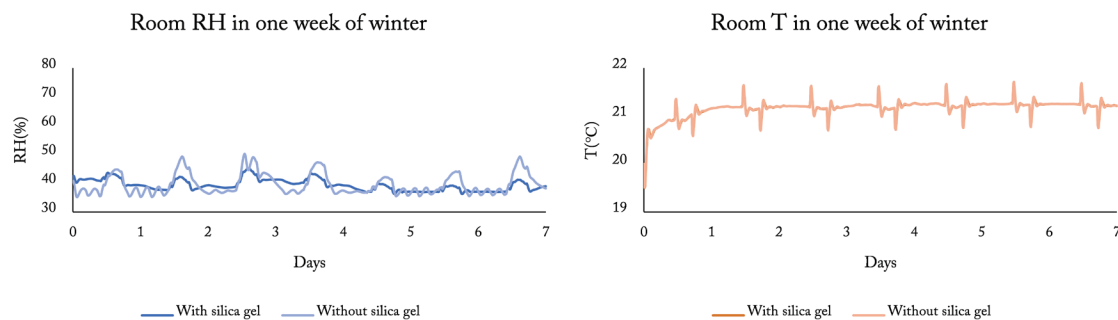


Figure 7.3: Relative humidity and temperature in scenario e1 and e2

7.1.2 Evaluation

The results in Figure 7.1, Figure 7.2 and Figure 7.3 shows that the silica gel does not have a significant influence on the temperature in the room. So, only the effect on the fluctuation of relative humidity and energy demand in one year are evaluated.

7.1.2.1 Relative Humidity

Relative humidity data for each scenario is collected to make box plots.

In spring, the fluctuation reduces by 41.1% when silica gel packed bed is applied in the room, with the range changing from between 47% and 57% to between 43% and 60%. While the average RH almost keeps the same at around 49%. And it is inferred the change of temperature does not have a large influence on relative humidity by observing original plots of temperature and RH. The effect is still huge in other seasons. However, there are outliers on the box plot in summer, which results from the inappropriate setpoint of RH. Probably the accepted fluctuation range is needed to increase to match climate conditions in summer. By excluding these outliers, the fluctuation reduces by around 63.6%. While fluctuation decreases by 35.7% with the application of silica gel in winter.

The reason why the moisture buffering effect is very considerable in summer and relatively smaller in winter is discussed. On the one hand, there are more visitors in summer than that in winter. So, the difference between the case with and without silica gel is larger. On the other hand, the hygrothermal performance of the packed bed is checked. Its temperature fluctuation range in winter is almost two times larger than that in summer, which weakens the moisture buffering effect of silica gel, according to the conclusions in chapter 5.

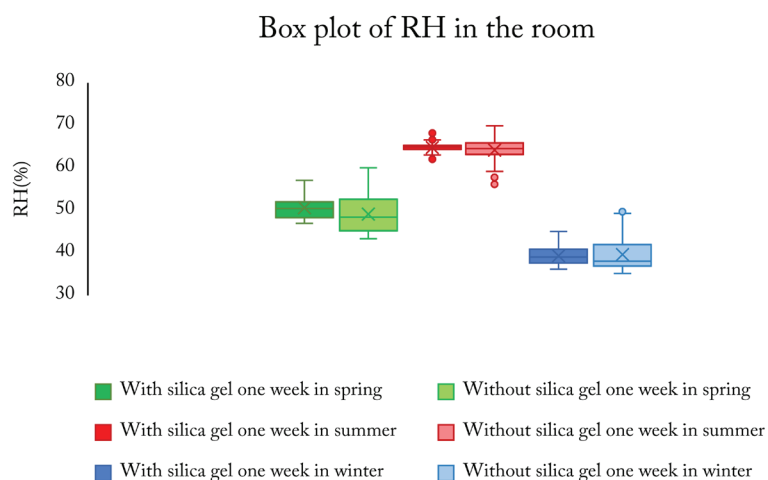


Figure 7.4: *Box plot of RH in the room*

7.1.2.2 Energy Demand

As Figure 7.5 shows, there is a decrease in energy demand in all seasons. And the application of silica gel contributes to more energy saving of humidification than that of dehumidification. The reduction in humidification energy in each season is between 26.9% and 66.4%. While the decrease of dehumidification energy is from 8.4% to 46.1%. In total, the 18.9% of energy in one year is saved.

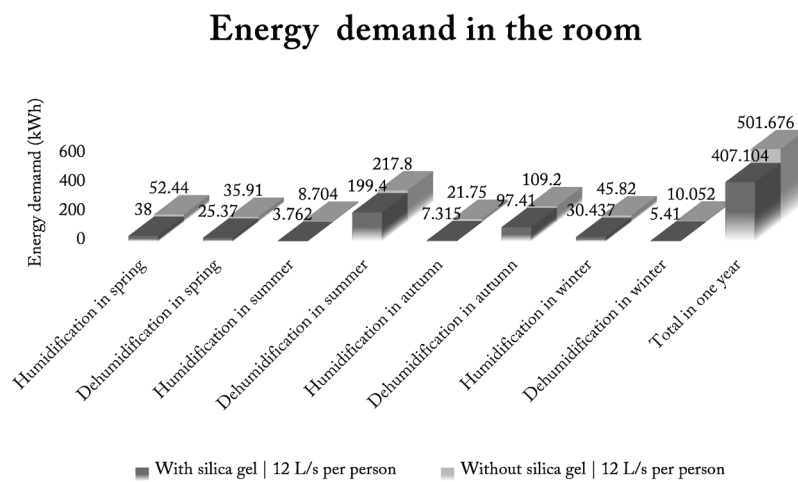


Figure 7.5: Energy demand in the room of scenario f1 and f2

7.2 Simulation of the Whole Building

Both the reduction in energy demand and ventilation flow rate are studied based on the building model. The results are presented in section 7.2.1 at first. Then they are evaluated in section 7.2.2.

7.2.1 Results

The variation of RH in the building for one year is shown in Figure 7.6, Figure 7.7, and Figure 7.8. The scenario when there is no silica gel in the room is compared with three scenarios: when the silica gel is applied with 12 L/s per person, 9 L/s per person, and 6 L/s per person, respectively.

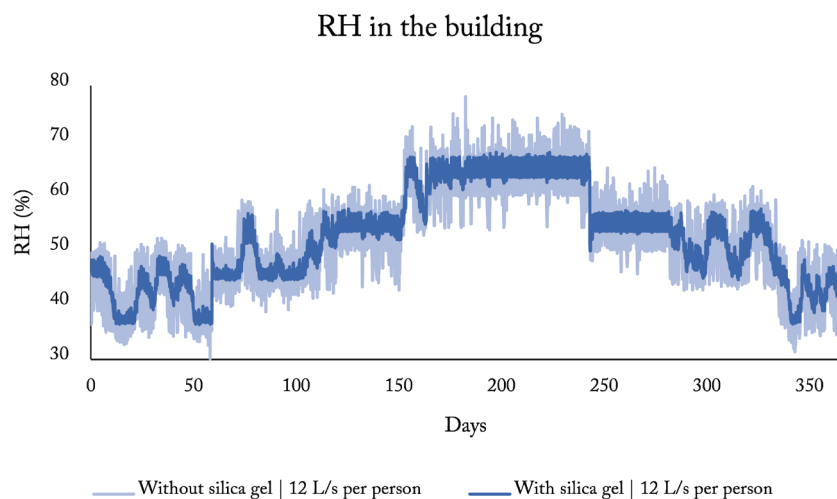


Figure 7.6: *RH of scenario g1 and g2*

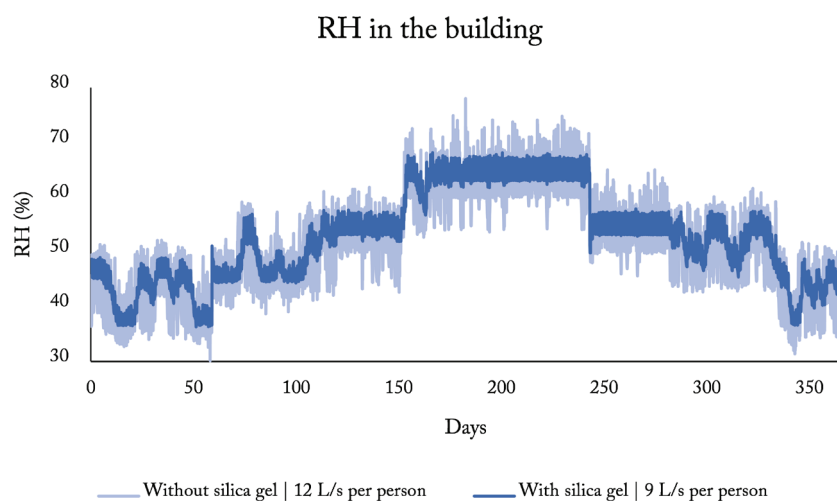


Figure 7.7: *RH of scenario g2 and b*

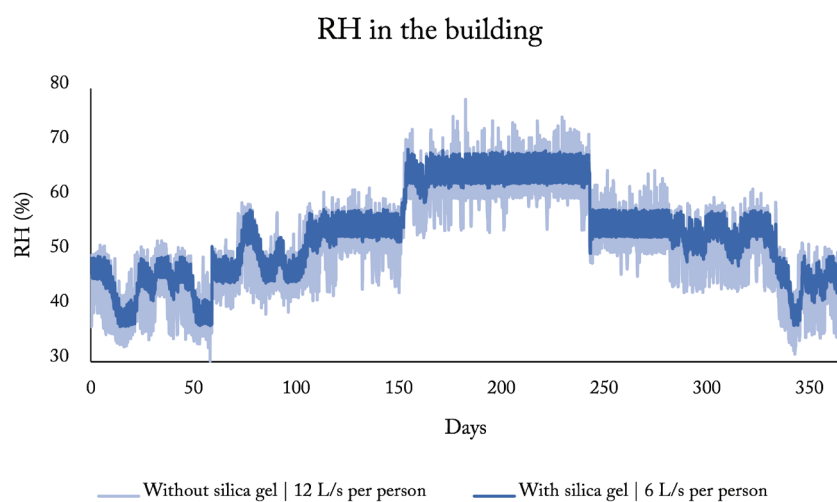


Figure 7.8: *RH of scenario g2 and i*

7.2.2 Evaluation

7.2.2.1 Relative Humidity

Box plots are used again to evaluate the effect on the relative humidity in different seasons in one year by comparing data from scenario g1 and g2. Firstly, the average RH in spring and autumn is around 50%, and the average value in winter is 42%, which is consistent with the setpoint. However, the average value in summer is 3% higher than the setpoint. So, a minor change on the setpoint is still needed. In terms of fluctuation, it drops by over half in spring and summer with the application of silica gel. While there is a 40% reduction in autumn and winter. Furthermore, the results are consistent with those in the room model due to the fact that the effect in summer is more significant than that in winter.

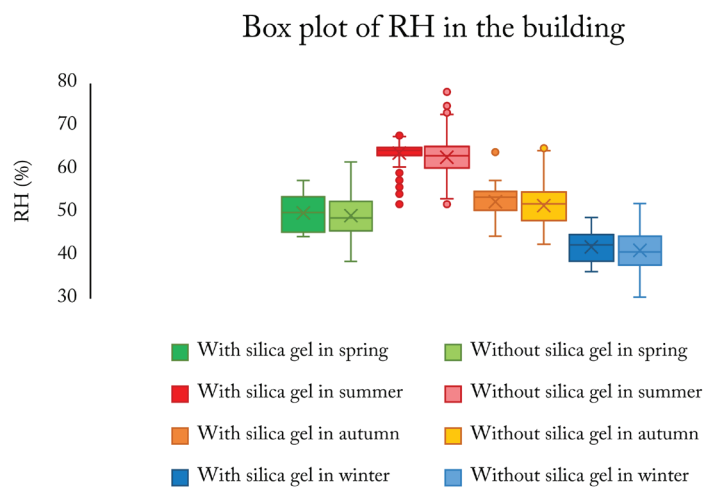


Figure 7.9: *Fluctuation of RH of scenario g1 and g2*

The range of relative humidity fluctuation in climate class A1 is defined by seasonal running average plus seasonal rise or minus seasonal drop. Since the process of calculating these three values is a little complicated, it is simplified in an alternative way. The average seasonal value is calculated in each season separately at first. Then the range is illustrated in yellow lines at the lower diagram of Figure 7.10. It is formed by average value plus or minus 5%, which is the acceptable short fluctuation in climate class A1.

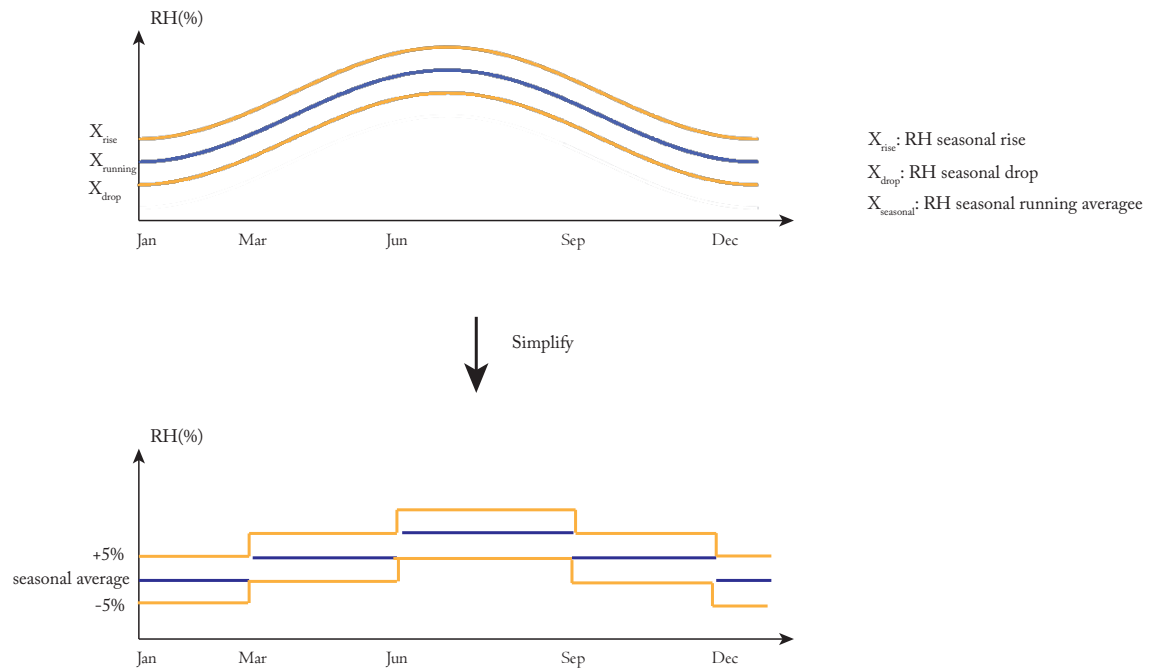


Figure 7.10: *Simplified the range of climate class A1*

The data from scenario g1, g2, h, and i are collected to check what percentage is within the limit of class A1 in Figure 7.11, Figure 7.12, Figure 7.13, and Figure 7.14. It shows that the proportion of data that meet the A1 requirement rises from 72.3% to around 90% with the silica gel. Furthermore, the lower ventilation flow rate does not influence the matching degree since the percentage in scenario g2, h, and i is quite similar.

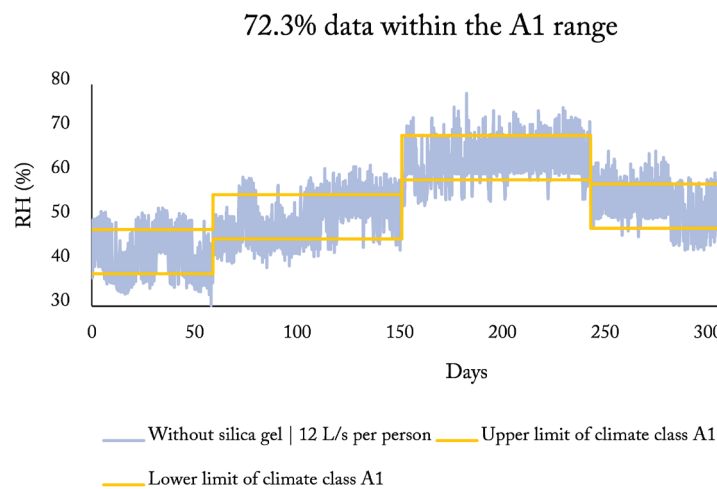


Figure 7.11: *Evaluation of climate class A1 in scenario g1*

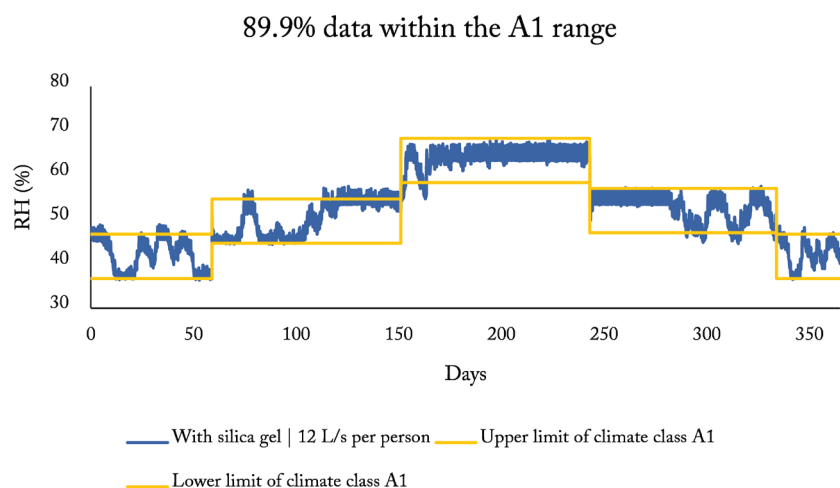


Figure 7.12: *Evaluation of climate class A1 in scenario g2*

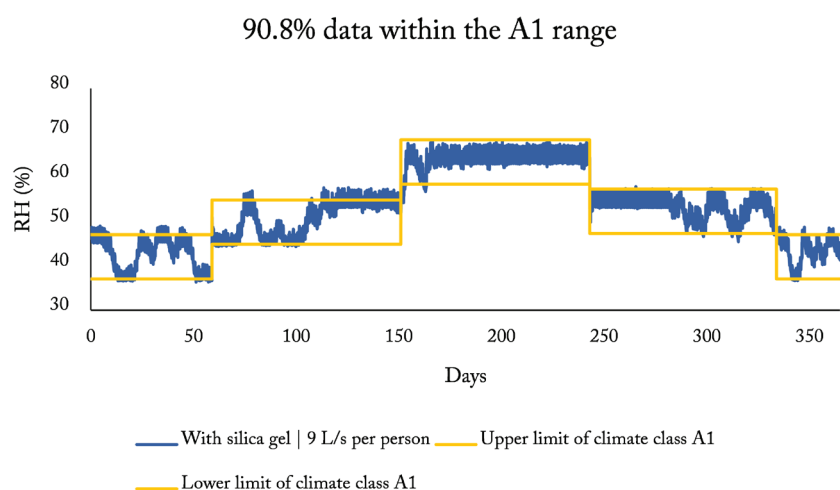


Figure 7.13: *Evaluation of climate class A1 in scenario h*

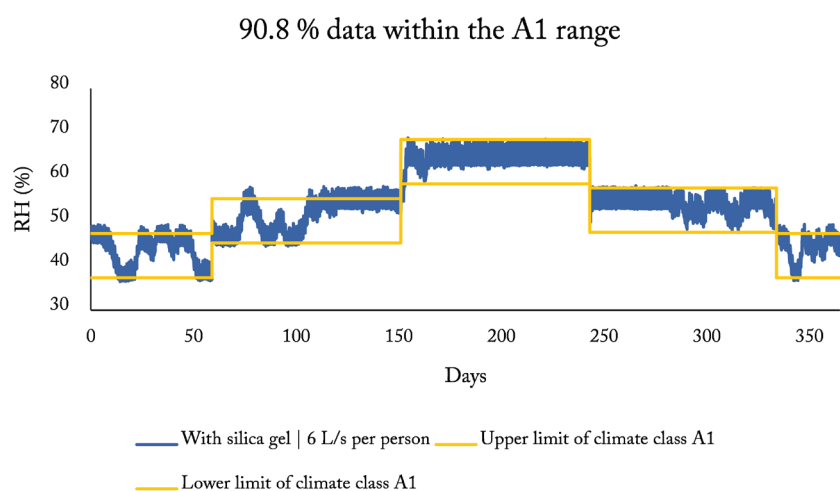


Figure 7.14: *Evaluation of climate class A1 in scenario i*

7.2.2.2 Energy Demand and Ventilation Flow Rate

There is more dehumidification energy required in summer and no dehumidification in winter in Figure 7.15. It matches the reality since the air is humid in summer and dry in winter. By comparing scenario g1 and g2, energy demand in all seasons decreases. For instance, the energy demand for dehumidification in spring drops by 34.1%, and the energy demand for humidification in autumn decrease by 59.3%. In total, 16.2% of energy is saved in one year.

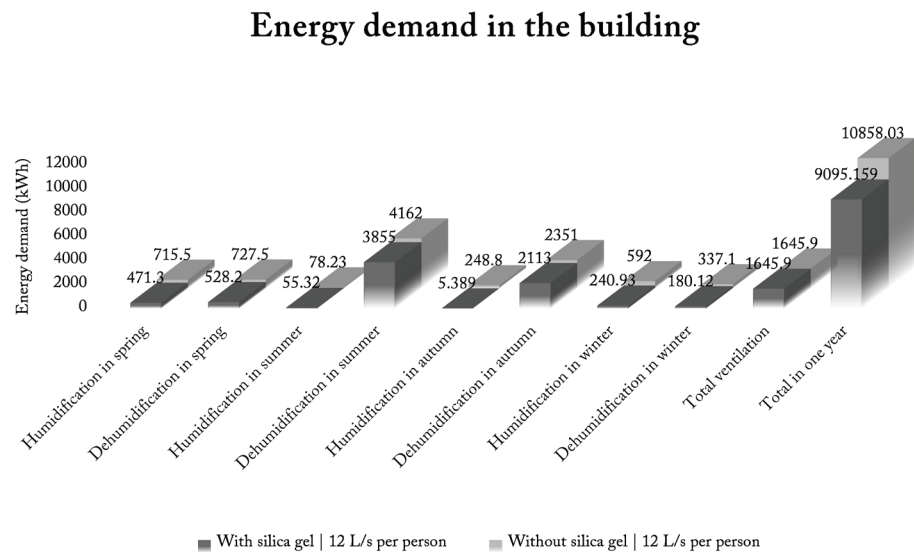


Figure 7.15: Energy demand of scenario g1 and g2

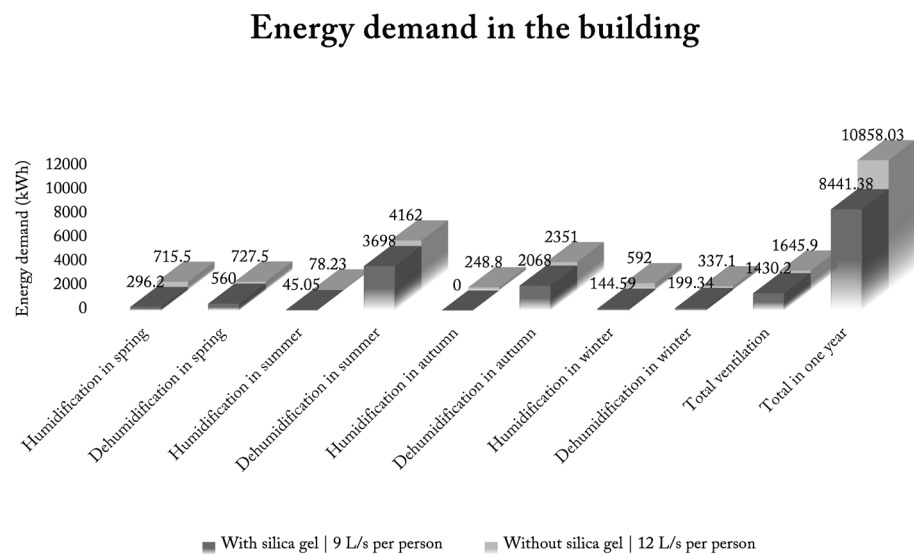


Figure 7.16: Energy demand of scenario g2 and h

Energy demand in the building

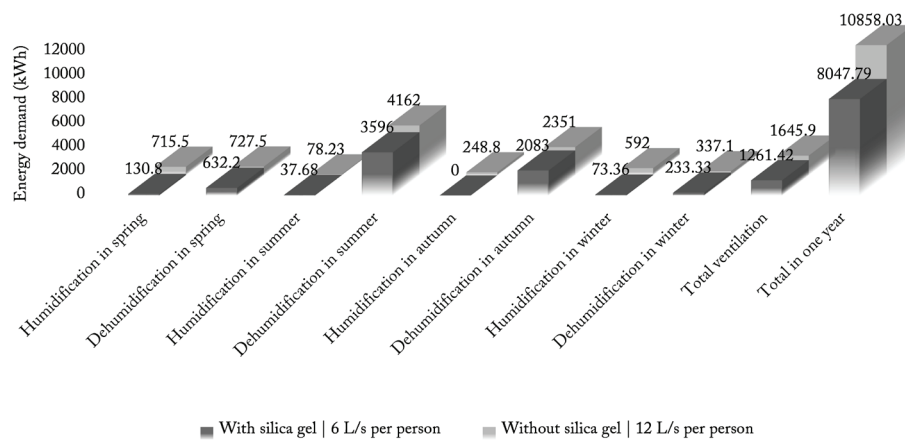


Figure 7.17: Energy demand of scenario g2 and i

The results also show the possibility of a reduction in the ventilation flow rate. In Figure 7.16 and Figure 7.17, it decreases to 9 L/s per person and 6 L/s per person when the silica gel is present in the room. And the climate is still more stable than that of scenario g1 when the silica gel is absent with the ventilation flow rate of 12 L/s per person. Besides, a lower ventilation flow rate saves more electricity to drive fans. At the same time, it also reduces even more energy consumption for humidifying and dehumidifying air in the room since the smaller change occurs on the total amount of vapor in the room. Yearly energy demand reduces 22.3% and 25.9% in scenario h and i, respectively.

7.3 Design Concept of Humidity Control Device

The amount of silica gel needed in one room is around 0.126 m^3 . And the form of the packed bed does not influence the buffering effect. The pressure drop at the access should be as low as possible to have silent small supply fans for recirculation, and it saves energy as well. Since the pressure drop depends much on the length of the packed bed, it indicates that a larger diameter and smaller height are preferable. Some possible dimensions of the packed bed are shown in Table 7.1.

Table 7.1: The dimension of packed bed

Length (m)	Diameter(m)	Cross section(m^2)	Pressure drop (Pa)
0.444	0.6	0.283	47.11
0.327	0.7	0.385	25.49
0.25	0.8	0.503	14.92
0.198	0.9	0.636	9.34
0.16	1	0.785	6.11

Based on Darcy' law, the pressure drop along the length of the packed bed can be calculated as follow:

$$Q_{re} = \frac{kA_c}{\mu L_b} \Delta p \quad (7.1)$$

Where k is the permeability of packed bed, which is around $5 \times 10^{-8} \text{ m}^2$. A is the cross section area [m^2], μ is the dynamic viscosity, which is around $1.8 \times 10^{-5} \text{ Pa} \cdot \text{s}$. Δp is the pressure drop. Q_{re} is the volumetric flow rate of recirculation [m^3/s].

Since the recirculation mass flow is 0.1 kg/s , the pressure drop along the packed bed with different dimensions is calculated in Table 7.2.

Table 7.2: The pressure drop along the packed bed

Length (m)	Diameter(m)	Cross section(m^2)	Volume(m^3)
0.444	0.6	0.283	0.126
0.327	0.7	0.385	0.126
0.25	0.8	0.503	0.126
0.198	0.9	0.636	0.126
0.16	1	0.785	0.126

The larger diameter, the smaller the pressure drop is. However, it is hard to achieve a uniform flow since more supply fans are needed. So, the container with a diameter of 0.8 m is chosen, and five computer fans with a diameter of 0.2 m are installed at the top of the cylinder container.

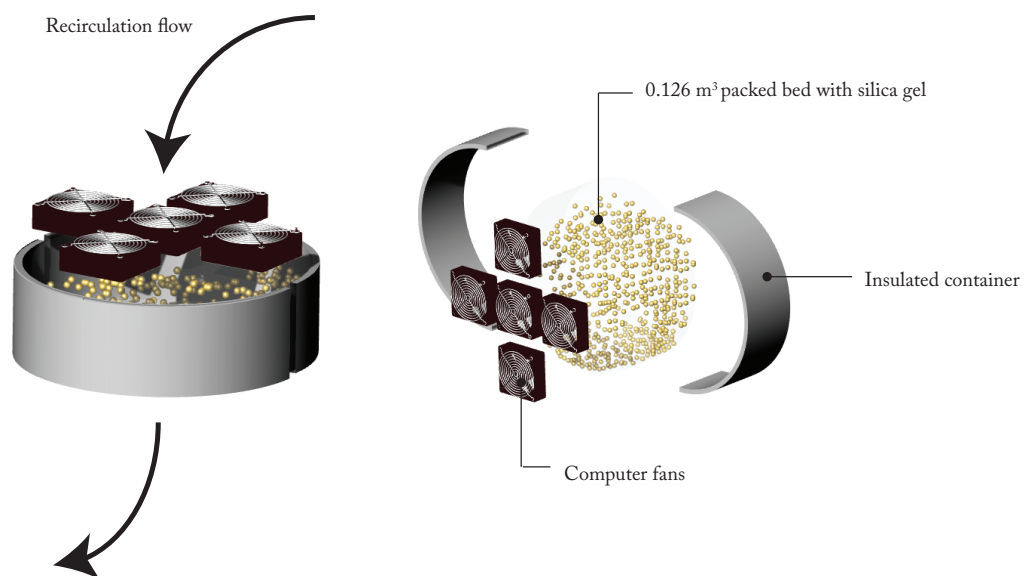


Figure 7.18: The humidity control device

The power of the supply fan can be approximately calculated by:

$$P_{fan} = \frac{Q_{re} \Delta p}{\eta_{fan}} \quad (7.2)$$

So the power of one supply fan is around 0.8W. So, yearly energy consumption of five fans is 7kWh, which is negligible, compared with the reduction effect on humidification, dehumidification, and ventilation energy.

7.4 Conclusions

The effect on the stability of relative humidity, energy savings, and reduction in ventilation rate with the application of silica gel in the room is studied by evaluating results from both room and building level. And it is concluded that silica gel takes effect on these three aspects.

Firstly, silica gel is capable of reducing the relative humidity fluctuation by factor 2 in both the room and building with the amount equal to 0.1 % of room volume. Secondly, silica gel also can reduce humidification and dehumidification energy demand because of its excellent buffering effect. The yearly energy usage can be saved over one-tenth. Thirdly, even the ventilation flow rate can be minimized to 6 L/s per person under the premise of maintaining good air quality and acceptable relative humidity. Based on this value, the total supply airflow reduces by half, which indicates the possibility of reducing the size of AHU. Besides, the design concept also shows the feasibility of combining silica gel with the climate system in reality. Meanwhile, it is energy-efficient and has a tiny volume.

8

Discussion

8.1 Chapter 2 Literature Study

8.2 Chapter 3 Feasibility Study

8.3 Chapter 4 Model Development

8.4 Chapter 5 Model Verification and Validation

8.5 Chapter 6 Simulation Conditions

8.6 Chapter 7 Simulation Results

8 Discussion

The previous work is discussed chapter by chapter. It includes the incompleted tasks, the supplementary explanation of modeling assumptions, and the issues of the imperfect model.

8.1 Chapter 2 Literature Study

The previous plan of visiting more museums in the Netherlands and writing a section about the summary of active and passive design approaches is not achieved due to the time limit and coronavirus situations. Moreover, the study on the control technology of HVAC is not studied in depth. So, it is not written in this chapter.

8.2 Chapter 3 Feasibility Study

Due to a lack of setting of boundary conditions in model 1.0, the relative humidity value exceeds 100% sometimes, resulting from the low ventilation rate. However, this is just the feasibility study to check the reduction in the fluctuation of RH mathematically instead of simulating the real conditions.

8.3 Chapter 4 Model Development

There are still some parts that are needed to improve in both model 2.0 and 3.0. Firstly, the hygric part is quite simple since the moisture transfer between the air in the room and construction is neglected. Although it is proved that the effect is only one-tenth of the advection effect in chapter 5, it is still slightly different from the real conditions, which reduces the accuracy of the model.

Secondly, the moisture sorption and desorption isotherms are simplified as a linear function with the slope of 350 since the real hysteresis is hard to model. However, the real desorption isotherm has a smaller slope than that of sorption isotherm. So, the silica gel's ability to release moisture is overestimated slightly.

Thirdly, the air handling unit part is simplified since only the humidifier and dehumidifier are modeled, and it is assumed the perfect process where the humidity ratio is directly used. So, it is possible to create a more advanced model so that the energy performance can be evaluated more accurately. The effect on heating and cooling can be simulated as well. In addition, the setpoint in summer is inappropriate in the current case. The PI controller is not always stable since it is only tuned by simple trial and error method, which causes fluctuation in results sometimes. As the results in chapter 7 shows, the fluctuation of RH due to the defective is more noticeable in the case with silica gel than the case without silica gel.

8.4 Chapter 5 Model Verification and Validation

Due to the fact that the National Holocaust Museum is closed for renovation and the climate chamber at the faculty is not available for students, the experiment part is eliminated. So, the validation is achieved by using Design Builder as comparative software. Although it is well-validated, there are still some drawbacks of modeling hygric conditions. The humidity control is too ideal since it directly controls the relative humidity value to setpoint range, namely, there is no data exceeding the control range in results. So the humidity control part in model 3.0 can be validated sufficiently. The simulated scenarios are defined as simple as possible so that the cause for the difference between the two models can be found. The more complicated scenarios are not included due to the time limit.

8.5 Chapter 6 Simulation Conditions

Since there is no available data on the number of visitors in the past years, the occupancy is simplified as the normal distribution function every day. However, the situations are more complicated. For instance, there could be fewer visitors in museums sometimes. Moreover, there is no specific function of occupancy. But the scenarios that are defined in this chapter can be regarded as the worst. If the silica gel is effective enough in these scenarios, it will be more capable in reality.

The building model is assumed as one large room model. The case in reality is much more complicated since the climate in every exhibition room is different from each other. Besides, all the silica gel packed bed is combined as a larger one with a large recirculation flow going through in the building model instead of placing them in every room separately, which might cause more optimistic results.

8.6 Chapter 7 Simulation Results

The initial conditions of RH and temperature in silica gel nodes have a key role in the simulation results. It is preferable to set these two parameters consistent with those in the air node in the room. The initial conditions of RH is 50% in spring or autumn, 63% in summer, and 45% in winter. The inappropriate setting weakens the buffering effect of silica gel since it needs a period of time to reach the dynamic equilibrium with the relative humidity in the room.

As mentioned in 8.3, the simplified desorption isotherm causes the higher moisture capacity of silica gel when it releases the moisture, enhancing its effect on saving humidification energy.

The buffering effect of silica gel is expected to compare with that of wood or lime plaster. It is not done due to the limited time.



Conclusions

9.1 Conclusions to Sub-questions

9.2 Conclusions to General Questions

9 Conclusions

This chapter answers the questions in chapter 1. Both of sub-research and general research questions are solved.

9.1 Conclusions to Sub-questions

The effect of high-capacity of hygroscopic materials on climate in museums is studied schematically in the whole project. All the research questions are answered individually in corresponding chapters.

1. What simulation tools are available and what is their expected accuracy in estimating the hygric conditions in the exhibition space?

In chapter 3 and 4, three models with different complexity are developed, which forms a schematic study of modeling methods. Model 1.0 focuses on the feasibility of applying silica gel in the room with the low ventilation rate. Since it is quite simple, its validity is not discussed. Both model 2.0 and 3.0 consists of three parts: the thermal part, the hygric part and, air handling unit part. The main difference between the two models is whether the silica gel is modeled as separate nodes.

By comparing with Design Builder model in three simple scenarios, it is observed that the combination of heat and moisture transfer between silica gel and the air in the room and the estimation of humidity load from visitors in model 3.0 are accurate enough since difference on fluctuation range is less than 2% from the Design Builder model. While the perfect contact between silica gel and air in model 2.0 results in more stable values, which is not realistic. However, the humidity control in model 3.0 is not validated sufficiently since the control in Design Builder is too ideal. Therefore, the heat and moisture transfer conditions in the exhibition space can be estimated well in model 3.0, and the accuracy of its humidity control needs further research.

2. To what extent can the fluctuation of relative humidity be reduced by using the high capacity hygroscopic material?

In model 1.0, it is found that the proper amount of silica gel is 0.1% of room volume. The buffering effect is quite optimistic because the model is quite simple. It is not discussed here, and only the simulation results from model 3.0 are evaluated.

The simulation in chapter 7 is done on the level of both the room and the building. In the room model, scenarios with a period of one week in different seasons are analyzed. It is discovered that the reduction in fluctuation is between 35.7% and 63.6% when the silica

gel is used in the exhibition room. The effect varies from seasons to seasons, and it is more effective in summer than winter. Because the temperature fluctuation of the packed bed in winter is larger than that in summer, weakening its moisture buffering effect. In the building model, the performance of silica gel is consistent with that in the room model with over 50% reduction in spring and summer and around 40% reduction in autumn and winter. Besides, the matching degree with ASHRAE climate class A1 raises from 73% to 90%. In short, it is concluded that the fluctuation can reduce by a factor of 2 with the use of the silica gel in exhibition space, and it is preferable that the temperature in the room is kept constant to avoid the adverse impact.

3. What is the influence on energy demand by using the high capacity hygroscopic material?

With all the exhibition space being equipped with the silica gel packed bed, the yearly energy in the whole building can be saved around 16.2%. Because of the high moisture capacity of the silica gel, it can release moisture when the surrounding air becomes dry and absorb moisture when the air becomes humid. With this moisture buffering effect, the load on the air handling unit is lightened. So, it is concluded that the conservative estimation of energy demand for humidification and dehumidification can be reduced by a factor of 0.9.

4. To what extent can the ventilation rate of air handling be reduced by using high-capacity moisture buffering materials?

On the premise that indoor air quality in exhibition space is maintained, the ventilation flow rate is reduced to 9 L/s per person and 6 L/s per person when the silica gel is used. Compared with the scenario when there is no silica gel in the room with a standard value of 12 L/s per person, the indoor climate is still more stable in the scenario with lower ventilation flow rate in relative humidity aspects. Because of the excellent moisture buffering effect of silica gel, less ventilation is needed in the room. The existing total supply capacity is 8000 m³/h, and it is possible to decrease it to 4000 m³/h when 6 L/s per person is used as the standard value.

5. How could buffering materials be integrated into construction or climate systems?

The fifth sub-questions are solved by designing a humidity control device, and it is a flat cylinder container with five computer fans on the top to introduce the recirculation flow. The diameter of cross section of the container is 0.8m, and its length is 0.25m. A rough calculation shows it is silent since the small pressure drop is needed. Furthermore, it is energy-efficient because the yearly energy consumption is 7kWh, which is negligible compared with the amount of saved energy.

9.2 Conclusions to General Questions

Silica gel can be used not only in the display case but also in the exhibition room by integrating a packed bed with a simple climate system. Firstly, the on stabilization effect on the relative humidity is significant, which is beneficial to the conservation of the exposed collection, the comfort of humans, and the interior historic construction surface in the exhibition space. In terms of energy performance, a small amount of humidification and dehumidification energy can be saved due to the moisture buffering effect of silica gel. Furthermore, there is a possibility of using a smaller air handling unit with less complexity since less ventilation is needed when the silica gel is used in the room. So, the cost of producing and buying a more complicated installation is reduced. In a word, the silica gel as a kind of hygroscopic material is evaluated excellent in aspects of its effect on air conditions and energy performance in the exhibition space of museums.

10

Recommendations

10.1 Recommendations to Museums

10.2 Recommendations to Future Research

10 Recommendations

10.1 Recommendations to Museums

The thesis shows the potential of using silica gel to stabilize the relative humidity in the room. It is recommended to use this small humidity control device in one of the exhibition rooms as a trial. At the same time, a sensor can be used to monitor the data and it can be compared with relative humidity in other rooms without silica gel or with traditional buffering materials. A little more silica gel is needed in practice when it is used on the higher floor level because the warmer air contains more moisture. Besides, it is preferable to control the room temperature to constant value since it weakens the moisture buffering effect.

In terms of the setpoint of the air handling unit, it is not necessary to follow the ASHRAE requirement. As shown in chapter 7, the RH control range from 55% to 65% in summer is improper in this project. It should match the RH varying in the room. So, it is suggested to monitor the relative humidity and calculate the appropriate range, which can give better humidity control in the room.

Furthermore, it is suggested that the number of visitors is recorded because it is useful values for analysis of indoor climate in the future.

10.2 Recommendations to Future Research

This project can be used as the first step to study the application of this humidity control approach in exhibition space.

Further study on the humidity control device can continue. For instance, the hygrothermal performance of packed bed can be extended in inlet air conditions, and whether the performance can improve when the heating and cooling are combined with simple supply fans.

The model also can be extended to a complete building model, which can be applied to analysis in more museums. To achieve it, the moisture transfer between construction and air in the room can be added at first. Then, a more advanced air handling unit model with the addition of a heating and cooling coil can be developed to replace the existing simple one. Besides, the control part also can be tuned and optimized to get more stable and precise values.

The experiment in the climate chamber or in one museum can be done if it is possible,

which can not only prove the simulation results but also compare it with that of other hygroscopic materials, such as wood and lime plaster.

As for the production of the device, it can also be utilized by industrial design to integrate engineering concepts with artwork in museums.

11 Appendix

11.1 Appendix A: Implementation of Model 1.0

11.1.1 Matlab Script

```
% Simple thermal and hygric model in exhibition room

clear; % clear all the data in the workplace

% -----PHYSICAL INPUT -----

% construction parameters
l_room      = 5.663;          % length of the room (m)
w_room      = 5.480;          % width of the room (m)
h_room      = 4;              % height of the room (m)
V_silica_gel = 0.259;         % silica gel volume (m3)
V_room = l_room*w_room*h_room; % room air volume (m3)

% constants
rho_air      = 1.2;           % mass density of air (kg/m3)
rho_silica_gel = 600;         % mass density of silica gel (kg/m3)

% hygric parameters
c            = 0.034;         % corelation coefficient between isotherm curve o
flow_in      = 0.149;         % mass flow rate ventilation air (kg/s)
x_in         = 0.0073;        % humidity ratio outdoor air(kg/kg)
g_person     = 77.575*10^(-5); % moisture production per second(kg/s)
x_sat        = 0.014659;      % saturation humidity ratio of air
T_period     = 14400;

% mass balance
x_i = [];
x_i(1) = x_in;
dt = 1;
T(1)= dt;
i=1;

for j=1:200

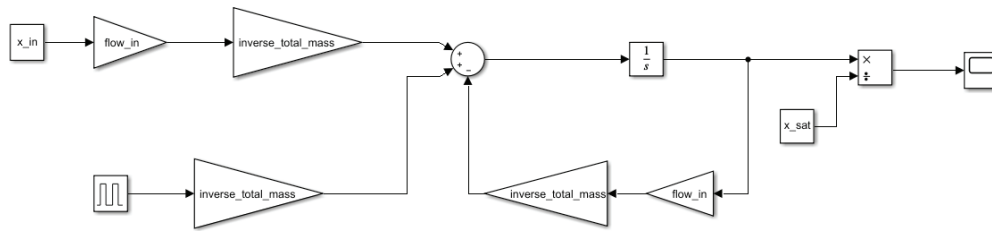
    if mod(j,2)==0
        G=0;
    else
        G=g_person;
    end

    while i*dt<j*T_period/2
        dxdt(i) = (G + flow_in * (x_in - x_i(i)))/(rho_air * V_room + rho_silica_gel *
        x_i(i+1) = x_i(i) + dxdt(i) * dt;
        T(i+1)=i*dt;
        i=i+1;
    end

end

RH=x_i/x_sat*100;
plot(T/3600,RH, '-');
xlabel('Hour(h)');
ylabel('RH(%)');
```

11.1.2 Simulink Code



11.2 Appendix B: Feasibility Study Data

11.2.1 Group 1: 0 kg/m² Silica Gel

Ventilation rate (L/s/m ²)	Humidity load (kg/s/m ²)	Period (h)	ΔRH (%)	\overline{RH} (%)
0.5	0.625	0.25	2.01	84.62
		1	7.99	84.62
		4	29.99	84.62
	1.25	0.25	4	119.4
		1	16	119.4
		4	59.95	119.4
	2.5	0.25	8	189.1
		1	31.9	189.1
		4	119.9	189.1
1	0.625	0.25	2.01	67.68
		1	7.91	67.68
		4	25.61	67.68
	1.25	0.25	4.01	85.56
		1	15.82	85.56
		4	51.05	85.56
	2.5	0.25	8	121.3
		1	31.6	121.3
		4	102.41	121.3
2	0.625	0.25	2.02	58.74
		1	7.58	58.74
		4	16.93	58.74
	1.25	0.25	4.03	67.68
		1	15.17	67.68
		4	33.89	67.68
	2.5	0.25	8.06	85.56
		1	30.31	85.56
		4	67.84	85.58
4	0.625	0.25	2.02	54.24
		1	6.46	54.24
		4	8.87	54.24
	1.25	0.25	4.03	58.68
		1	12.92	58.68
		4	17.74	58.68
	2.5	0.25	8.06	67.56
		1	25.84	67.56
		4	35.47	67.56

11.2.2 Group 2: 2.5 kg/m² Silica Gel

Ventilation rate (L/s/m ²)	Humidity load (kg/s/m ²)	Period (h)	ΔRH (%)	\overline{RH} (%)
0.5	0.625	0.25	0.13	84.62
		1	0.49	84.62
		4	1.96	84.6
	1.25	0.25	0.3	119.45
		1	1	119.4
		4	3.9	119.45
	2.5	0.25	0.5	189.05
		1	1.9	189.05
		4	7.9	189.05
1	0.625	0.25	0.12	67.68
		1	0.49	67.68
		4	1.96	67.68
	1.25	0.25	0.25	85.56
		1	0.99	85.56
		4	3.93	85.56
	2.5	0.25	0.5	121.35
		1	2	121.3
		4	7.8	121.3
2	0.625	0.25	0.12	58.74
		1	0.49	58.74
		4	1.96	58.74
	1.25	0.25	0.25	67.68
		1	0.98	67.83
		4	4.21	67.68
	2.5	0.25	0.49	85.56
		1	1.97	85.56
		4	7.83	85.56
4	0.625	0.25	0.12	54.24
		1	0.49	54.24
		4	1.93	54.25
	1.25	0.25	0.24	58.68
		1	0.98	58.68
		4	3.85	58.67
	2.5	0.25	0.49	67.56
		1	1.97	67.56
		4	7.69	67.54

11.2.3 Group 3: 5 kg/m² Silica Gel

Ventilation rate (L/s/m ²)	Humidity load (kg/s/m ²)	Period (h)	ΔRH (%)	\overline{RH} (%)
0.5	0.625	0.25	0.06	84.61
		1	0.25	84.62
		4	1.01	84.60
	1.25	0.25	0.1	119.45
		1	0.5	119.45
		4	2	119.3
	2.5	0.25	0.3	189.05
		1	1	189.1
		4	4.1	189.05
1	0.625	0.25	0.06	67.68
		1	0.25	67.68
		4	1.01	67.68
	1.25	0.25	0.13	85.56
		1	0.51	85.56
		4	2	85.56
	2.5	0.25	0.2	121.3
		1	1	121.3
		4	4	121.3
2	0.625	0.25	0.06	58.74
		1	0.25	58.74
		4	1.01	58.74
	1.25	0.25	0.13	67.68
		1	0.51	67.68
		4	2.02	67.67
	2.5	0.25	0.25	85.56
		1	1.01	85.56
		4	4.03	85.55
4	0.625	0.25	0.06	54.24
		1	0.25	54.24
		4	1	54.24
	1.25	0.25	0.13	58.68
		1	0.5	58.68
		4	2.01	58.68
	2.5	0.25	0.25	67.56
		1	1.01	67.56
		4	4.02	67.56

11.2.4 Group 4: 10 kg/m² Silica Gel

Ventilation rate (L/s/m ²)	Humidity load (kg/s/m ²)	Period (h)	ΔRH (%)	\overline{RH} (%)
0.5	0.625	0.25	0.04	84.56
		1	0.13	84.60
		4	0.51	84.62
	1.25	0.25	0.07	119.39
		1	0.20	119.4
		4	1.00	119.4
	2.5	0.25	0.10	188.95
		1	0.50	188.95
		4	2.10	189.05
1	0.625	0.25	0.03	67.68
		1	0.13	67.68
		4	0.51	67.68
	1.25	0.25	0.06	85.55
		1	0.25	85.56
		4	1.03	85.56
	2.5	0.25	0.20	121.3
		1	0.50	121.35
		4	2.00	121.3
2	0.625	0.25	0.03	58.74
		1	0.13	58.74
		4	0.51	58.74
	1.25	0.25	0.06	67.68
		1	0.26	67.68
		4	1.03	67.68
	2.5	0.25	0.13	85.56
		1	0.51	85.56
		4	2.05	85.56
4	0.625	0.25	0.03	54.24
		1	0.13	54.24
		4	0.51	54.24
	1.25	0.25	0.07	58.67
		1	0.26	58.67
		4	1.03	58.67
	2.5	0.25	0.13	67.56
		1	0.51	67.56
		4	2.04	67.55

11.3 Appendix C: Implementation of Model 2.0

11.3.1 Matlab Script

```
% Model 2.0

clear;

% ----- VARIABLES -----

building_function_type = 1; % 1 = NHM, 2 = residence
building_age_type = 2;      % affects building_facade_type, 1 = new, 2 = old
building_method_type = 2;   % see facade_values, 1= light-weight, 2= medium-weight, 3
infiltration_type = 2;      % 1 = no infiltration, 2 quite airtight, 3 normal, 4 quit
WWR_type = 1;              % see WWR_values, window to wall ratio
glazing_type = 2;          % see glazing_values
orientation = 30;          % in degrees. 0 degrees means that facade with orien1 =
                           % 90 degrees means that facade with orien1 =
                           % 180 degrees means that facade with orien1 =
                           % etc.
                           % orientation must be a real number between 0 and 360

% ----- SCRIPT -----

start_time = 0*86400; % start time of the simulation
stop_time = 365*86400; % stop time of the simulation

% Glazing data for calculation of transmission of direct solar as function of inciden
glazing_transmission_data = [
1.470E-02    1.486E+00   -3.852E+00    3.355E+00   -1.474E-03
5.546E-01    3.563E-02   -2.416E+00    2.831E+00   -2.037E-03
7.709E-01   -6.383E-01   -1.576E+00    2.448E+00   -2.042E-03
3.462E-01    3.963E-01   -2.582E+00    2.845E+00   -2.804E-04
2.883E+00   -5.873E+00    2.489E+00    1.510E+00   -2.577E-03
3.025E+00   -6.366E+00    3.137E+00    1.213E+00   -1.367E-03
3.229E+00   -6.844E+00    3.535E+00    1.088E+00   -2.891E-03
3.334E+00   -7.131E+00    3.829E+00    9.766E-01   -2.952E-03
3.146E+00   -6.855E+00    3.931E+00    7.860E-01   -2.934E-03
3.744E+00   -8.836E+00    6.018E+00    8.407E-02    4.825E-04];

glazing_values = [
1.6  0.7  5
1.65 0.3  6
0.7  0.5  5
0.7  0.1 10]; % All values for U, SHGC and transmission type

glazing_properties = glazing_values(glazing_type,:);

% Define glazing transmission type for calculation of transmission of direct solar as
% function of incidence angle. See report 'Modeling Windows in Energy Plus
% with Simple Performance Indices', LBNL report 2804E, October 2009
glazing_transmission_type = glazing_properties(3);
% 1 = A- 3mm clear
% 2 = B- 3mm bronze
% 3 = C- 6mm bronze
% 4 = D-Single Coated
% 5 = E-Double clear 3mm
% 6 = F-Double coated 3mm clear
% 7 = G-Double 3mm tinted 3 mm clear
```

```

% 8 = H-Double glazing: coated - 6mm clear
% 9 = I-Double Glazing:6mm tinted - 6mm clear
% 10= J-Triple-Coated-3mm clear- coated

WWR_values = [ % Window to wall ratio of facade at orien1, orient2, orient3 and orien
0.23 0.0 0.0 0.0 % room with one facade orientated on orien1
0.0 0.0 0.3 0.0]; % room with one facade orientated on orien3

TinIC = 20; % initial temperature in all nodes (23 is average of heating a

room.depth = 5.48;
room.width = 5.465; % in this case width is in orien2-orien4 direction
room.height = 4.6;
room.volume = room.depth*room.width*room.height; % air volume room, depth x width
room.area = room.depth*room.width;

WWR_properties = WWR_values(WWR_type,:);

A_gl_orien1 = WWR_properties(1)*room.width*room.height; % surface area glass orien1
A_gl_orien2 = WWR_properties(2)*room.depth*room.height; % surface area glass orien2
A_gl_orien3 = WWR_properties(3)*room.width*room.height; % surface area glass orien3
A_gl_orien4 = WWR_properties(4)*room.depth*room.height; % surface area glass orien4

% window U values (glazing + frame)
U_gl = glazing_properties(1);

U_gl_orien1 = U_gl; % don't change this
U_gl_orien2 = U_gl; % don't change this
U_gl_orien3 = U_gl; % don't change this
U_gl_orien4 = U_gl; % don't change this

% Solar heat gain coefficient glass without sunblinds
SHGC_orien1 = glazing_properties(2);
SHGC_orien2 = SHGC_orien1;
SHGC_orien3 = SHGC_orien1;
SHGC_orien4 = SHGC_orien1;

% Solar heat gain coefficient glass with sunblinds
SHGC_orien1_SB = SHGC_orien1;
SHGC_orien2_SB = SHGC_orien2;
SHGC_orien3_SB = SHGC_orien3;
SHGC_orien4_SB = SHGC_orien4;

glazing_transmission_coef = glazing_transmission_data(glazing_transmission_type,:);

ThresholdSBoff = 22; % Operative room temperature below which the sunblinds
ThresholdSBon = 24; % Operative room temperature above which the sunblinds
ThresholdSBIso = 100; % incoming solar radiative power below which the sunbl

CFsol = 0.2; % convection factor solar radiation entering the room

working_days = 7; % number of (consecutive) 'working days' in a week, m

building_function_values = [ % int. heat production, hour people present wd, hour peo

```

```
15 11 17 11 17 1.0/3600 0 24 0 24 0 24
6 19 9 0 24 0.7/3600 19 7 0 24 0 24]; % All values for corresponding building funct

building_function_properties = building_function_values(building_function_type,:); %

p_i_wd = building_function_properties(1); % total sensible internal heat production
p_i_nwd = building_function_properties(1); % total sensible internal heat production

hour_people_present_wd = [building_function_properties(2),building_function_properti
hour_people_present_nwd = [building_function_properties(4),building_function_properti

ThresholdWindowOpen = 100; % Room air temperatuer above which the windows are
ThresholdWindowClosed = 100; % Room air temperature below which the windows are
VentRateOpenWindow = 2/3600; % Additional ventilation rate with windows open [per

ventilation_rate = building_function_properties(6);
hour_vent_flow_wd = [building_function_properties(7),building_function_properties(
hour_vent_flow_nwd = [building_function_properties(9),building_function_properties(
WTW_efficiency = 0.75;

building_infiltration_values = [
0.0/3600 % no infiltration
0.1/3600 % quite airtight
0.2/3600 % normal
0.4/3600 % quite leaky
0.8/3600];% very leaky

infiltration_rate = building_infiltration_values(infiltration_type,:); %infiltratic

Threshold_Toper_night_ventilation_on = 24; % Threshold operative room temperaure abo
Threshold_Toper_night_ventilation_off = 22; % Threshold operative room temperaure bel
% night ventilation period is defined as
Threshold_Toper_bypass_on = 24; % Threshold operative room temperaure abo
Threshold_Toper_bypass_off = 22; % Threshold operative room temperaure bel

hour_heat_cool_on = [building_function_properties(11),building_function_properties(1

% thermostat setpoint and heating control
heating_setpoint = 20; % setpoint temperature (oC), only applies when peo
heating_proportional = 2000; % proportional part of PI-controller (W/K)
heating_integral = 0.1; % integral part of PI-controller (W/Ks)
heating_max_power = 10000; % maximum power heating (W)
cooling_setpoint = 24; % setpoint temperature, only applies when people a
cooling_proportional = 2000; % proportional part of PI-controller (W/K)
cooling_integral = 0.1; % integral part of PI-controller (W/Ks)
cooling_max_power = 10000; % maximum power heating (W)

% ----- construction material parameters -----

if building_age_type == 1 % new building
    facade_values = [ % 3x thickness, 3x density, 3x heat capacity, 3x lambda, for ea
```

```

0.05 0.10 0.05      800 35 800      1880 1470 1880      0.22 0.027
0.10 0.17 0.1      2000 35 7850      840 1470 500      1.00 0.027
0.10 0.11 0.10     2400 35 2100      840 1470 840      1.70 0.027
roof_values = [ % 3x thickness, 3x density, 3x heat capacity, 3x lambda, for ea
0.05 0.10 0.05      800 35 800      1880 1470 1880      0.22 0.027
0.10 0.12 0.005     2000 35 7850      840 1470 500      1.00 0.027
0.10 0.11 0.10     2400 35 2100      840 1470 840      1.70 0.027
floor_values = [ % 3x thickness, 3x density, 3x heat capacity, 3x lambda, for ea
0.05 0.10 0.05      800 35 800      1880 1470 1880      0.22 0.027
0.10 0.12 0.005     2000 35 7850      840 1470 500      1.00 0.027
0.20 0.11 0.10     2400 35 2100      840 1470 840      1.70 0.027

elseif building_age_type == 2 % old building
    facade_values = [ % 3x thickness, 3x density, 3x heat capacity, 3x lambda, for ea
0.05 0.04 0.05      800 35 800      1880 1470 1880      0.22 0.027
0.10 0.17 0.20     2000 20 2000      840 830 1000      0.96 0.04
0.10 0.04 0.10     2400 35 2100      840 1470 840      1.70 0.027
    roof_values = [ % 3x thickness, 3x density, 3x heat capacity, 3x lambda, for ea
0.05 0.04 0.05      800 35 800      1880 1470 1880      0.22 0.027
0.10 0.05 0.005     2000 35 7850      840 1470 500      1.00 0.027
0.10 0.04 0.10     2400 35 2100      840 1470 840      1.70 0.027
    floor_values = [ % 3x thickness, 3x density, 3x heat capacity, 3x lambda, for ea
0.05 0.04 0.05      800 35 800      1880 1470 1880      0.22 0.027
0.10 0.13 0.10     2000 20 2000      840 830 1000      0.96 0.04 0
0.20 0.04 0.10     2400 35 2100      840 1470 840      1.70 0.027

end

facade_properties = facade_values(building_method_type,:);
roof_properties   = roof_values(building_method_type,:);
floor_properties  = floor_values(building_method_type,:);

% orien1, external construction 1 layer 1.
e1_constr(1).d = facade_properties(1); % thickness, inside layer (sand-lime bric
e1_constr(1).rho = facade_properties(4); % density
e1_constr(1).c = facade_properties(7); % spec. heat capacity
e1_constr(1).la = facade_properties(10); % heat conduction coefficient
% external construction 1 layer 2
e1_constr(2).d = facade_properties(2); % thickness, middle layer (insulation:min
e1_constr(2).rho = facade_properties(5); % density
e1_constr(2).c = facade_properties(8); % spec. heat capacity
e1_constr(2).la = facade_properties(11); % heat conduction coefficient
% external construction 1 layer 3
e1_constr(3).d = facade_properties(3); % thickness, outside layer (brickwork)
e1_constr(3).rho = facade_properties(6); % density
e1_constr(3).c = facade_properties(9); % spec. heat capacity
e1_constr(3).la = facade_properties(12); % heat conduction coefficient
% surface area external construction 1
e1_constr_A = room.width*room.height-A_gl_orien1; % surface area external cons

% orien2, external construction 2 layer 1. REPRESENTS ALL SIDE WALLS AND ROOF AND FL
e2_constr(1).d = facade_properties(1); % thickness, inside layer (sand-lime bric
e2_constr(1).rho = facade_properties(4); % density
e2_constr(1).c = facade_properties(7); % spec. heat capacity
e2_constr(1).la = facade_properties(10); % heat conduction coefficient
% external construction 1 layer 2
e2_constr(2).d = facade_properties(2); % thickness, middle layer (insulation)
e2_constr(2).rho = facade_properties(5); % density
e2_constr(2).c = facade_properties(8); % spec. heat capacity

```

```
e2_constr(2).la = facade_properties(11);    % heat conduction coefficient
% external construction 1 layer 3
e2_constr(3).d = facade_properties(3);      % thickness, outside layer (brickwork)
e2_constr(3).rho = facade_properties(6);    % density
e2_constr(3).c = facade_properties(9);     % spec. heat capacity
e2_constr(3).la = facade_properties(12);    % heat conduction coefficient
% surface area external construction 2
e2_constr_A = room.depth*room.height-A_gl_orien2;    % surface area external cons

% orien3, SAME AS ORIEN2, external construction 3 layer 1
e3_constr(1).d = facade_properties(1);      % thickness, inside layer (sand-lime bric
e3_constr(1).rho = facade_properties(4);    % density
e3_constr(1).c = facade_properties(7);     % spec. heat capacity
e3_constr(1).la = facade_properties(10);    % heat conduction coefficient
% external construction 1 layer 2
e3_constr(2).d = facade_properties(2);      % thickness, middle layer (insulation)
e3_constr(2).rho = facade_properties(5);    % density
e3_constr(2).c = facade_properties(8);     % spec. heat capacity
e3_constr(2).la = facade_properties(11);    % heat conduction coefficient
% external construction 1 layer 3
e3_constr(3).d = facade_properties(3);      % thickness, outside layer (brickwork)
e3_constr(3).rho = facade_properties(6);    % density
e3_constr(3).c = facade_properties(9);     % spec. heat capacity
e3_constr(3).la = facade_properties(12);    % heat conduction coefficient
% surface area external construction 3
e3_constr_A = room.width*room.height-A_gl_orien3;    % surface area external cons

% orien4, external construction 4 layer 1
e4_constr(1).d = facade_properties(1);      % thickness, inside layer (sand-lime bric
e4_constr(1).rho = facade_properties(4);    % density
e4_constr(1).c = facade_properties(7);     % spec. heat capacity
e4_constr(1).la = facade_properties(10);    % heat conduction coefficient
% external construction 1 layer 2
e4_constr(2).d = facade_properties(2);      % thickness, middle layer (insulation)
e4_constr(2).rho = facade_properties(5);    % density
e4_constr(2).c = facade_properties(8);     % spec. heat capacity
e4_constr(2).la = facade_properties(11);    % heat conduction coefficient
% external construction 1 layer 3
e4_constr(3).d = facade_properties(3);      % thickness, outside layer (brickwork)
e4_constr(3).rho = facade_properties(6);    % density
e4_constr(3).c = facade_properties(9);     % spec. heat capacity
e4_constr(3).la = facade_properties(12);    % heat conduction coefficient
% surface area external construction 4
e4_constr_A = room.depth*room.height-A_gl_orien4;    % surface area external cons

% ROOF, external construction 5 layer 1
e5_constr(1).d = roof_properties(1);        % thickness, inside layer (sand-lime bric
e5_constr(1).rho = roof_properties(4);      % density
e5_constr(1).c = roof_properties(7);       % spec. heat capacity
e5_constr(1).la = roof_properties(10);      % heat conduction coefficient
% external construction 1 layer 2
e5_constr(2).d = roof_properties(2);        % thickness, middle layer (insulation)
e5_constr(2).rho = roof_properties(5);      % density
e5_constr(2).c = roof_properties(8);       % spec. heat capacity
e5_constr(2).la = roof_properties(11);      % heat conduction coefficient
% external construction 1 layer 3
e5_constr(3).d = roof_properties(3);        % thickness, outside layer (brickwork)
```

```

e5_constr(3).rho = roof_properties(6);      % density
e5_constr(3).c   = roof_properties(9);      % spec. heat capacity
e5_constr(3).la  = roof_properties(12);     % heat conduction coefficient
% % surface area external construction 5
e5_constr_A      = room.width*room.depth;   % surface area external construction 5 =

% FLOOR, external construction 6 layer 1
e6_constr(1).d   = floor_properties(1);     % thickness, inside layer (sand-lime bric
e6_constr(1).rho = floor_properties(4);     % density
e6_constr(1).c   = floor_properties(7);     % spec. heat capacity
e6_constr(1).la  = floor_properties(10);    % heat conduction coefficient
% external construction 1 layer 2
e6_constr(2).d   = floor_properties(2);     % thickness, middle layer (insulation)
e6_constr(2).rho = floor_properties(5);     % density
e6_constr(2).c   = floor_properties(8);     % spec. heat capacity
e6_constr(2).la  = floor_properties(11);    % heat conduction coefficient
% external construction 1 layer 3
e6_constr(3).d   = floor_properties(3);     % thickness, outside layer (brickwork)
e6_constr(3).rho = floor_properties(6);     % density
e6_constr(3).c   = floor_properties(9);     % spec. heat capacity
e6_constr(3).la  = floor_properties(12);    % heat conduction coefficient
% surface area external construction 6
e6_constr_A      = room.width*room.depth;   % surface area external construction 6 =

A_total = e1_constr_A+e2_constr_A+e3_constr_A+e4_constr_A+e5_constr_A+e6_constr_A;

e1_alpha_i      = 2.7;      % convective surface heat transfer coefficient inside con
e2_alpha_i      = 2.7;      % convective surface heat transfer coefficient inside con
e3_alpha_i      = 2.7;      % convective surface heat transfer coefficient inside con
e4_alpha_i      = 2.7;      % convective surface heat transfer coefficient inside con
e5_alpha_i      = 2.7;      % convective surface heat transfer coefficient inside con
e6_alpha_i      = 2.7;      % convective surface heat transfer coefficient inside con

e1_alpha_e      = 25;      % total outside surface heat transfer coefficient constru
    e2_alpha_e      = 0;      % total outside surface heat transfer coefficient cons
    e3_alpha_e      = 0;      % total outside surface heat transfer coefficient cons
    e4_alpha_e      = 0;      % total outside surface heat transfer coefficient cons
    e5_alpha_e      = 0;      % total outside surface heat transfer coefficient cons
    e6_alpha_e      = 0;      % total outside surface heat transfer coefficient con

e1_sol_abs      = 0.5;      % solar absorption coefficient outside surface constructi
    e2_sol_abs      = 0.0;      % solar absorption coefficient outside surface constr
    e3_sol_abs      = 0.0;      % solar absorption coefficient outside surface constr
    e4_sol_abs      = 0.0;      % solar absorption coefficient outside surface constr
    e5_sol_abs      = 0.0;      % solar absorption coefficient outside surface constr

% -----END OF INPUT -----

% mass matrix sensible part
M_r_s(1,1)=0.5* e1_constr(1).d*e1_constr(1).rho*e1_constr(1).c*e1_constr_A;
M_r_s(2,2)=0.5*(e1_constr(1).d*e1_constr(1).rho*e1_constr(1).c*e1_constr_A + e1_constr
M_r_s(3,3)=0.5*(e1_constr(2).d*e1_constr(2).rho*e1_constr(2).c*e1_constr_A + e1_constr
M_r_s(4,4)=0.5* e1_constr(3).d*e1_constr(3).rho*e1_constr(3).c*e1_constr_A;
M_r_s(5,5)=0.5* e2_constr(1).d*e2_constr(1).rho*e2_constr(1).c*e2_constr_A;
M_r_s(6,6)=0.5*(e2_constr(1).d*e2_constr(1).rho*e2_constr(1).c*e2_constr_A + e2_constr
M_r_s(7,7)=0.5*(e2_constr(2).d*e2_constr(2).rho*e2_constr(2).c*e2_constr_A + e2_constr

```

```

M_r_s(8,8)=0.5* e2_constr(3).d*e2_constr(3).rho*e2_constr(3).c*e2_constr_A;
M_r_s(9,9)=0.5* e3_constr(1).d*e3_constr(1).rho*e3_constr(1).c*e3_constr_A;
M_r_s(10,10)=0.5*(e3_constr(1).d*e3_constr(1).rho*e3_constr(1).c*e3_constr_A + e3_con
M_r_s(11,11)=0.5*(e3_constr(2).d*e3_constr(2).rho*e3_constr(2).c*e3_constr_A + e3_con
M_r_s(12,12)=0.5* e3_constr(3).d*e3_constr(3).rho*e3_constr(3).c*e3_constr_A;
M_r_s(13,13)=0.5* e4_constr(1).d*e4_constr(1).rho*e4_constr(1).c*e4_constr_A;
M_r_s(14,14)=0.5*(e4_constr(1).d*e4_constr(1).rho*e4_constr(1).c*e4_constr_A + e4_con
M_r_s(15,15)=0.5*(e4_constr(2).d*e4_constr(2).rho*e4_constr(2).c*e4_constr_A + e4_con
M_r_s(16,16)=0.5* e4_constr(3).d*e4_constr(3).rho*e4_constr(3).c*e4_constr_A;
M_r_s(17,17)=0.5* e5_constr(1).d*e5_constr(1).rho*e5_constr(1).c*e5_constr_A;
M_r_s(18,18)=0.5*(e5_constr(1).d*e5_constr(1).rho*e5_constr(1).c*e5_constr_A + e5_con
M_r_s(19,19)=0.5*(e5_constr(2).d*e5_constr(2).rho*e5_constr(2).c*e5_constr_A + e5_con
M_r_s(20,20)=0.5* e5_constr(3).d*e5_constr(3).rho*e5_constr(3).c*e5_constr_A;
M_r_s(21,21)=0.5* e6_constr(1).d*e6_constr(1).rho*e6_constr(1).c*e6_constr_A;
M_r_s(22,22)=0.5*(e6_constr(1).d*e6_constr(1).rho*e6_constr(1).c*e6_constr_A + e6_con
M_r_s(23,23)=0.5*(e6_constr(2).d*e6_constr(2).rho*e6_constr(2).c*e6_constr_A + e6_con
M_r_s(24,24)=0.5* e6_constr(3).d*e6_constr(3).rho*e6_constr(3).c*e6_constr_A;
M_r_s(25,25)=1200*room.volume*4; %rho*c*air_volume times 4 to inclu

nnr_r = 25; % number of nodes room (constructions and room
nnr_out = nnr_r+1; % outside air temperature
nk_tot = nnr_out; % total number of nodes in the model
nk_v_tot = 1; % number of fixed nodes in the model (in this c
nkl_tot = nk_tot-nkv_tot; % number of free nodes in the model

% define de 'conductivity' values between the nodes
% matrix Y(i,j) contains de conductivity between node i and j where i<j
% use an imaginary number for a direction-dependent flow element
% for example flow from 1 to 3: Y(1,3)=20i
% use a negative number for a reversed flow
% for example flow from 3 to 1: Y(1,3)=-20i

% stiffness matrix (excludes the glazing; that is done in Simulink)
Y_r1=zeros(nk_tot);
Y_r1(1,2) = e1_constr(1).la*e1_constr_A/e1_constr(1).d; % conduction
Y_r1(2,3) = e1_constr(2).la*e1_constr_A/e1_constr(2).d; % conduction
Y_r1(3,4) = e1_constr(3).la*e1_constr_A/e1_constr(3).d; % conduction
Y_r1(5,6) = e2_constr(1).la*e2_constr_A/e2_constr(1).d; % conduction
Y_r1(6,7) = e2_constr(2).la*e2_constr_A/e2_constr(2).d; % conduction
Y_r1(7,8) = e2_constr(3).la*e2_constr_A/e2_constr(3).d; % conduction
Y_r1(9,10) = e3_constr(1).la*e3_constr_A/e3_constr(1).d; % conduction
Y_r1(10,11) = e3_constr(2).la*e3_constr_A/e3_constr(2).d; % conduction
Y_r1(11,12) = e3_constr(3).la*e3_constr_A/e3_constr(3).d; % conduction
Y_r1(13,14) = e4_constr(1).la*e4_constr_A/e4_constr(1).d; % conduction
Y_r1(14,15) = e4_constr(2).la*e4_constr_A/e4_constr(2).d; % conduction
Y_r1(15,16) = e4_constr(3).la*e4_constr_A/e4_constr(3).d; % conduction
Y_r1(17,18) = e5_constr(1).la*e5_constr_A/e5_constr(1).d; % conduction
Y_r1(18,19) = e5_constr(2).la*e5_constr_A/e5_constr(2).d; % conduction
Y_r1(19,20) = e5_constr(3).la*e5_constr_A/e5_constr(3).d; % conduction
Y_r1(21,22) = e6_constr(1).la*e6_constr_A/e6_constr(1).d; % conduction
Y_r1(22,23) = e6_constr(2).la*e6_constr_A/e6_constr(2).d; % conduction
Y_r1(23,24) = e6_constr(3).la*e6_constr_A/e6_constr(3).d; % conduction
Y_r1(4,nnr_out) = e1_alpha_e*e1_constr_A; % convection bet
Y_r1(8,nnr_out) = e2_alpha_e*e2_constr_A; % convection bet
Y_r1(12,nnr_out) = e3_alpha_e*e3_constr_A; % convection bet
Y_r1(16,nnr_out) = e4_alpha_e*e4_constr_A; % convection bet
Y_r1(20,nnr_out) = e5_alpha_e*e5_constr_A; % convection bet
Y_r1(24,nnr_out) = e6_alpha_e*e6_constr_A; % convection bet

```

```

Y_r1(1,25)      = e1_alpha_i*e1_constr_A;           % convection bet
Y_r1(5,25)      = e2_alpha_i*e2_constr_A;           % convection bet
Y_r1(9,25)      = e3_alpha_i*e3_constr_A;           % convection bet
Y_r1(13,25)     = e4_alpha_i*e4_constr_A;           % convection bet
Y_r1(17,25)     = e5_alpha_i*e5_constr_A;           % convection bet
Y_r1(21,25)     = e6_alpha_i*e6_constr_A;           % convection bet
Y_r1(1,5)       = 5*e2_constr_A/(A_total-e1_constr_A)*e1_constr_A; % radiation exch
Y_r1(1,9)       = 5*e3_constr_A/(A_total-e1_constr_A)*e1_constr_A; % radiation exch
Y_r1(1,13)      = 5*e4_constr_A/(A_total-e1_constr_A)*e1_constr_A; % radiation exch
Y_r1(1,17)      = 5*e5_constr_A/(A_total-e1_constr_A)*e1_constr_A; % radiation exch
Y_r1(1,21)      = 5*e6_constr_A/(A_total-e1_constr_A)*e1_constr_A; % radiation exch
Y_r1(5,9)       = 5*e3_constr_A/(A_total-e2_constr_A)*e2_constr_A; % radiation exch
Y_r1(5,13)      = 5*e4_constr_A/(A_total-e2_constr_A)*e2_constr_A; % radiation exch
Y_r1(5,17)      = 5*e5_constr_A/(A_total-e2_constr_A)*e2_constr_A; % radiation exch
Y_r1(5,21)      = 5*e6_constr_A/(A_total-e2_constr_A)*e2_constr_A; % radiation exch
Y_r1(9,13)      = 5*e4_constr_A/(A_total-e3_constr_A)*e3_constr_A; % radiation exch
Y_r1(9,17)      = 5*e5_constr_A/(A_total-e3_constr_A)*e3_constr_A; % radiation exch
Y_r1(9,21)      = 5*e6_constr_A/(A_total-e3_constr_A)*e3_constr_A; % radiation exch
Y_r1(13,17)     = 5*e5_constr_A/(A_total-e4_constr_A)*e4_constr_A; % radiation exch
Y_r1(13,21)     = 5*e6_constr_A/(A_total-e4_constr_A)*e4_constr_A; % radiation exch
Y_r1(17,21)     = 5*e6_constr_A/(A_total-e5_constr_A)*e5_constr_A; % radiation exch

%definition of weight factors for determining the approximate radiation temperature i
Rf_r1 = zeros(1,nk_tot);
Rf_r1(nnr_out) = (A_gl_orien1*(U_gl_orien1/7.7)+A_gl_orien2*(U_gl_orien2/7.7)+A_gl_o
Rf_r1(1)      = e1_constr_A;
Rf_r1(5)      = e2_constr_A;
Rf_r1(9)      = e3_constr_A;
Rf_r1(13)     = e4_constr_A;
Rf_r1(17)     = e5_constr_A;
Rf_r1(21)     = e6_constr_A;
temp = sum(Rf_r1);
Rf_r1 = Rf_r1/temp;

% create empty initial stiffness matrix with nk rows and columns
Si_r1 = zeros(nk_tot);

% fill Si with values
% first row is node 1
% second row is node 2
% etc
for i=1:nk_tot-1
    for j=i+1:nk_tot
        Si_r1=fillS(Si_r1,Y_r1,i,j); %subroutine in fillS.m
    end
end

% definition of stiffness matrix
% take only the part of Si that reflects the free nodes
S_r1 = Si_r1(1:nkl_tot,1:nkl_tot);

% the part Si(1:nkl_r,nkl_r+1:nk_r) is moved to the load vector
S_r1_fixed = Si_r1(1:nkl_tot,nkl_tot+1:nk_tot);

% climatic data

```



```
load('Te_NEN5060_2018');
load('qsol_NEN5060_2018');
load('xe_NEN5060_2018');

Te = Te_NEN5060_2018;
qtemp = qsol_NEN5060_2018;
xe = xe_NEN5060_2018;

% adjust solar data so that first column in qsol gives solar radiation on orien1
qsol(:,1) = qtemp(:,1);
for j=0:2
    if orientation >= 0 && orientation < 45
        qsol(:,2+9*j) = (45-orientation)/45*qtemp(:,2+9*j)+orientation/45*qtemp(:,3+9
        qsol(:,3+9*j) = (45-orientation)/45*qtemp(:,3+9*j)+orientation/45*qtemp(:,4+9
        qsol(:,4+9*j) = (45-orientation)/45*qtemp(:,4+9*j)+orientation/45*qtemp(:,5+9
        qsol(:,5+9*j) = (45-orientation)/45*qtemp(:,5+9*j)+orientation/45*qtemp(:,6+9
        qsol(:,6+9*j) = (45-orientation)/45*qtemp(:,6+9*j)+orientation/45*qtemp(:,7+9
        qsol(:,7+9*j) = (45-orientation)/45*qtemp(:,7+9*j)+orientation/45*qtemp(:,8+9
        qsol(:,8+9*j) = (45-orientation)/45*qtemp(:,8+9*j)+orientation/45*qtemp(:,9+9
        qsol(:,9+9*j) = (45-orientation)/45*qtemp(:,9+9*j)+orientation/45*qtemp(:,2+9
    elseif orientation >= 45 && orientation < 90
        qsol(:,2+9*j) = (90-orientation)/45*qtemp(:,3+9*j)+(orientation-45)/45*qtemp(
        qsol(:,3+9*j) = (90-orientation)/45*qtemp(:,4+9*j)+(orientation-45)/45*qtemp(
        qsol(:,4+9*j) = (90-orientation)/45*qtemp(:,5+9*j)+(orientation-45)/45*qtemp(
        qsol(:,5+9*j) = (90-orientation)/45*qtemp(:,6+9*j)+(orientation-45)/45*qtemp(
        qsol(:,6+9*j) = (90-orientation)/45*qtemp(:,7+9*j)+(orientation-45)/45*qtemp(
        qsol(:,7+9*j) = (90-orientation)/45*qtemp(:,8+9*j)+(orientation-45)/45*qtemp(
        qsol(:,8+9*j) = (90-orientation)/45*qtemp(:,9+9*j)+(orientation-45)/45*qtemp(
        qsol(:,9+9*j) = (90-orientation)/45*qtemp(:,2+9*j)+(orientation-45)/45*qtemp(
    elseif orientation >= 90 && orientation < 135
        qsol(:,2+9*j) = (135-orientation)/45*qtemp(:,4+9*j)+(orientation-90)/45*qtemp
        qsol(:,3+9*j) = (135-orientation)/45*qtemp(:,5+9*j)+(orientation-90)/45*qtemp
        qsol(:,4+9*j) = (135-orientation)/45*qtemp(:,6+9*j)+(orientation-90)/45*qtemp
        qsol(:,5+9*j) = (135-orientation)/45*qtemp(:,7+9*j)+(orientation-90)/45*qtemp
        qsol(:,6+9*j) = (135-orientation)/45*qtemp(:,8+9*j)+(orientation-90)/45*qtemp
        qsol(:,7+9*j) = (135-orientation)/45*qtemp(:,9+9*j)+(orientation-90)/45*qtemp
        qsol(:,8+9*j) = (135-orientation)/45*qtemp(:,2+9*j)+(orientation-90)/45*qtemp
        qsol(:,9+9*j) = (135-orientation)/45*qtemp(:,3+9*j)+(orientation-90)/45*qtemp
    elseif orientation >= 135 && orientation < 180
        qsol(:,2+9*j) = (180-orientation)/45*qtemp(:,5+9*j)+(orientation-135)/45*qtem
        qsol(:,3+9*j) = (180-orientation)/45*qtemp(:,6+9*j)+(orientation-135)/45*qtem
        qsol(:,4+9*j) = (180-orientation)/45*qtemp(:,7+9*j)+(orientation-135)/45*qtem
        qsol(:,5+9*j) = (180-orientation)/45*qtemp(:,8+9*j)+(orientation-135)/45*qtem
        qsol(:,6+9*j) = (180-orientation)/45*qtemp(:,9+9*j)+(orientation-135)/45*qtem
        qsol(:,7+9*j) = (180-orientation)/45*qtemp(:,2+9*j)+(orientation-135)/45*qtem
        qsol(:,8+9*j) = (180-orientation)/45*qtemp(:,3+9*j)+(orientation-135)/45*qtem
        qsol(:,9+9*j) = (180-orientation)/45*qtemp(:,4+9*j)+(orientation-135)/45*qtem
    elseif orientation >= 180 && orientation < 225
        qsol(:,2+9*j) = (225-orientation)/45*qtemp(:,6+9*j)+(orientation-180)/45*qtem
        qsol(:,3+9*j) = (225-orientation)/45*qtemp(:,7+9*j)+(orientation-180)/45*qtem
        qsol(:,4+9*j) = (225-orientation)/45*qtemp(:,8+9*j)+(orientation-180)/45*qtem
        qsol(:,5+9*j) = (225-orientation)/45*qtemp(:,9+9*j)+(orientation-180)/45*qtem
        qsol(:,6+9*j) = (225-orientation)/45*qtemp(:,2+9*j)+(orientation-180)/45*qtem
        qsol(:,7+9*j) = (225-orientation)/45*qtemp(:,3+9*j)+(orientation-180)/45*qtem
        qsol(:,8+9*j) = (225-orientation)/45*qtemp(:,4+9*j)+(orientation-180)/45*qtem
        qsol(:,9+9*j) = (225-orientation)/45*qtemp(:,5+9*j)+(orientation-180)/45*qtem
    elseif orientation >= 225 && orientation < 270
        qsol(:,2+9*j) = (270-orientation)/45*qtemp(:,7+9*j)+(orientation-225)/45*qtem
```

```

        qsol(:,3+9*j) = (270-orientation)/45*qtemp(:,8+9*j)+(orientation-225)/45*qtem
        qsol(:,4+9*j) = (270-orientation)/45*qtemp(:,9+9*j)+(orientation-225)/45*qtem
        qsol(:,5+9*j) = (270-orientation)/45*qtemp(:,2+9*j)+(orientation-225)/45*qtem
        qsol(:,6+9*j) = (270-orientation)/45*qtemp(:,3+9*j)+(orientation-225)/45*qtem
        qsol(:,7+9*j) = (270-orientation)/45*qtemp(:,4+9*j)+(orientation-225)/45*qtem
        qsol(:,8+9*j) = (270-orientation)/45*qtemp(:,5+9*j)+(orientation-225)/45*qtem
        qsol(:,9+9*j) = (270-orientation)/45*qtemp(:,6+9*j)+(orientation-225)/45*qtem
    elseif orientation >= 270 && orientation < 315
        qsol(:,2+9*j) = (315-orientation)/45*qtemp(:,8+9*j)+(orientation-270)/45*qtem
        qsol(:,3+9*j) = (315-orientation)/45*qtemp(:,9+9*j)+(orientation-270)/45*qtem
        qsol(:,4+9*j) = (315-orientation)/45*qtemp(:,2+9*j)+(orientation-270)/45*qtem
        qsol(:,5+9*j) = (315-orientation)/45*qtemp(:,3+9*j)+(orientation-270)/45*qtem
        qsol(:,6+9*j) = (315-orientation)/45*qtemp(:,4+9*j)+(orientation-270)/45*qtem
        qsol(:,7+9*j) = (315-orientation)/45*qtemp(:,5+9*j)+(orientation-270)/45*qtem
        qsol(:,8+9*j) = (315-orientation)/45*qtemp(:,6+9*j)+(orientation-270)/45*qtem
        qsol(:,9+9*j) = (315-orientation)/45*qtemp(:,7+9*j)+(orientation-270)/45*qtem
    elseif orientation >= 315 && orientation <= 360
        qsol(:,2+9*j) = (360-orientation)/45*qtemp(:,9+9*j)+(orientation-315)/45*qtem
        qsol(:,3+9*j) = (360-orientation)/45*qtemp(:,2+9*j)+(orientation-315)/45*qtem
        qsol(:,4+9*j) = (360-orientation)/45*qtemp(:,3+9*j)+(orientation-315)/45*qtem
        qsol(:,5+9*j) = (360-orientation)/45*qtemp(:,4+9*j)+(orientation-315)/45*qtem
        qsol(:,6+9*j) = (360-orientation)/45*qtemp(:,5+9*j)+(orientation-315)/45*qtem
        qsol(:,7+9*j) = (360-orientation)/45*qtemp(:,6+9*j)+(orientation-315)/45*qtem
        qsol(:,8+9*j) = (360-orientation)/45*qtemp(:,7+9*j)+(orientation-315)/45*qtem
        qsol(:,9+9*j) = (360-orientation)/45*qtemp(:,8+9*j)+(orientation-315)/45*qtem
    end
    qsol(:,10+9*j) = qtemp(:,10+9*j);
end

% constant parameters
L_lv = 2.5e6; % latent heat of vaporization of wat
R_v = 461.5; % gas constant of water (J/(kg.K))
rho_a = 1.2; % density of dry air(kg/m3)

% silica gel packed bed
rho_g = 700; % density of silica gel(kg/m3)
V_bed = 0; % the volume of packed bed(m3)
e_bed = 0.36; % porosity of the packed bed
ksi_sorp = 500; % slope of sorption isotherm(kg/m3)
V_gel = V_bed*(1-e_bed); % the volume of silica gel beads(m3)

% enthalpy wheel
eta_v_max = 0.7; % maximum efficiency of enthalpy whe

% the occupancy
Occupancy = [0 0 0 0 0 0 0 0 0 0 2 3 4 5 4 3 2 0 0 0 0 0 0]; % the number of people
Clothing = [0 0 0 0 0 0 0 0 0 0 1 1 1 1 1 1 0 0 0 0 0 0 0]; % clothing load in one

% the humidity load
g_people = 0.05; % humidity load per person(kg/h)
Humidity_load = g_people*Occupancy + g_wet_clothing*Clothing; % humidity

% the ventilation flow rate
min_value = 0.5/1000*3600*room.area; % minimum ventilation flow rate(m3/h)
normal_value = 12/1000*3600; % normal ventilation flow rate(m3/h per
max_value = 5/1000*3600*room.area; % supply capacity (m3/h)

Min flow rate =[min value min value min value min value min value min value min value

```

```
Normal_flow_rate = normal_value*Occupancy; % ventilation flow rate with occupancy(m3/

Ventilation_flow_rate = Min_flow_rate + Normal_flow_rate;

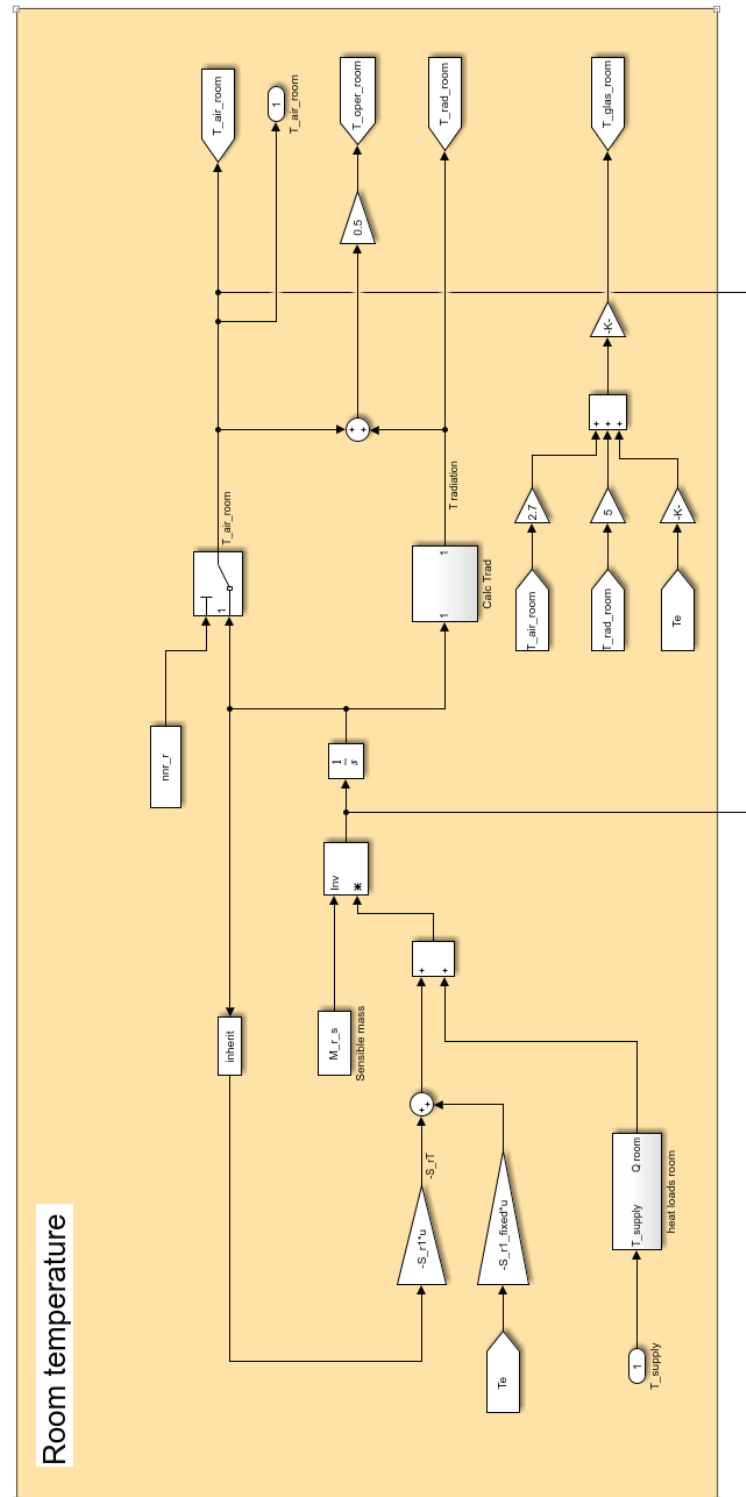
Ventilation_flow_rate(Ventilation_flow_rate>max_value)= max_value; % check the maximu
Ventilation_flow_rate(Ventilation_flow_rate<min_value)= min_value; % check the minimu

clear qtemp Te_NEN5060_2018 qsoltot_NEN5060_2018 xe_NEN5060_2018
```

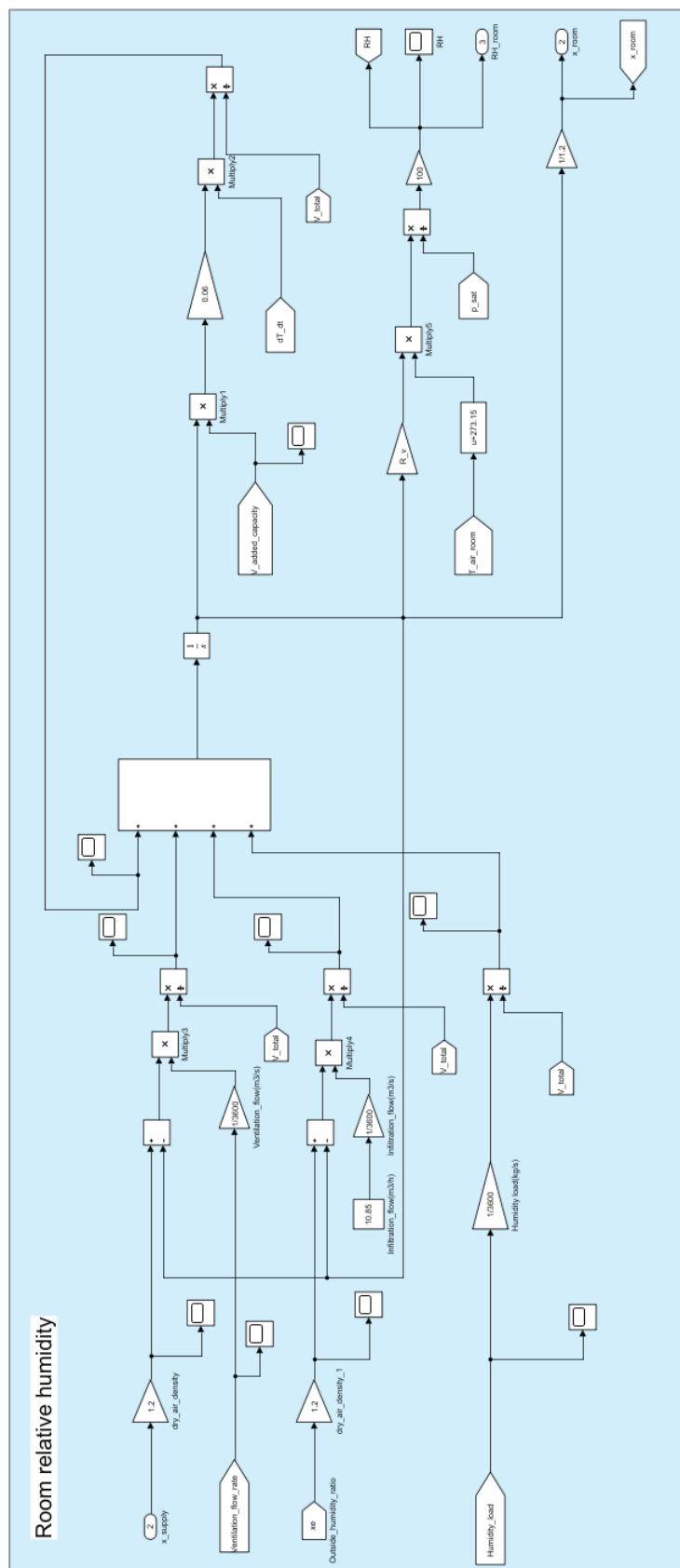
11.3.2 Simulink Code

Only main parts are shown.

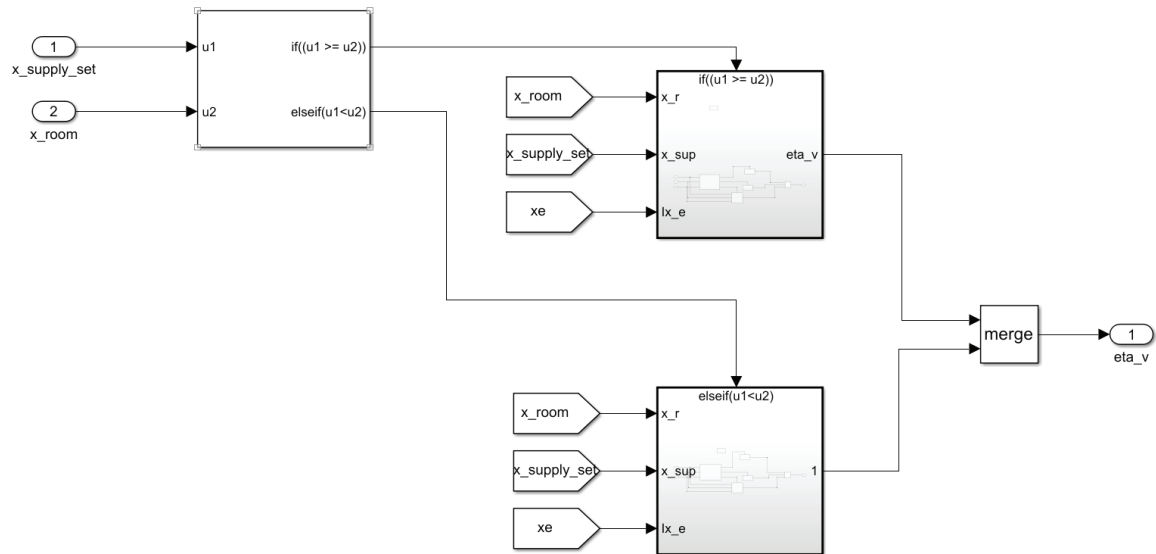
11.3.2.1 Temperature Calculation in the Room



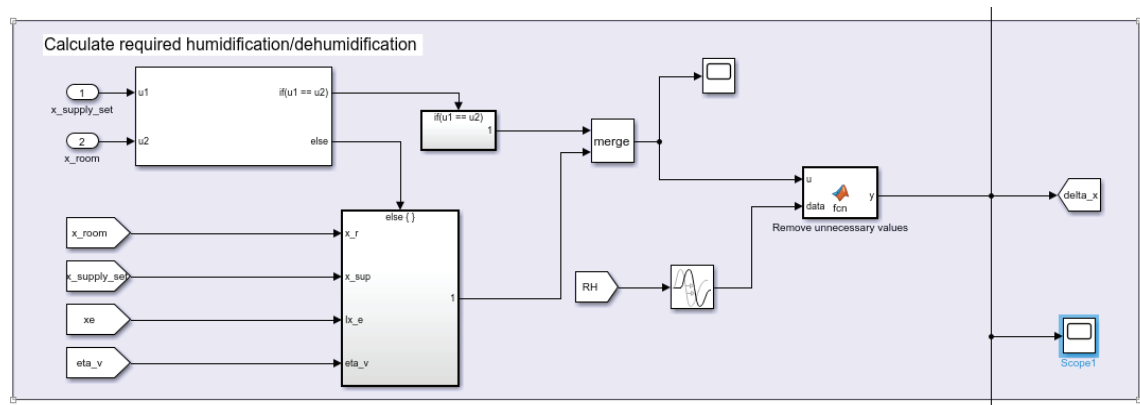
11.3.2.2 Relative Humidity Calculation in the Room



11.3.2.3 Enthalpy wheel



11.3.2.4 Humidifier and Dehumidifier



11.4 Appendix D: Implementation of Model 3.0

11.4.1 Matlab Script

Only the different part from model 2.0 is shown

```
% heat and moisture transfer in a column packed bed of silica gel

R_v = 461.5; % gas constant of water (J/(kg.K))
L_lv = 2.5e6; % latent heat of vaporization of wat
L_bed = 1; % length of packed bed (along the ai
D_bed = 0.4; % diameter of cylindrical packed bed
nk_bed = 10; % number of control volumes in the p
e_bed = 0.36; % porosity of packed bed
V_room = room.volume; % the volume of room(m3)

rho_gel = 700; % mass density of dry silica gel (kg
rho_air = 1.2; % mass density of dry air (kg/m3)

c_gel = 1000; % specific heat capacity of dry sili
c_liq = 4280; % specific heat capacity of liquid w
c_vap = 1860; % specific heat capacity of water va
c_air = 1000; % specific heat capacity of dry air

Flow_bed = 0.1; % flow rate through packed bed (kg/s

V_c_bed = 0.25*pi*L_bed*(D_bed)^2/nk_bed; % volume of one control volume

eta_v_max = 0.7; % maximum efficiency of sorption whe

% help matrix, airflow through packed bed,
S_help=zeros(nk_bed,nk_bed+1);
for k=1:nk_bed
    S_help(k,k)= 1;
    S_help(k,k+1)= -1;
end

% the occupancy
Occupancy = [0 0 0 0 0 0 0 0 0 0 0 0 0 0 0 0 0 0 0 0 0]; % the number of people
Clothing = [0 0 0 0 0 0 0 0 0 0 0 0 0 0 0 0 0 0 0 0 0]; % clothing load in one

% the humidity load
g_people = 0.05; % humidity load from people (kg/
g_wet_clothing = 0.03; % humidity load from wet clothin
Humidity_load = g_people*Occupancy + g_wet_clothing*Clothing; % humidity

% the ventilation flow rate
min_value = 0.5/1000*3600*room.area; % minimum ventilation flow rate(m3/h)
normal_value = 12/1000*3600; % normal ventilation flow rate(m3/h per
max_value = 5/1000*3600*room.area; % supply capacity (m3/h)

Min_flow_rate =[min_value min_value min_value min_value min_value min_value min_value

Normal_flow_rate = normal_value*Occupancy; % ventilation flow rate with occupancy(m3/

Ventilation_flow_rate = Min_flow_rate + Normal_flow_rate;

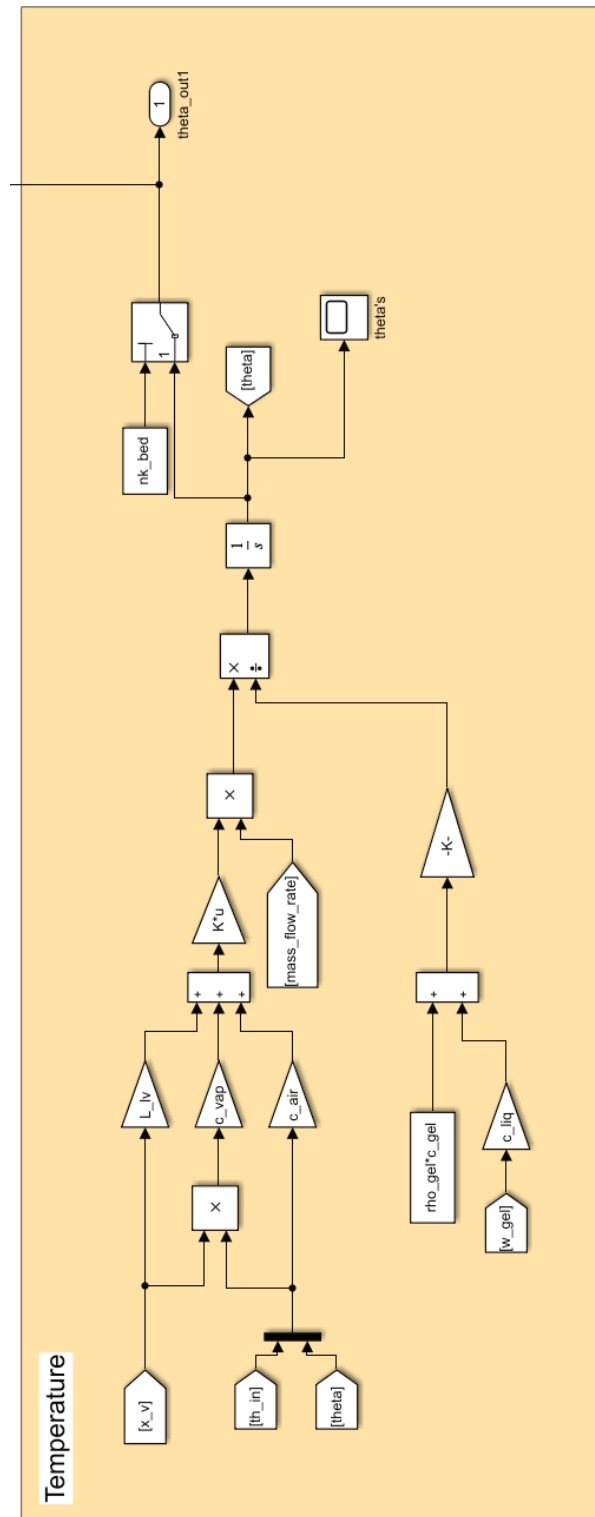
Ventilation_flow_rate(Ventilation_flow_rate>max_value)= max_value; % check the maximu
Ventilation_flow_rate(Ventilation_flow_rate<min_value)= min_value; % check the minimu

clear atemp Te NEN5060 2018 asoltot NEN5060 2018 xe NEN5060 2018
```

11.4.2 Simulink Code

Only the main part is shown, and the same part with model 2.0 is not shown.

11.4.2.1 Temperature Calculation in the Packed Bed





11.5 Appendix E: Design Builder Model Settings

The construction in scenario a1, a2, and a3 is the same. So, only settings of scenario a3 is shown since it is the most complicated one among them.

11.5.1 Activity

Activity Template	
Template	Public Assembly Spaces - Museum (children's
Sector	General
Zone type	1-Standard
Zone multiplier	1
<input checked="" type="checkbox"/> Include zone in thermal calculations	
<input checked="" type="checkbox"/> Include zone in Radiance daylighting calculations	
Floor Areas and Volumes	
Occupancy	
Occupancy density (people/m2)	0.2700
Schedule	NHM
Metabolic	
Activity	Walking about
Factor (Men=1.00, Women=0.85, Children=0.75)	0.75
CO2 generation rate (m3/s-W)	0.0000000382
Clothing	
Clothing schedule definition	1-Generic summer and winter clothing
Winter clothing (clo)	1.00
Summer clothing (clo)	0.50
Comfort Radiant Temperature Weighting	
Calculation type	1-Zone averaged
Contaminant Generation and Removal	
<input type="checkbox"/> Contaminant generation/removal	
DHW	
Environmental Control	
Heating Setpoint Temperatures	
Heating (°C)	20.0
Heating set back (°C)	13.0
Cooling Setpoint Temperatures	
Cooling (°C)	24.0
Cooling set back (°C)	32.0
Humidity Control	
RH Humidification setpoint (%)	45.0
RH Dehumidification setpoint (%)	55.0
Ventilation Setpoint Temperatures	
Minimum Fresh Air	
Lighting	
Computers	
<input type="checkbox"/> On	
Office Equipment	
<input type="checkbox"/> On	
Miscellaneous	

11.5.2 Construction

Construction Template		«
Template	Project construction template	
Construction		«
External walls	Facade1	
Below grade walls	Project below grade wall	
Flat roof	Ceiling1	
Pitched roof (occupied)	Project pitched roof	
Semi-Exposed		«
Semi-exposed ceiling	Project semi-exposed ceiling	
Semi-exposed floor	Project semi-exposed floor	
Floors		«
Ground floor	Ground floor	
External floor	Project external floor	
Internal floor	Project internal floor	
Sub-Surfaces		«
Walls	Project wall sub-surface construction	
Internal	Project internal wall sub-surface construction	
Roof	Project roof sub-surface construction	
External door	Project external door	
Internal Thermal Mass		«
Construction	Project internal mass	
Exposed area (m2)	0.00	
Adjacency		«
Adjacency	1-Auto	▼
Geometry, Areas and Volumes		«
Fixed Surface Thicknesses		>>
Void Depths		>>
Surface Convection		«
Heating Design		>>
Cooling Design		>>
Simulation		>>
Linear Thermal Bridging at Junctions		>>
Airtightness		«
<input type="checkbox"/> Model infiltration		
Cost		>>

11.5.3 Opening

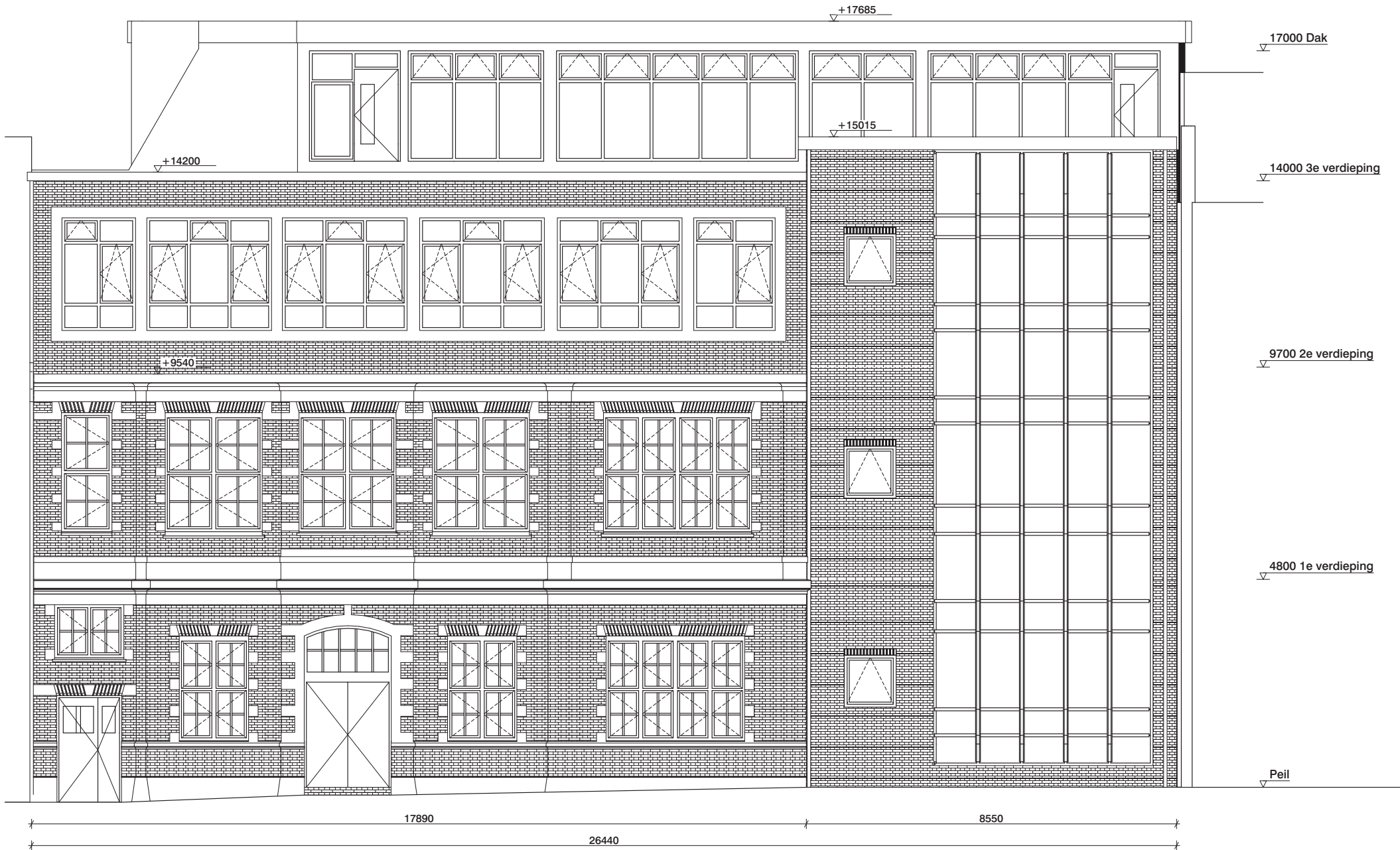
Glazing Template		«
Template	Project glazing template	
External Windows		«
Glazing type	Dbl LoE Spec Sel Clr 6mm/13mm Air	
Layout	Preferred height 1.5m, 30% glazed	
Dimensions		«
Type	3-Preferred height ▼	
Window to wall %	38	
Window height (m)	3.00	
Window spacing (m)	1.00	
Sill height (m)	0.80	
Outside reveal depth (m)	0.000	
Frame and Dividers		»
Shading		«
<input type="checkbox"/> Window shading		
<input type="checkbox"/> Local shading		
Airflow Control Windows		»
Free Aperture		»
Internal Windows		»
Sloped Roof Windows/Skylights		»
Doors		»

11.5.4 HVAC

	HVAC Template	
	Template	Fan Coil Unit (4-Pipe), Air cooled Chiller
	Mechanical Ventilation	
<input checked="" type="checkbox"/>	On	
	Outside air definition method	1-By zone
	Outside air (ac/h)	1.000
	Operation	
	Schedule	On 24/7
	Economiser (Free Cooling)	>>
	Heat Recovery	>>
	Auxiliary Energy	>>
	Heating	
<input checked="" type="checkbox"/>	Heated	
	Fuel	1-Electricity from grid
	Heating system seasonal CoP	0.850
	Sizing Zone Equipment	>>
	Type	>>
	Operation	
	Schedule	On 24/7
	Cooling	
<input checked="" type="checkbox"/>	Cooled	
	Cooling system	Default
	Fuel	1-Electricity from grid
	Cooling system seasonal CoP	1.800
	Supply Air Condition	>>
	Operation	
	Schedule	On 24/7
	Humidity Control	
<input checked="" type="checkbox"/>	Humidification	
	Humidification control type	2-Humidistat
<input checked="" type="checkbox"/>	Dehumidification	
	Dehumidification control type	2-Humidistat
	DHW	
<input type="checkbox"/>	On	
	Natural Ventilation	
<input type="checkbox"/>	On	
	Earth Tube	>>
	Air Temperature Distribution	>>
	Cost	>>

11.6 Appendix F: Renovation Design from Winhov and ABT

11.6.1 Front Elevation



Project
NHM Kweekschool

Middenlaan 27, 1018 DB Amsterdam

Onderdeel
Gevelaanzichten

Voorgevel
bestaande toestand

Tekeningnummer
2550 DO KS BS 031

Datum	Schaal	Formaat
15/05/2020	1:100	A3

Wijzigingsdatum

Fase	Status
Definitief ontwerp	-

Opdrachtgever
Stichting Hollandsche Schouwburg

Architect
OFFICE WINHOV

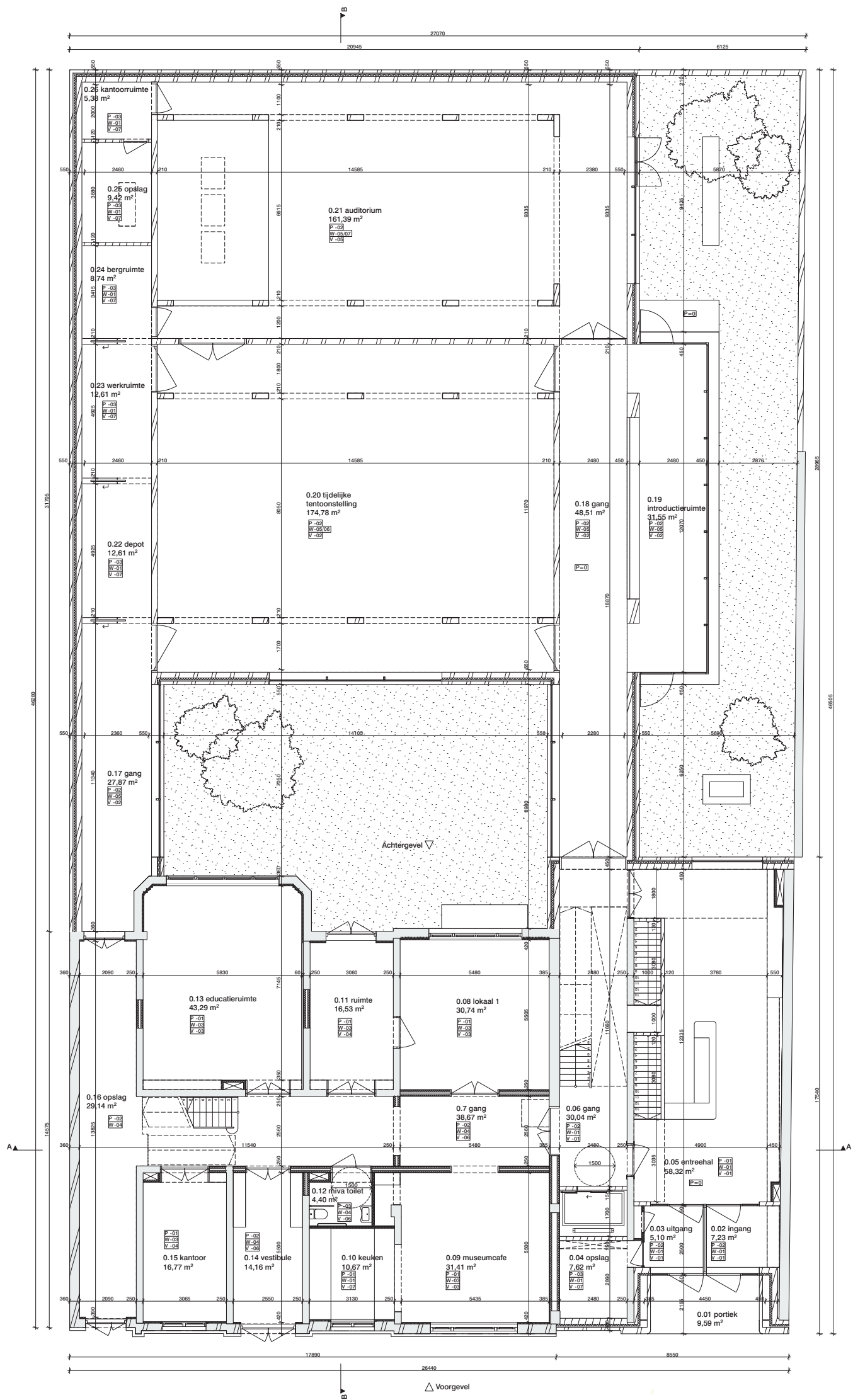
Johan van Hasseltweg 2 E1, 1022 WV Amsterdam,
tel. +31 20 684 44 46, office@winhov.nl

11.6.2 Back Elevation



Project		
NHM Kweekschool		
Middenlaan 27, 1018 DB Amsterdam		
Onderdeel		
Gevelaanzichten		
Achtergevel		
bestaande toestand		
Tekeningnummer		
2550 DO KS BS 032		
-		
Datum	Schaal	Formaat
15/05/2020	1:100	A3
Wijzigingsdatum		
-		
Fase	Status	
Definitief ontwerp	-	
Opdrachtgever		
Stichting Hollandsche Schouwburg		
Architect		
OFFICE WINHOV		
Johan van Hasseltweg 2 E1, 1022 WV Amsterdam tel. +31 20 684 44 46, office@winhov.nl		

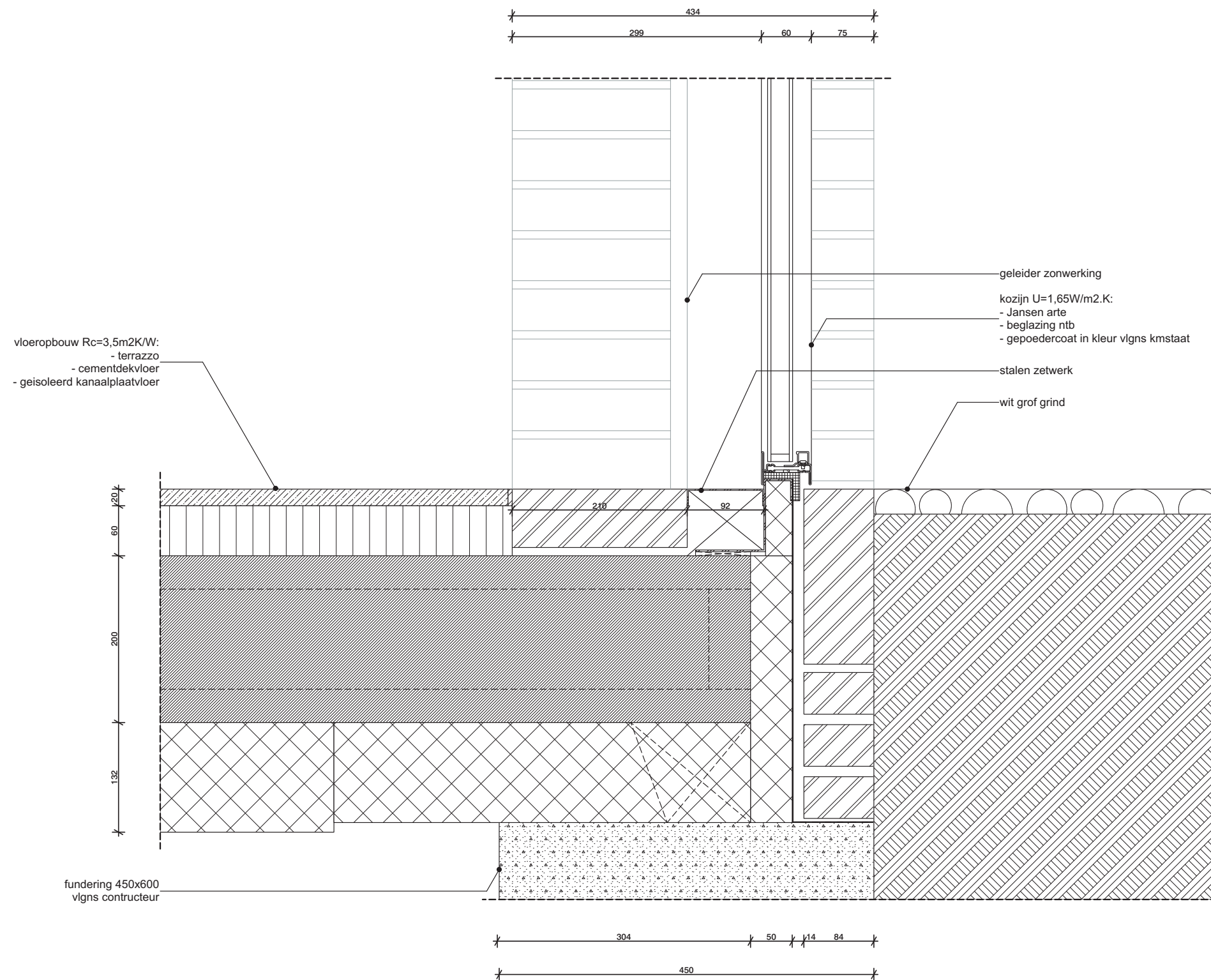
11.6.3 Floor Plan of the Ground Floor



Project		
NHM Kweekschool		
Middenlaan 27, 1018 DB Amsterdam		
Onderdeel		
Plattegronden		
Begane grond		
nieuwe toestand		
Tekeningnummer		
2550 DO KS 020 NS		
-		
Datum	Schaal	Formaat
30/04/2020	1:100	A2
Wijzigingsdatum		
-		
Fase		Status
Definitief ontwerp		-
Opdrachtgever		
Stichting Hollandsche Schouwburg		
Architect		
OFFICE WINHOV		
Johan van Hasseltweg 2 E1, 1022 WV Amsterdam, tel. +31 20 684 44 46, office@winhov.nl		



11.6.5 Details of the Glazing and Ground



blad

D.201V1

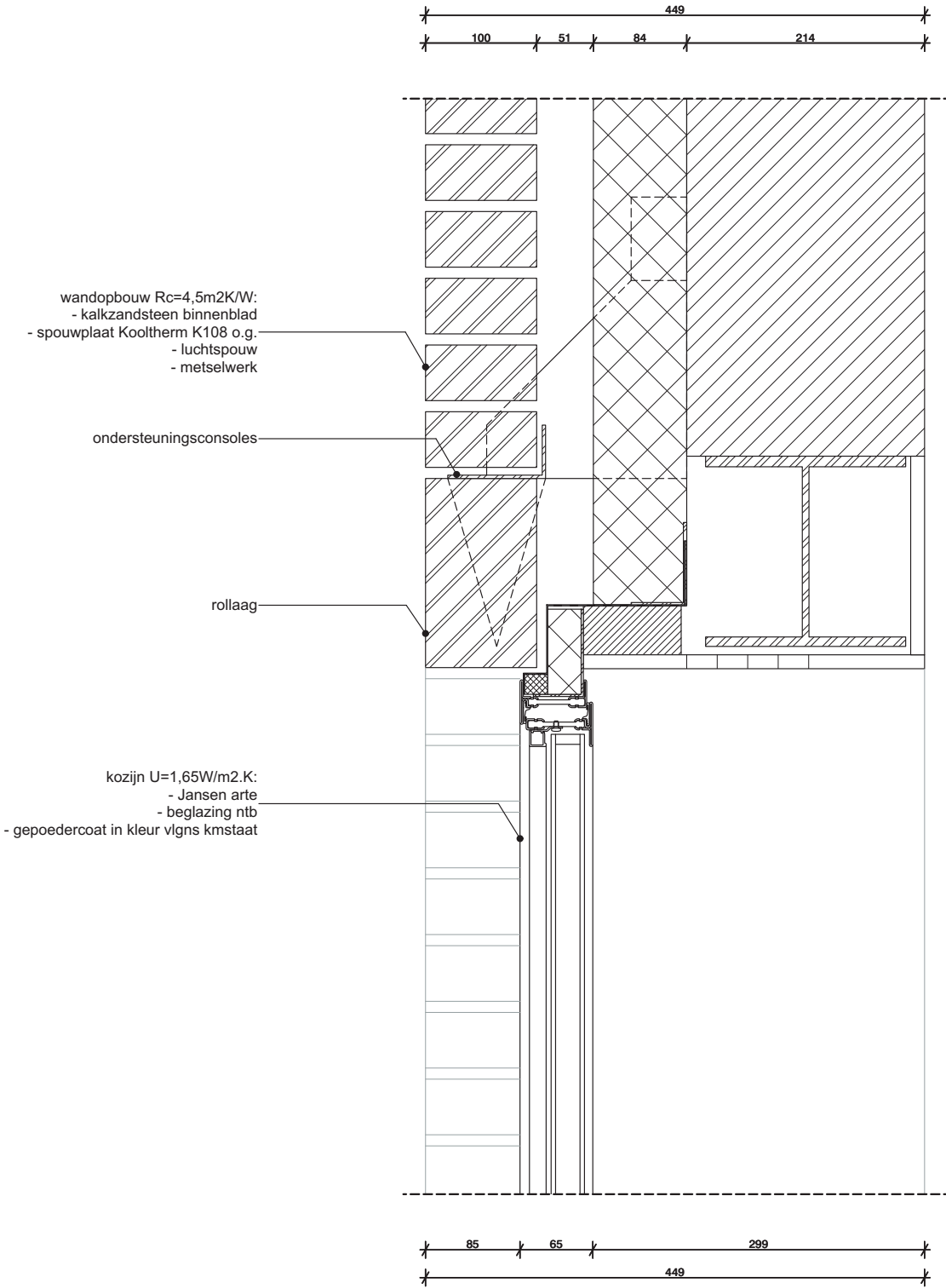
Details

Datum	Schaal	Formaat
15/05/2020	1:5	A3

Tekeningnummer
2550 DO KS 100

OFFICE WINHOV

11.6.6 Details of the Facade and Glazing



blad		
D.309V2		
Details		
Datum	Schaal	Formaat
15/05/2020	1:5	A3
Tekeningnummer		
2550 DO KS 100		

OFFICE WINHOV

12 Nomenclature

Δp	pressure drop [Pa]
ΔRH	fluctuation of RH when the system is in equilibrium in model 1.0
Δx	difference between humidity ratio of air that goes into and out the humidifier or dehumidifier [kg/kg]
AHU	air handling unit
A_c	cross section area of packed bed [m ²]
A_i	inside surface of construction (i = 1, 5, 9, 13, 17, 21) [m ²]
A_r	surface area where air and beads interact [m ²]
a	slope of the line that describe the relation between moisture content of the pore space and the air right at the silica gel surface
b	the y-intercept of the line that describe the relation between moisture content of the pore space and the air right at the silica gel surface
CoP_{dehum}	coefficient of performance of humidifier
CoP_{hum}	coefficient of performance of dehumidifier
C_{eq}	concentration of water vapor at equilibrium
C_l	heat capacity of liquid water [J/K]
C_s	heat capacity of solid parts in the porous materials [J/K]
C_v	heat capacity of water vapor [J/K]
c	correlation factor between the humidity ratio of air and silica gel
c_1	slope of sorption isotherm
c_2	y-intercept of sorption isotherm
c_a	specific heat capacity of dry air [J/(K·kg)]
c_g	specific heat capacity of silica gel [J/(K·kg)]
c_l	specific heat capacity of liquid water [J/(K·kg)]
c_v	specific heat capacity of water vapor [J/(K·kg)]
D	difference between the RH in the display case and outside RH
EMC	equilibrium moisture content
E_{hum}	humidification energy demand
E_{dehum}	dehumidification energy demand
F	maximum acceptable range of RH fluctuation in the display case
$G_{AHU}(t)$	advection effect by ventilation [kg/s]
$G_{inf}(t)$	advection effect by infiltration [kg/s]
$G_v(t)$	humidity load [kg/s]
g	mass flux density [kg/m ² s]
g_l	mass flux density of liquid transport [kg/m ² s]
g_v	mass flux density of vapor transport [kg/m ² s]

h_l	the enthalpy of liquid water [J/kg]
h_v	the enthalpy of water vapor [J/kg]
k	permeability of packed bed [m ²]
L_{lv}	specific latent heat of vaporization of water [J/kg]
M	specific moisture reservoir
M_H	corrected specific moisture reservoir
M_w	molar weight of water [g/mol]
\dot{m}	mass flow rate of air in model 1.0 [kg/s]
m_a	mass of air [kg]
m_g	mass of silica gel [kg]
N	air exchange rate per day
p	pressure [Pa]
p_e	water vapor pressure in the air [Pa]
P_{fan}	power of fan [W]
p_s	water vapor pressure on the surface of construction [Pa]
p_{sat}	water vapor pressure at saturation [Pa]
Q_{AHU}	flow rate of ventilation [m ³ /s]
Q_{inf}	flow rate of infiltration [m ³ /s]
$Q_{per}(t)$	heat gain from people [W]
$Q_{add}(t)$	heating or cooling energy [W]
$Q_{sol}(t)$	solar gain [W]
\vec{q}	heat flux [W/m ²]
\vec{q}_l	heat flux transferred by liquid [W/m ²]
\vec{q}_v	heat flux transferred by vapor [W/m ²]
\overline{RH}	average RH when the the system is in equilibrium in model 1.0
RH	relative humidity
R_v	gas constant of water vapor [J/(kg.K)]
T	temperature [K]
T_i	temperature of node($i = 1, 5, 9, 13, 17, 21$) in model 2.0 and 3.0 [K]
t	time [s]
t_{min}	minimum days that the exhibition should be preserved under the acceptable range of RH
V_c	volume of one control volume of silica gel packed bed in model 3.0 [m ³]
V_{case}	volume of display case [m ³]
V_g	volume of the packed bed [m ³]
V_r	volume of the room [m ³]
w	moisture content of the silica gel [kg/m ³]
w_a	moisture content of the pore space [kg/m ³]

w_{a-g}	moisture content of the air right at the surface of silica gel beads [kg/m ³]
w_g	moisture content of the silica gel [kg/m ³]
x_e	humidity ratio of outside air [kg/kg]
x_g	humidity ratio of silica gel [kg/kg]
$x_{g,sat}$	humidity ratio of silica gel at saturation [kg/kg]
x_r	humidity ratio of air in the room [kg/kg]
$x_{r,sat}$	humidity ratio of air in the room at saturation [kg/kg]
x_s	humidity ratio of supply air [kg/kg]
x_{set}	desired humidity ratio [kg/kg]
α_c	convection coefficient [W/m ² K]
β_c	moisture transfer coefficient between the air in the packed bed and in the room [m/s]
β_{c-g}	moisture transfer coefficient between void space and the surface of silica gel beads [m/s]
β_p	surface vapour transfer coefficient [s/m]
δ_p	moisture permeability [kg/m·Pa·s]
ε	porosity of the packed bed
η_{wheel}	working efficiency of enthalpy wheel
η_{fan}	working efficiency of fan
η_{max}	maximum working efficiency of enthalpy wheel
μ	dynamic viscosity [Pa·s]
ξ	moisture capacity of silica gel [kg/m ³]
ρ_a	density of dry air [kg/m ³]
ρ_l	density of liquid water [kg/m ³]
ρ_s	density of solid parts in the porous materials [kg/m ³]
$\rho_{sat,g(T)}$	density of water vapor in saturation condition at temperature T [kg/m ³]
ρ_v	density of water vapor [kg/m ³]
$\rho_{v,25}$	vapor density of air in the room in model 3.0 [kg/m ³]
$\rho_{v,a}$	vapor density of air in the room in model 2.0 [kg/m ³]
$\rho_{v,g}$	vapor density of silica gel in model 2.0 [kg/m ³]
ϕ	relative humidity
ϕ_N	relative humidity of node N(N=I, II, ... , XII) in model 3.0

13 List of Figures

Chapter 1

Figure 1.1: A climate design concept in the National Holocaust Museum (ABT & Winhov, 2019)	4
Figure 1.2: Outline of the thesis	6
Figure 1.3: Methodology of the thesis	7

Chapter 2

Figure 2.1: Nine steps to manage the indoor climate in museums (Ankersmit & Stappers, 2017)	11
Figure 2.2: Temperature and humidity for visible mold (left). The time required for visible mold (right)	12
Figure 2.3: Schematic HVAC system	16
Figure 2.4: Indicating silica gel (Giebel Adsorbents)	18
Figure 2.5: Sorption isotherms of three types of silica gel (Long Life for Art, 2017)	18
Figure 2.6: Moisture transfer in the packed bed (Chang Lara, 2015)	19
Figure 2.7: Relationship between the moisture content of silica gel beads and that of air right at the surface (left). Sorption isotherm of silica gel (right).	21
Figure 2.8: Floor plan of the National Holocaust Museum in Amsterdam	24
Figure 2.9: The facade of the front building (left). Details on the window (right).	25

Chapter 3

Figure 3.1: Assumption and mass transfer network of model 1.0	29
Figure 3.2: The simplified moisture sorption isotherm of air and silica gel	30
Figure 3.3: Periodic moisture production	32
Figure 3.4: The illustration of dependent variables	32
Figure 3.5: The combination of variables for each group	33
Figure 3.6: 0 kg/m ² silica gel, ventilation rate=0.5 L/s/m ²	34
Figure 3.7: 0 kg/m ² silica gel, ventilation rate=1 L/s/m ²	34
Figure 3.8: 0 kg/m ² silica gel, ventilation rate=2 L/s/m ²	34
Figure 3.9: 0 kg/m ² silica gel, ventilation rate=4 L/s/m ²	34
Figure 3.10: 2.5 kg/m ² silica gel, ventilation rate=0.5 L/s/m ²	35
Figure 3.11: 2.5 kg/m ² silica gel, ventilation rate=1 L/s/m ²	35
Figure 3.12: 2.5 kg/m ² silica gel, ventilation rate=2 L/s/m ²	35
Figure 3.13: 2.5 kg/m ² silica gel, ventilation rate=4 L/s/m ²	35
Figure 3.14: 5 kg/m ² silica gel, ventilation rate=0.5 L/s/m ²	36
Figure 3.15: 5 kg/m ² silica gel, ventilation rate=1 L/s/m ²	36

Figure 3.16: 5 kg/m ² silica gel, ventilation rate=2 L/s/m ²	36
Figure 3.17: 5 kg/m ² silica gel, ventilation rate=4 L/s/m ²	36
Figure 3.18: 10 kg/m ² silica gel, ventilation rate=0.5 L/s/m ²	37
Figure 3.19: 10 kg/m ² silica gel, ventilation rate=1 L/s/m ²	37
Figure 3.20: 10 kg/m ² silica gel, ventilation rate=2 L/s/m ²	37
Figure 3.21: 10 kg/m ² silica gel, ventilation rate=4 L/s/m ²	37
Figure 3.22: The reduction effect on average relative humidity with different ventilation and moisture production rate	39

Chapter 4

Figure 4.1: Definition of construction and nodes in the thermal	39
Figure 4.2: Heat transfer network of model 2.0	40
Figure 4.3: Thermodynamic equilibrium in the packed bed	41
Figure 4.4: Mass transfer network of model 2.0	41
Figure 4.5: Simplified mass transfer network of model 2.0	43
Figure 4.6: Simplified AHU model	44
Figure 4.7: Humidity control components in Simulink	44
Figure 4.8: Heat transfer network of model 3.0	47
Figure 4.9: Definition of control volumes and assumption of moisture transfer	49
Figure 4.10: Mass transfer network of model 3.0	49

Chapter 5

Figure 5.1: The simplified version of the model development process (Sargent, 1981)	55
Figure 5.2: Illustration of Design Builder model	57
Figure 5.3: Comparison of RH in scenario a1	58
Figure 5.4: Comparison of RH in scenario a2	59
Figure 5.5: Comparison of RH in scenario a3	59
Figure 5.6: Moisture transfer between construction and air	61
Figure 5.7: Input T in scenario b1	63
Figure 5.8: Output T in scenario b1	63
Figure 5.9: Output RH in scenario b1	64
Figure 5.10: Output humidity ratio in scenario b1	64
Figure 5.11: Input humidity ratio in scenario b2	65
Figure 5.12: Output T in scenario b2	65
Figure 5.13: Output RH in scenario b2	66
Figure 5.14: Output humidity ratio in scenario b2	66

Chapter 6

Figure 6.1: The overview renovation design of the National Holocaust Museum (ABT &Winhov, 2020)	71
Figure 6.2: Simulated objects (ABT &Winhov, 2020)	72
Figure 6.3: Occupancy in one exhibition room in spring and autumn	73
Figure 6.4: Occupancy in one exhibition room in summer	73
Figure 6.5: Occupancy in one exhibition room in winter	73
Figure 6.6: Internal humidity load in one exhibition room in spring and autumn	74
Figure 6.7: Internal humidity load in one exhibition room in summer	74
Figure 6.8: Internal humidity load in one exhibition room in winter	74
Figure 6.9: Ventilation flow rate in one exhibition room in spring and autumn	75
Figure 6.10: Ventilation flow rate in one exhibition room in summer	75
Figure 6.11: Ventilation flow rate in one exhibition room in winter	75

Chapter 7

Figure 7.1: Relative humidity and temperature in scenario c1 and c2.	83
Figure 7.2: Relative humidity and temperature in scenario d1 and d2	83
Figure 7.3: Relative humidity and temperature in scenario e1 and e2	83
Figure 7.4: Box plot of RH in the room	84
Figure 7.5: Energy demand in the room of scenario f1 and f2	85
Figure 7.6: RH of scenario g1 and g2	86
Figure 7.7: RH of scenario g2 and h	86
Figure 7.8: RH of scenario g2 and i	86
Figure 7.9: Fluctuation of RH of scenario g1 and g2	87
Figure 7.10: Simplified the range of climate class A1	88
Figure 7.11: Evaluation of climate class A1 in scenario g1	88
Figure 7.12: Evaluation of climate class A1 in scenario g2	89
Figure 7.13: Evaluation of climate class A1 in scenario h	89
Figure 7.14: Evaluation of climate class A1 in scenario i	89
Figure 7.15: Energy demand of scenario g1 and g2	90
Figure 7.16: Energy demand of scenario g2 and h	90
Figure 7.17: Energy demand of scenario g2 and i	91
Figure 7.18: The humidity control device	92

14 List of Tables

Chapter 2

Table 2.1: Temperature and relative humidity specifications for collection (ASHRAE, 2019)	12
Table 2.2: Specific moisture reservoir at 20 °C (Tétreault & Bégin, 2018)	17

Chapter 3

Table 3.1: Amount of silica gel	27
Table 3.2: Ventilation flow rate	27
Table 3.3: Humidity load	27
Table 3.4: Period	28
Table 3.5: Division of groups	29
Table 3.6: Average ΔRH of every group	34
Table 3.7: Average \overline{RH} of every group	34

Chapter 4

Table 4.1: Working efficiency of enthalpy when the room needs humidification	45
Table 4.2: Working efficiency of enthalpy when the room needs dehumidification	46
Table 4.3: Summary of model 2.0 and 3.0	50

Chapter 5

Table 5.1: Summary of scenarios	57
Table 5.2: Comparison of fluctuation of RH in scenario a1, a2, and a3	60
Table 5.3: Input variables of the packed bed	62

Chapter 6

Table 6.1: Summary of simulation scenarios in one room with period of one week	72
Table 6.2: Scenario f1 when there is no silica gel in the room with period of one year	73
Table 6.3: Scenario f2 when there silica gel is applied in the room with period of one year	73
Table 6.4: Scenario g1 when there is no silica gel with 12 L/s/ per person ventilation rate	75
Table 6.5: Scenario g2 when silica gel is applied with 12 L/s per person ventilation rate	75
Table 6.6: Scenario when silica gel is applied with 9 L/s per person ventilation rate	76
Table 6.7: Scenario when silica gel is applied with 6 L/s per person ventilation rate	76

Chapter 7

Table 7.1: The dimension of packed bed	91
Table 7.2: The pressure drop along the packed bed	92

15 Reference

ASHRAE, A. (2013). Standard 62.1-2013 Ventilation for acceptable indoor air quality. American Society of Heating, Refrigerating and Air-Conditioning Engineers, Inc., Atlanta, GA, 40.

ASHRAE, A. (2019). Museums, Galleries, Archives and Libraries. ASHRAE Handbook–HVAC Applications..

ABT, & Winhov. (2019). Nationaal Holocaust Museum & Hollandsche Schouwburg VO fase

ABT, & Winhov. (2020). Nationaal Holocaust Museum Visiedocument definitief ontwerp

Andersson, A. C. (1985). Verification of calculation methods for moisture transport in porous building materials. Document-Swedish Council for Building Research, (D6).

Ankersmit, B., & Stappers, M. (2017). Managing indoor climate risks in museums. Springer.

Ayerst, G. (1968). Prevention of biodeterioration by control of environmental conditions. In Biodeterioration of materials. Microbiological and allied aspects. Proceedings of the 1st international symposium. Southampton, 9th-14th september, 1968 (pp. 223-241).

Chang Lara, C. (2015). The Passive Display Case.

DesignBuilder User Manual.(2006). Retrieved from: http://www.designbuildersoftware.com/docs/designbuilder/DesignBuilder_2.1_Users-Manual_Ltr.pdf

Erhardt, D., & Mecklenburg, M. (1994). Relative humidity re-examined. Studies in Conservation, 39(sup2), 32-38.

Ferreira, C., de Freitas, V. P., & Delgado, J. M. P. Q. (2020). The Influence of Hygroscopic Materials on the Fluctuation of Relative Humidity in Museums Located in Historical Buildings. Studies in Conservation, 65(3), 127-141.

GiebelAdsorbents. Products. Retrieved from: <https://www.giebel-adsorber.de/en/products/adsorbents-silicagel>

- Groom, P., Panisset T. (1933) Studies in penicillium chrysogenum thom in relation to temperature and relative humidity of the air. *Ann. Appl. Biol.*, 20, pp. 633-660
- Hagentoft, C.E. (2001). HAMSTAD- WP 2 Modelling: Determination of liquid water transfer properties of porous building materials and development of numerical assesment methods. Chalmers University of Technology Report R-02:9.
- Hens, H.L.S.C. (1993). Mold risk: Guidelines and practice, commenting the results of the International Energy Agency EXCO on energy conservation in buildings and community systems, Annex 14: Condensation energy. In Bugs, Mold and Rot III: Moisture Specifications and Control in Buildings, pp. 19-28. W. Rose and A. Tenwolde, eds. National Institute of Building Sciences, Washington, D.C.
- Hillston, J. (2003). Model validation and verification. Edinburgh: University of Edinburgh.
- Kramer, R. P. (2017). Clever climate control for culture: energy efficient indoor climate control strategies for museums respecting collection preservation and thermal comfort of visitors.
- Long life for art. (2017). Climate Control. Retrieved from: <https://llfa.eu/climate-control/prosorb.html>
- Lord, B., Lord, G. D., & Dexter, G. (2002). The Manual of Museum Exhibitions. Rowman Altamira.
- Martens, M. H. J. (2012). Climate risk assessment in museums: degradation risks determined from temperature and relative humidity data.
- Ministerie van Onderwijs, C. en W. (2018). Managing indoor climate risks—Publication—Cultural Heritage Agency. Ministerie van Onderwijs, Cultuur en Wetenschap. Retrieved from: <https://english.cultureelerfgoed.nl/publications/publications/2018/01/01/managing-indoor-climate-risks>
- Osanyintola, O. F., & Simonson, C. J. (2006). Moisture buffering capacity of hygroscopic building materials: Experimental facilities and energy impact. *Energy and Buildings*, 38(10), 1270-1282.
- Padfield, T. (1999). On the usefulness of water absorbent materials in museum walls. In 12th Triennial Meeting of the Committee for Conservation of the International Council

of Museums. James and James Science Publishers Ltd, London (pp. 83-87).

Sargent, R. G. (1981). An Assessment Procedure and a Set of Criteria for Use in the Evaluation of 'Computerized Models and Computer-Based Modelling Tools' (No. WP-80-016).

Sargent, R. G. (2013). Verification and validation of simulation models. *Journal of simulation*, 7(1), 12-24.

Schrijver, E., & Bijvoet, L. Bouwen ann het National Holocaust Museum

Sedlbauer, K. (2001). Prediction of mould fungus formation on the surface of and inside building components. *Fraunhofer Institute for Building Physics*, 75-141.

Tétreault, J. (2003). Airborne Pollutants in Museums, Galleries and Archives: Risk Assessment, Control Strategies and Preservation Management. Canadian Conservation Institute.

Tétreault, J., & Bégin, P. (2018). Silica Gel: Passive Control of Relative Humidity. Canadian Conservation Institute, Department of Canadian Heritage.

Thomson, G. (1977). Stabilization of RH in exhibition cases: Hygrometric half-time. *Studies in Conservation*, 22(2), 85-102.

Trechsel, H. R. (2001). Moisture analysis and condensation control in building envelopes. ASTM.

Van Belleghem, M. (2013). Modelling coupled heat and moisture transfer between air and porous materials for building applications (Doctoral dissertation, Ghent University).

Van Unen, J. (2019). The energy and Comfort Performance of a Lightweight Translucent Adaptable Trombe Wall in Different Buildings and Climates: A numerical study.

Wang, S. (2019). Museums' Responses to Tourism Sessonality: A Case Study in Umeå, Sweden.

Weintraub, S. (2002). Demystifying silica gel. Object Specialty Group.

White, J. (2013). Literature review on adsorption cooling systems. *Lat. Am. Caribb. J. Eng.*

Educ.

Yang, K. S., Wang, J. S., Wu, S. K., Tseng, C. Y., & Shyu, J. C. (2017). Performance Evaluation of a Desiccant Dehumidifier with a Heat Recovery Unit. *Energies*, 10(12), 2006.

Yu, D., Klein, S. A., & Reindl, D. T. (2001). An evaluation of silica gel for humidity control in display cases.



**nationaal
holocaust
museum**